



Exploring the pathways of stemness in the healthy and cancerous canine mammary gland

Meike Philipsen
3904261

Supervisors
Dr. ir. J.A. Mol
Ing. E.P.M. Timmermans-Sprang

Department of Clinical Sciences of Companion Animals
Faculty of Veterinary Medicine, Utrecht University, the Netherlands

2015-2016

Table of Contents

Chapter I: General introduction and aim of the study	5
Chapter II: Is there a relation between high basal Wnt activity and the expression of integrin markers in canine mammary tumor cell lines?	8
Summary	8
Introduction	8
Materials & methods	11
Cell culture	11
cDNA synthesis and quantitative PCR	11
TCF/LEF reporter assay	12
Labeling with fluorescently labeled antibodies and flow cytometry analysis	13
TCF/LEF reporter assay to compare Wnt activity of integrin $\alpha 6^{\text{high}}$ and integrin $\alpha 6^{\text{low}}$ cells from CMT-U27 and CIPm cell lines sorted by flow cytometry	13
Extracellular matrix culture	15
Statistics	15
Results	16
Quantitative RT-PCR	16
Flow cytometry analysis of PE anti-CD49f labeled CMT1, CMT-U27, CMT9 and CIPp cell lines	17
Comparison of Wnt activity in relation to level of CD49f expression	20
Extracellular matrix culture	21
Discussion	22
Chapter III: Neither integrin adaptor expression levels, nor a mutation in the integrin adaptor P140CAP are clearly associated with high basal Wnt activity in 3 canine mammary tumor cell lines	25
Summary	25
Introduction	25
Materials & methods	28
qPCR of integrin adaptors and CSK	28
Exome sequencing of P140CAP in canine mammary tumor cell lines	28
PCR and gel electrophoresis of P140CAP	28
Transfection with P140CAP-pcDNA3.1 for protein isolation and western blotting	29
Co-transfection with P140CAP-pcDNA3.1, TOP or FOP and Renilla plasmids and TCF/LEF reporter assay	29
Culture of P140CAP-pcDNA3.1 transfected and untransfected CMT-U27 and CIPm with and without Wnt pathway stimulation for Wnt target gene qPCR	30

RNA isolation, cDNA synthesis and qPCR of Wnt target genes.....	30
Transfection of CMT-U27 dsRED with P140CAP-pcDNA3.1 and subsequent injection into zebrafish embryos to study metastasis	31
Statistics	32
Results	33
qPCR of integrin adaptors.....	33
Exome sequencing of SRCIN1 in canine mammary tumor cell lines	37
Western blot of P140CAP transfected cells	39
The effect of transfection with murine P140CAP expression plasmid on Wnt activity	39
qPCR of Wnt target genes	44
Effect of P140CAP overexpression on metastasis of CMT-U27 dsRed in zebrafish.....	46
Discussion.....	47
Chapter IV: Attempts at long-term 3D canine mammary organoid culture.....	50
Summary	50
Introduction	50
Materials & methods.....	52
Canine mammary gland tissue	52
Isolation of mammary organoids	52
Organoid culture method and culture media	53
Passaging of canine mammary organoids	54
Results	55
Summarizing table of individual dog records, conditions and results	55
Isolation of mammary organoids	56
Organoid culture with the van Amerongen medium + 3 μ M CHIR	57
Organoid culture with the mini-gut organoid growth medium	57
Discussion.....	58
Chapter V: General discussion	60
References.....	62
Acknowledgements	72
Supplements.....	73
Supplement 1: Genorm results of cDNA of the panel of 12 CMT cell lines	73
Supplement 2: PE CD49f ^{high} and CD49f ^{low} gates.....	74
Supplement 3: Individual qPCR data of integrins in a panel of 12 CMT cell lines	75
Supplement 4: Results FACS CD49f CIPm.....	77

Supplement 5: Optimization of transfection conditions.....	78
Supplement 6: Genorm results of Wnt target qPCR.....	80
Supplement 7: Results of NEDD9 and IPP-complex qPCR	81
Supplement 8: Results of preliminary P140CAP TCF/LEF reporter assays of CIPm.....	84
Supplement 9: Results of putative Wnt target gene qPCR	85
Supplement 10: Courses followed during the HP year.....	91

Chapter I: General introduction and aim of the study

As the second most common cancer in the world, with an estimated 1.67 million new cases diagnosed worldwide in 2012, breast cancer remains a global health challenge (1). Although intensive screening and improved treatment options have increased the 5 year survival rate to over 80% in high income countries, it is still the second cause of cancer death in women from developed regions (1,2). In less developed regions, breast cancer remains the leading cause of cancer death in women, with survival rates ranging between 40% and 60% (1,2).

Breast cancer is a heterogeneous disease that can be classified into at least three major subtypes based on the expression of molecular markers. These markers are of both therapeutic and prognostic value. Most breast cancers are of the estrogen receptor positive (ER⁺) subtype: they are defined by estrogen receptor alpha (ER α) expression and/or progesterone receptor (PR) expression. These tumors are targeted with endocrine therapy: in premenopausal women, the standard treatment for these cancers is Tamoxifen (a selective estrogen receptor modulator with anti-estrogenic activity in breast cancer cells); in postmenopausal women they are treated with aromatase inhibitors to prevent local mammary synthesis of estrogens. Although the initial prognosis of these tumors has improved, recurrence due to endocrine resistance remains a therapeutic challenge (3). The second breast cancer subtype is characterized by gene amplification and/or overexpression of the human epidermal growth factor receptor 2 (HER2/ERBB2/Neu). Approximately 20% of breast cancers have HER2 overexpression, which is associated with more aggressive tumor behavior and a worse prognosis (4). Targeting these tumors with Trastuzumab, an anti-HER2 humanized monoclonal antibody, has improved the outcome for both patients with early and metastasized HER2+ disease (5). However, high resistance rates to Trastuzumab remain a problem. 65% of patients with HER2+ disease show primary resistance, meaning they do not respond to initial Trastuzumab treatment. Additionally, 70% of patients who show an initial response develop secondary resistance within a year after the initial treatment (4). The third subtype is defined by the absence of ER, PR and HER2 expression, and is known as triple negative breast cancer (TNBC). This highly aggressive subtype accounts for 10-15% of breast cancers (6). As it lacks any target for which specific treatment has been developed, the primary treatment for TNBC is chemotherapy (3). Although 40% of patients with a primary tumor respond well to chemotherapy, the prognosis of the 60% that does not respond to chemotherapy is unfavorable: the 5-year disease-free survival is less than 50% (7).

Regardless of breast cancer subtype, most cancer-related death is due to therapy resistance and metastasis of the primary tumor. Cancer stem cells (CSCs) are thought to be drivers of metastasis, cancer progression and therapy resistance. CSCs are a small population of cells within the tumor with stem-cell like properties such as self-renewal and multi-lineage differentiation (8). Stem cells are thought to be of particular importance in the mammary gland, seeing as it is a tissue that can develop and undergo involution extensively throughout life. However, CSCs do not necessarily originate from normal tissue stem cells. It is thought that in the process of tumorigenesis, mutations in stem-, progenitor- or even differentiated cells can all cause these cells to gain stem-cell like abilities (9). CSCs may explain intra- and intertumor heterogeneity by their ability to give rise to heterogeneous progeny. Similar to the older clonal evolution theory, the cancer stem cell theory offers an explanation for intra- and intertumor heterogeneity. One of the main differences is that the cancer stem cell theory supposes a form of cellular hierarchy: the cancer stem cell maintains the tumor by dividing and differentiating into the different cell types that make up the tumor (9). In the clonal evolution theory a single cell receives an oncogenic hit and starts dividing. During these cell divisions, the daughter cells will acquire different mutations. Some cells will acquire advantageous mutations and become dominant clones. Other clones may lack tumorigenicity. However, there is no

cellular hierarchy, meaning there is not a parent subtype that gives rise to the other subtypes. Instead, each subtype replicates to sustain itself (10).

From a clinical perspective, the cancer stem cell theory offers attractive explanations for the biggest therapeutic challenges: therapy resistance, cancer recurrence and a lack of curative treatment for metastatic disease. Normal tissue stem cells appear to have an intrinsic resistance therapeutic strategies commonly employed to target cancer cells. Most (chemotherapeutic) drugs target highly active cells, yet stem cells reside in a state of relative quiescence (8). Additionally, stem cells highly express certain transmembrane drug transporters, causing them to be resistant to many drugs and toxins (8). Moreover, stem cells have a more active DNA damage checkpoint response and a higher DNA repair capacity, rendering them more resistant to radiotherapy (8). If CSCs have similar properties as normal tissue stem cells, it appears plausible that current treatment strategies insufficiently target CSCs. The survival of CSCs that remain dormant in the body for many years is thought to be a cause of cancer recurrence and subsequent metastasis.

However, the CSC model is not undisputed. Most evidence for the existence of CSCs has been derived from studies that assessed the tumor-initiating capacity of supposed human CSCs by transplanting these into immune-deficient mice. Some argue these transplantation assays may not reflect cell behavior in patients. One study showed that transplanting lymphomas and leukemia's of mouse origin into recipient mice led to a very high frequency of tumor growth, challenging the concept that only rare CSCs are able to initiate tumor growth (11).

Pet dogs have been suggested as a good animal model for human breast cancer. The epidemiology of canine mammary tumors (CMTs) resembles that of human breast cancer. CMTs occur spontaneously at a high incidence (200-250/100.000 dogs/year in Europe) (12-14). The main risk factor for developing CMTs is exposure to steroid hormones, as is demonstrated by the drastically lower incidence in bitches that have been spayed after the first estrous cycle when compared to uncastrated bitches, an effect that is still present although less effective after spaying before the 2nd estrus cycle but after this is absent (15). As in humans, increasing age is a risk factor for developing mammary tumors (16). Seeing as pet dogs have a shared environment with their human owners, they may also prove a valuable model to study environmental risk factors for developing breast cancer. Histologically, canine simple carcinomas, which have only epithelial proliferation, closely resemble human *in situ* or invasive ductal or lobular carcinomas (17). Canine mammary carcinomas may also, more often than human breast cancer, appear as complex carcinomas suggesting a real stem cell origin with a variety in cellular differentiation whereas simple carcinomas may have an origin in mutations of progenitor cells (17). On the cellular level, CMTs and human breast cancer share many signaling pathways commonly altered in carcinogenesis, including PI3K/AKT, KRAS, PTEN, Wnt- β -catenin and MAPK signaling (18). There is some evidence the BRCA 1/2 complex is involved in canine mammary tumorigenesis (19). Studies investigating the role of HER2 overexpression have produced conflicting results, with one study finding increased survival in dogs with malignant mammary tumors overexpressing HER2 (20-22).

Previous work of the Comparative and Translational Oncology group has shown that in a panel of 12 canine mammary tumor cell lines, 3 have highly activated canonical Wnt signaling in association with high HER2 expression and PTEN silencing (23). Seeing as Wnt activity is known to play an important role in both normal mammary gland development and tumor formation, and is thought to be a stem cell marker, the high Wnt activity in these 3 cell lines has been the focus of research for the past years. It has been shown that the high Wnt activity is not caused by a mutation in any of the components of the Wnt pathway, as is common in colorectal cancer (23). It can, however, be further induced by PI3K/mTOR inhibition, and is sensitive to cSRC inhibition (24). Nevertheless, the ultimate cause of the high Wnt activity is yet to be discovered.

As cSRC is, among other pathways, activated by integrin signaling, and the integrin $\alpha 6$ (also known as CD49f) is a specific marker for mammary stem cells, it was the aim of this project to further study the possible involvement of integrin signaling mechanisms in the highly elevated basal Wnt activity in some canine mammary cancer cell lines. Therefore the project studied if the presence of one stem cell marker, high Wnt activity, coincided with another, integrin $\alpha 6$, and whether they were functionally related. As will be explained in the next chapter, the initial found selective expression of CD49f in a subset of mammary cells with high basal Wnt activity appeared not to be reproducible and this path of research proved unworthy of pursuing. To move forward, we looked one step further in the integrin signaling pathway: could not the receptor, but a mutation in its adaptor P140CAP be the cause of the high Wnt activity? This path of research presented a technical difficulty, which made it necessary to develop an alternative way of measuring Wnt activity. Furthermore, it was attempted to culture canine mammary organoids to enable future studies of mammary stem cells in an environment bearing closer resemblance to the mammary stem cell niche *in vivo*.

The project is embedded into the faculty research program 'Regenerative medicine, stem cells and cancer', seeing as it has explored the concept of (cancer) stem cells in the context of the canine mammary gland.

Chapter II: Is there a relation between high basal Wnt activity and the expression of integrin markers in canine mammary tumor cell lines?

Summary

Active Wnt-signaling is thought to induce the development of mammary tumors from stem/progenitor cells, and is therefore used as a cancer stem cell marker. Likewise, integrin $\alpha 6$ (CD49f) is associated with cancer stemness. In this study, we investigated if highly activated Wnt-signaling and integrin expression are associated in canine mammary tumor cell lines. Expression of 7 integrin subunits, including integrin $\alpha 6$, was evaluated by RT-PCR of twelve canine mammary tumor cell lines with previously reported differential basal Wnt activity. Furthermore, the correlation between Wnt activity and integrin $\alpha 6$ expression was investigated in 3 canine mammary tumor cell lines with high basal Wnt activity (CMT1, CMT-U27 and CMT9) and in 2 canine mammary tumor cell lines with absent basal Wnt activity (CIPm and CIPp). Cells from these 5 cell lines were transfected with TOPflash or FOPflash and Renilla, subsequently labeled with PE-anti CD49f antibody and sorted into integrin $\alpha 6$ positive and negative populations by flow cytometry. Wnt-activity of integrin $\alpha 6$ positive and negative populations was measured using Dual Luciferase reporter assay. Additionally, Wnt activity of integrin $\alpha 6^{\text{high}}$ and integrin $\alpha 6^{\text{low}}$ cell fractions from CMT-U27 and CIPm cell lines was compared using a similar method. The functional activity of integrins in CMT-U27 and CIPm cell lines was tested by measuring Wnt activity after culture on ECM proteins such as collagen type I, Matrigel and laminins. In contrast to the hypothesis, cell lines with high basal Wnt activity showed an inverse relation with the mRNA expression of various integrins. Flow cytometry of PE-anti integrin $\alpha 6$ labeled cell lines revealed that nearly 100% of cells from both cell lines with high and low Wnt activity expressed integrin $\alpha 6$ on the cell surface. Comparison of Wnt activity of integrin $\alpha 6$ positive and negative populations was therefore not possible. Wnt activity did not differ significantly between integrin $\alpha 6^{\text{high}}$ and integrin $\alpha 6^{\text{low}}$ cell fractions in CMT-U27 and CIPm cell lines, nor between conditions cultured on various ECM proteins versus control uncoated. Integrin $\alpha 6$ is not a specific marker of high Wnt activity in canine mammary tumor cell lines, and integrins in general do not appear to influence Wnt activity. Their suitability as a cancer stem cell marker in canine mammary tumors may be limited.

Introduction

Cancer stem cells (CSCs) are thought to be a driver of metastasis, cancer progression and therapy resistance in many forms of cancer, including breast cancer. Therefore they appear to be important therapeutic targets. However, in order to be able to develop effective therapeutic strategies, these cells must first be isolated. In order to do so, reliable CSC markers are needed.

The mammary gland is a dynamic organ that develops mostly post-natal and undergoes extensive development during each period of pregnancy and lactation followed by subsequent involution. The activity of developmental cell signaling pathways in mammary stem cell is thought to be essential for this plasticity. One of the pathways implicated in mammary stem cell activity is the Wnt signaling pathway. The Wnt signaling pathway is a complex evolutionarily conserved pathway that is essential for the embryonic development of many organ systems and the maintenance of tissues throughout life (25). Wnt-signaling cascades are often categorized as canonical/ β -catenin dependent or non-canonical/ β -catenin independent, although this division does not appear to be absolute (26). Canonical Wnt activity is initiated by binding of extracellular Wnt ligand to Frizzled membrane

receptor and low-density lipoprotein 5 or 6 (LRP5/LRP6) co-receptor. This binding attracts Disheveled, which inhibits the β -catenin destruction complex. In absence of Wnt signaling, the β -catenin destruction complex, which consists of GSK-3, Axin, CK1 α and APC, marks β -catenin for ubiquitin-mediated destruction. Activation of the Wnt pathways leads to inhibition of the β -catenin destruction complex. As β -catenin is no longer destructed, it will accumulate in the cytosol and nucleus. In the nucleus β -catenin will form an activation complex with DNA binding proteins of the nuclear TCF/Lymphoid Enhancer Factor (LEF) family, resulting in transcription of TCF/LEF regulated genes (26-28).

Wnt signaling has been implicated in multiple stages of normal mammary gland development as well as oncogenic transformation (29-31). Studies using Wnt-reporter mice and mice with genetic modifications to Wnt pathway component genes have revealed the Wnt pathway to be essential for mammary stem cell function and thereby embryonic development of the mammary gland (32-34). The role of Wnt activity in pubertal development and adult tissue maintenance is not as apparent (35). In pregnancy, however, Wnt activity appears to play a part in stem cell renewal and differentiation required for mammary development (35). *In vitro* Wnt proteins have been shown to be self-renewal factors for normal mammary stem cells in culture (36).

With regard to cancer initiation, activation of the Wnt pathway in mouse models of breast cancer has been shown to induce tumor formation (37,38). Preneoplastic lesions in these mouse models have a greater proportion of cells that exhibit progenitor markers and the tumors that arise in these mouse models are heterogeneous, as would be expected from a tumor with a stem cell origin (38). Studies of human breast cancer suggest a role for Wnt activity in tumor initiation and progression (39). High Wnt activity in basal breast cancer is associated with poor outcome (40). Unlike in other types of cancers such as colon carcinoma, genetic mutations in principal components of the Wnt pathway are rare in breast cancer. Alternative mechanisms of Wnt activation found in breast cancer include excessive production of Wnt ligands, increased activity of Wnt receptors, decreased expression of endogenous Wnt pathway inhibitors, loss of antagonizing non-canonical Wnt activity and Wnt ligand-independent β -catenin activation (39).

As the Wnt pathway is essential for normal stem cell functioning and in cancer appears to give rise to a greater number of tumor cells with stem cell or progenitor phenotype, Wnt activity appears to be a functional CSC marker. In our lab, we have a panel of 12 canine mammary tumor cell lines. Three of these CMT cell lines, CMT1, CMT-U27 and CMT9, have high canonical Wnt activity which can be attenuated by cSrc inhibition as previously reported (23,24). However, the ultimate cause of this high Wnt activity is unknown. Preliminary experiments with lyoplates have shown that 12.7% of cells in the cell lines with high Wnt activity express integrin $\alpha 6$ on the cell surface, compared to 0.01% in CIPm and CIPp cell lines with low Wnt activity. These findings prompted an interest in integrin $\alpha 6$, and integrins in general, as these have been implicated in normal stem cell maintenance and cancer stem cell regulation (41), and activation of cSRC.

Integrins are heterodimeric cell surface receptors that mediate cell-extracellular matrix attachment. Additionally, they relay signals between the extracellular environment and the cell through the association of their cytosolic domain with intracellular signaling proteins (42). As such, integrins are responsible for cell survival, proliferation, attachment and migration. In mammals there are 18 α and 8 β subunits that are known to combine into 24 distinct heterodimers (42). Integrin $\beta 1$ is one of two β integrins capable of heterodimerization with integrin $\alpha 6$, integrin $\beta 4$ being the other partner. Both integrin $\alpha 6\beta 1$ and $\alpha 6\beta 4$ are laminin receptors. Integrins $\alpha 6$ and $\beta 1$ are both highly expressed in cells of the basal layer of the mammary gland, where the mammary stem cells are located (41). Furthermore, deletion of $\beta 1$ integrin in basal cells has been shown to lead to abnormal mammary morphogenesis and a reduced regeneration potential (43). Integrins $\alpha 6$ (CD49f) and $\beta 1$ (CD29) in

combination with CD24 have therefore been used in mice as markers to isolate mammary stem cells. Single cells isolated in this manner were able to repopulate a mammary gland (44,45).

Integrins have been implicated in cancer initiation, progression, drug resistance and metastasis (46). In part, this could be explained by the contribution of integrins to a CSC phenotype. Integrins involved in normal mammary stem cell maintenance are also thought to contribute to cancer stemness. Integrin $\alpha 6$ (CD49f) has been shown to further enrich for CSCs in a CD44^{high}/CD24^{low} breast cancer cell population (47) and to be necessary for tumorigenicity of a stem cell-like subset of the MCF7 breast cancer cell line (48). Conversely, integrin $\alpha 6$ has been repeatedly associated with poor outcome in breast cancer patients (49,50). Integrin $\beta 1$ is thought to be a normal mammary stem cell marker: it is primarily expressed in the basal cell layer and has been shown to be essential for normal mammary gland development (41,43). In both 3D-culture of human breast cancer cells and mouse mammary tumor models, higher integrin $\beta 1$ expression has been associated with increased tumor formation (51). Additionally, integrin $\beta 1$ has been combined with CD24 to enrich for CSCs in *Brca1* mouse mammary carcinoma cell lines (52). Integrin $\beta 1$ has been implicated in both pro-invasion/pro-metastatic and anti-invasion/anti-metastatic networks in different human breast cancer cell lines, indicating its function may depend on the molecular subtype (53-57). Studies on integrin $\beta 1$ expression as a prognostic marker have had mixed outcomes: some have found loss of integrin $\beta 1$ expression to be associated with more aggressive molecular subtype (58), others found high integrin $\beta 1$ expression to be a negative prognostic marker (59), or found no association between integrin $\beta 1$ expression and survival (60). Another set of integrins implicated in cancer progression are the $\alpha \nu \beta 3$ and $\alpha \nu \beta 6$ heterodimers. Integrin $\alpha \nu \beta 3$ contributes to adhesion and migration in breast cancer cell lines (61), and is thought to play a role in metastasis of breast cancer cells to bone (62). Pharmacological targeting or transcriptional silencing of $\alpha \nu$ -integrins has been shown to impair metastasis of human breast cancer cell lines in mouse, zebrafish and rat xenograft models (63,64). Furthermore, integrin $\alpha \nu \beta 3$ has been functionally linked to cancer stem cell properties such as tumor sphere formation and tumor initiation in human breast cancer cell lines (65).

Three canine mammary tumor cell lines in our lab appeared to have both high Wnt activity and integrin $\alpha 6$ expression, both of which are putative stem cell markers. We attempted to see if both markers overlapped, and if combining them could enrich for CSCs. First, we performed qPCR on a panel of 12 canine mammary tumor cell lines, including the cell lines with high Wnt activity, to see if any integrin associated in literature with breast cancer progression and/or CSC properties was specifically highly expressed in the cell lines with high Wnt activity. The proposed follow up experiment was to compare Wnt-activity using a TCF/LEF Wnt reporter assay between cells positive and negative for the integrin of interest. Furthermore, it was explored if there is a functional relation between the two. Does activating the integrin of interest by culturing the cells on matrix proteins further enhance Wnt activity, and thereby stemness?

Materials & methods

Cell culture

Five canine mammary tumor cell lines, CMT1, CMT-U27, CMT9, CIPm and CIPp, were brought into culture from frozen cell aliquots stored at -196°C. These cell lines originate from primary tumors diagnosed as carcinomas (CMT1, CMT-U27, CMT9 and CIPp) or its metastasis (CIPm). All cell lines were cultured in 75 cm² cell culture flasks (Greiner Bio-one, Alphen aan de Rijn, the Netherlands) in DMEM:F12 (Thermo Fisher Scientific, Breda, the Netherlands) with 10% Fetal Bovine Serum (FBS) (Thermo Fisher Scientific) and Penicillin/Streptomycin (P/S) (Thermo Fisher Scientific) at 37 °C with 5% CO₂ in a New Brunswick Scientific Innove CO-170 incubator (Eppendorf, Nijmegen, the Netherlands). Cells were passaged weekly at approximately 80% confluency.

cDNA synthesis and quantitative PCR

RNA used for cDNA synthesis was previously isolated from 2 passages of 12 canine mammary tumor cell lines using the RNeasy mini kit (Qiagen, Venlo, the Netherlands) according to manufacturer's protocol and stored at -80 °C. cDNA was synthesized using iScript cDNA synthesis kit (Bio-Rad, Veenendaal, the Netherlands) according to manufacturer's protocol. Quantitative PCR of 7 integrin genes and 7 reference genes was performed in duplicate using IQ SYBR green master mix (Bio-Rad) in a CFX384 Touch Real-Time PCR System (Bio-Rad) according to manufacturer's protocol. Primer sequences of target and reference genes are listed below in table 1. Stability of reference genes was tested using the Genorm method in RStudio 0.99.902 (RStudio, Boston, United States of America). Relative gene expression was calculated using the $\Delta\Delta CT$ -method (66). Reference gene rank, stability graph and variance graph are included in supplement 1.

Samples were grouped into three groups based on the Wnt activity of the respective cell line as previously reported (23). The high Wnt activity group included the following samples (P = passage number at time of RNA isolation): CMT1 P4, CMT1 P10, CMT-U27 P4, CMT-U27 P10, CMT9 P4, CMT9 P10. The moderate Wnt activity group included the following samples: CHMp P3, CHMp P20, CNMm P3, CNMm P18, CNMp P4, CNMp P7, P114 P4, and P114 P7. The low Wnt activity group included the following samples: CHMm P3, CHMm P19, CIPm P3, CIPm P19, CIPp P3, CIPp P19, CMT-U229 P4, CMT-U229 P7, CMT-U335 P4, and CMT-U335 P7.

Gene	Product Length	T _m (°C)	Forward/Reverse	Sequence 5'→3'
<i>ITGA5</i>	180	62	Forward	ATA-CCC-GGA-TCT-GAT-TGT-G
			Reverse	GTT-GAG-GCA-GAA-GCT-GAG
<i>ITGA6</i>	179	64	Forward	GGA-CCT-TGA-TAG-AAA-TTC-CTA-CC
			Reverse	TTC-ACC-TTG-AGG-CAT-ATC-CC
<i>ITGAV</i>	176	64	Forward	GCT-CAT-TTC-AGA-TCA-AGT-GG
			Reverse	GAA-ACA-AAG-TCA-TCT-ACG-CC
<i>ITGB1</i>	133	65.5	Forward	CAG-TTA-CAG-AAG-AAT-TTC-AGC-C
			Reverse	TGA-GGA-AAG-GGA-GTT-GTA-GG
<i>ITGB3</i>	135	64	Forward	CAA-CCA-TTA-TTC-TGC-CTC-CA
			Reverse	CTC-ACT-GTA-GTT-CTG-GTA-GAG
<i>ITGB4</i>	189	65.5	Forward	AAC-CAG-CAC-TCA-CTC-TAC-AC
			Reverse	CCT-CCT-CTC-CTT-TCT-TAA-GCT-C
<i>ITGB6</i>	167	62	Forward	GAC-CTC-AAT-ACA-ATC-AAA-GAG-CTG
			Reverse	GAA-GTA-TGG-AAT-ACT-ACT-GCA-AGG
<i>HMBS</i>	112	61	Forward	TCA-CCA-TCG-GAG-CCA-TCT
			Reverse	GTT-CCC-ACC-ACG-CTC-TTC-T
<i>HNRPH</i>	151	61	Forward	CTC-ACT-ATG-ATC-CAC-CAC-G
			Reverse	TAG-CCT-CCA-TAA-CCT-CCA-C
<i>RPS5</i>	141	62.5	Forward	TCA-CTG-GTG-AGA-ACC-CCC-T
			Reverse	CCT-GAT-TCA-CAC-GGC-GTA-G
<i>SRPR</i>	81	61	Forward	GCT-TCA-GGA-TCT-GGA-CTG-C
			Reverse	GTT-CCC-TTG-GTA-GCA-CTG-G
<i>RPS19</i>	95	62	Forward	CCT-TCC-TCA-AAA-AGT-CTG-GG
			Reverse	GTT-CTC-ATC-GTA-GGG-AGC-AAG
<i>TBP</i>	96	57	Forward	CTA-TTT-CTT-GGT-GTG-CAT-GAG-G
			Reverse	CCT-CGG-CAT-TCA-GTC-TTT-TC
<i>GAPDH</i>	100	58	Forward	TGT-CCC-CAC-CCC-CAA-TGT-ATC
			Reverse	CTC-CGA-TGC-CTG-CTT-CAC-TAC-CTT

Table 1 Primers sequences of integrins and reference genes.

TCF/LEF reporter assay

CMT1, CMT-U27 and CMT9 cell lines each were seeded in 2 24-well plates (Primaria, BD Biosciences, Breda, The Netherlands) in DMEM:F12 + 10% FCS + P/S at a density which would result in 80% confluency the following day. For CMT1 and CMT9, this optimal density was 100.000 cells/well, for CMT-U27 it was 150.000 cells/well. 24 H after seeding, transfection was initiated. Cells were washed in 1 ml Hank's Balanced Salt Solution (HBSS) (Thermo Fisher Scientific) per well, subsequently 400 µl DMEM:F12 was added to each well. For each well, 3 µl Lipofectamine 2000 (Thermo Fisher Scientific) was first added to 50 µl DMEM:F12 and incubated for 5 minutes at room temperature (RT). Afterwards, this was combined with 0.8 µg of either TOPFLASH- or FOPFLASH-TCF reporter plasmids (generous gift of prof Hans Clevers, Hubrecht Laboratory, Utrecht) and 0.5 ng Renilla (67) in 50 µl DMEM:F12 and incubated for 20 minutes at RT. Cells were transfected using 100 µl TOP or FOP transfection mixture per well. For each cell line, 1 24-well plate was transfected with TOP and the other 24-well plate with FOP. After incubating for 5 h at 37 °C with 5% CO₂, transfection was stopped by adding 500 µl DMEM:F12 with 20% FCS to each well. 48 H after transfection, cells were washed with 1 ml HANK's per well. Cells in columns 1-5 of each plate were detached with 100 µl TrypLE Express (Thermo Fisher Scientific) per well and used for flow cytometry. Cells in column 6 of each

plate were used as a control for transfection efficiency. After adding 100 µl 5x diluted Passive Lysis Buffer (Promega Benelux, Leiden, the Netherlands) to each well, the plates were put on an orbital shaker for 15 minutes at 300 rpm and then kept overnight at -20 °C. After transferring the thawed lysate to a v-shape 96 wells plate (Greiner Bio-one) it was centrifuged for 15 minutes at 2900 rpm in an Eppendorf 5804 centrifuge (Eppendorf). 20 µl of the supernatant was transferred to a white 96 wells assay plate (Corning, Amsterdam, the Netherlands) and analyzed using Dual-Luciferase Reporter Assay (Promega) according to manufacturer's protocol using a Centro LB 960 luminometer (Berthold Technologies, Vilvoorde, Belgium). TOP and FOP data were first corrected for the variation in transfection efficiency using the corresponding Renilla data, subsequently TOP/FOP ratio was calculated.

Labeling with fluorescently labeled antibodies and flow cytometry analysis

Flow cytometry experiments were at first performed with TOP/FOP transfected cells from CMT1, CMT-U27, CMT9, CIPm and CIPp cell lines on a BD Influx Cell Sorter (BD Biosciences). When it became apparent that the labeling procedure needed optimization and validation, subsequent experiments were performed using untransfected cells from the 5 cell lines on a BD Canto (BD Biosciences) as this was more convenient. The labeling protocol used for optimization and validation on the Canto will be described here, as it is the most complete. The labeling protocol used on the BD Influx Cell Sorter had the same basic procedure, but it used 10×10^6 cells, cells were detached from 24 wells Primaria plates and the protocol did not include the blocking step with rat serum step or the isotype control.

Cells of CMT1, CMT-U27, CMT9, CIPm and CIPp cell lines were detached from 75 cm² cell culture flasks using TrypLE Express, collected in HBSS and counted with 0,40% trypan blue dye (Bio-Rad) on a BioRad TC20 automated cell counter (Bio-Rad). 10^6 cells of CMT1, CMT-U27, CMT9, CIPm and CIPp cell lines were used per condition. The following conditions were used: unlabeled control, CD49f-labeled, CD-49f labeled with rat serum, isotype-labeled, isotype-labeled with rat serum and CD90-labeled. The following antibodies, purchased at BD Biosciences, were used: PE rat anti-human CD49f (#555736, clone GoH3, isotype rat (SD) IgG2a κ), PE rat IgG2a κ isotype control (#555844, clone GoH3) and PE mouse anti-human CD90 (#555596, clone 5E10, isotype mouse IgG1 κ). The collected cells were centrifuged for 5 minutes at 1400 rpm at room temperature (RT) in a Hettich Zentrifugen Rotofix 32A (Hettich Lab Technology, Tuttlingen, Germany) washed with Stain buffer with 5 mM EDTA added (SB + EDTA) (BD Biosciences) and centrifuged for 5 minutes at 1400 rpm at RT. After removing the supernatant, cells were incubated with SB + EDTA or SB + EDTA + 2% normal rat serum (collected from laboratory rats euthanized for other experiments) for 15 minutes at RT. The normal rat serum conditions were included to block aspecific binding of PE rat anti-human CD49f and PE rat isotype control. After the blocking step, the antibodies were added in volumes recommended by the manufacturer and incubated for 45 minutes on ice protected from light. Cells were washed twice to remove unbound antibodies, resuspended in 500 µl SB + EDTA, strained through a 40 µm cell strainer (Greiner Bio-one) and kept on ice protected from light until the sample was needed for flow cytometry.

Flow cytometry was performed on a BD Canto. The collected data was analyzed using FlowJo flow cytometry analysis software (FlowJo, Ashland, Oregon, United States of America). Gates were based on the unlabeled control of each cell line.

TCF/LEF reporter assay to compare Wnt activity of integrin $\alpha 6^{\text{high}}$ and integrin $\alpha 6^{\text{low}}$ cells from CMT-U27 and CIPm cell lines sorted by flow cytometry

CMT-U27 and CIPm cell lines were seeded on 20 Primaria 6-well plates in DMEM:F12 + 10% FCS + 1% P/S at densities of 500.000 and 275.000 cells/well respectively. 24 H after seeding, transfection was initiated. Cells were washed with HBSS, subsequently 1200 µl DMEM:F12 was added to each well. For

each well, 10 μ l Lipofectamine 2000 was first added to 150 μ l DMEM:F12 and incubated for 5 minutes at RT. Afterwards, this was combined with 2 μ g TOPFLASH or FOPFLASH-TCF reporter plasmids and 5 ng Renilla in 150 μ l DMEM:F12 and incubated for 20 minutes at RT. Cells were transfected using 300 μ l TOP or FOP transfection mixture per well. For each cell line, 10 6-well plates were transfected with TOP and 10 6-well plate with FOP. After incubating for 5 h at 37 °C with 5% CO₂, transfection was stopped by adding 1500 μ l DMEM:F12 + 20% FCS to each well. 48 H after transfection, cells were washed with HANK's and detached using TrypLE Express. Untransfected CMT-U27 and CIPm cells were concurrently detached from confluent 75 cm² cell culture flasks to be used for the control samples. For both CMT-U27 and CIPm, the following conditions were used: unlabeled untransfected control, PE anti-CD90 labeled untransfected control, PE anti-CD49f labeled TOP transfected, PE anti-CD49f labeled FOP transfected. 10⁶ cells for each control and 10x10⁶ cells for the TOP/FOP transfected samples were labeled following the procedure described earlier. Volumes of reagents were adjusted to the sample size. PE anti-CD49f labeling included blocking aspecific binding with normal rat serum. Samples were sorted on a BD Influx Sorter. Live, single cells were first gated using the unlabeled controls. Labeling procedure was verified with the PE anti-CD90 controls. In the PE anti-CD49f samples, the top 14-15% of cells with the highest PE signal and the bottom 9-10% of cells with the lowest PE signal were gated (figure 1 + supplement 2). Cells were sorted into tubes filled with DMEM:F12 + 10% FCS + P/S.

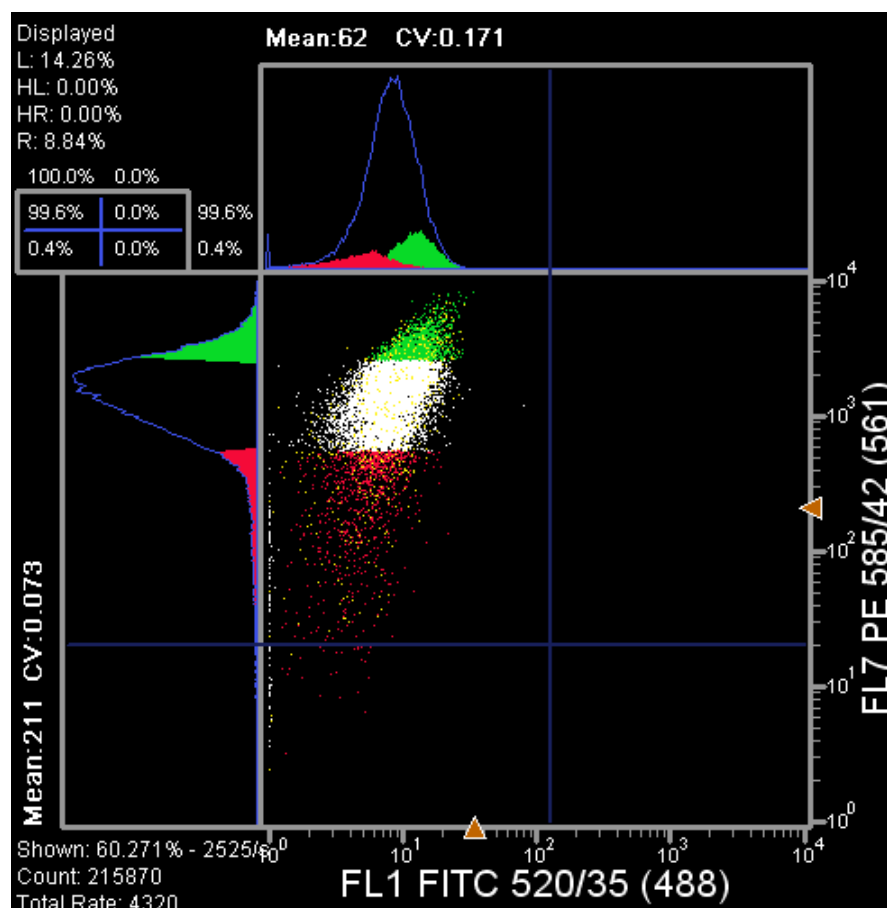


Figure 1 Example of gates drawn to sort CD49f^{high} and CD49f^{low} cells. Sample displayed here was PE anti-CD49f labeled TOP transfected CMT-U27 cell line. The top 14.26% cells with the highest PE signal were sorted into the left channel (green). The bottom 8.84% PE anti-CD49f TOP transfected CMT-U27 were sorted into the right channel (red). Cells outside of these two gates were discarded by the flow cytometer (white). Equivalent gating procedure was applied to all PE anti-CD49f labeled samples. Figures of gates in all PE anti-CD49f labeled samples are included in supplement 2.

For CMT-U27, 500.000 cells per condition were used in the TCF/LEF assay. For CIPm only 30.000 cells were used. After washing cells with HBSS, 5x diluted Passive Lysis Buffer was added (500 μ l to CMT-U27 samples, 60 μ l to CIPm samples) and tubes were put on an orbital shaker for 15 minutes at 300 rpm and then kept overnight at -20 °C. After transferring the thawed lysate to a v-shape 96 wells plate it was centrifuged for 15 minutes at 2900 rpm in an Eppendorf 5804 centrifuge. 20 μ l of the supernatant was transferred to a white 96 wells assay plate and analyzed using Dual-Luciferase Reporter Assay according to manufacturer's protocol using a Centro LB 960 luminometer. CMT-U27

samples were analyzed in triplicate, CIPm samples in duplicate. TOP and FOP data were first corrected for the number of cells present in the sample with corresponding Renilla data, subsequently TOP/FOP ratio was calculated.

Extracellular matrix culture

CMT-U27 and CIPm cell lines were cultured on various extracellular matrix proteins and then subjected to the TCF/LEF reporter assay. 2 different experiments were performed. In the first experiment the cells were cultured on collagen type 1 and Matrigel-coated Primaria 24-well plates and control uncoated Primaria 24 well plates. Primaria 24-well plates were coated with collagen type 1 (Sigma-Aldrich, Zwijndrecht, the Netherlands) by adding 16 µg collagen in 100 µl HBSS per well and incubating for 3 hours at RT. Primaria 24-well plates were coated with Matrigel Basement Membrane Matrix Growth Factor Reduced (Corning Life Sciences, Amsterdam, the Netherlands) by diluting Matrigel 1:2 with DMEM:F12 and adding 100 µl per well. In the second experiment, cells were cultured on control uncoated Primaria 24-well plates, ready-made Corning Biocoat Laminin 24 well plates (Corning) and on Primaria 24-well plates coated with laminin 521 (Biolamina, Sundbyberg, Sweden) according to manufacturer's protocol. In both experiments, CMT-U27 was seeded at a density of 100.000 cells/well, CIPm at a density of 70.000 in 1 ml DMEM:F12 + 10% FCS + P/S. Transfection with TOP/FOP reporter plasmid and TCF/LEF reporter assay were performed in triplicate as described above.

Statistics

In the qPCR experiment means of groups were compared using unpaired Mann-Whitney U test with Bonferroni correction. In TCF/LEF experiments, mean TOP/FOP ratios of samples of the same cell line were compared with paired Mann Whitney U test. All statistical analysis was performed in RStudio 0.99.902. Results were considered statistically significant at (corrected) $p < 0.05$.

Results

Quantitative RT-PCR

To determine if there is a relation between Wnt activity and integrin mRNA expression, the expression of the mRNAs encoding a variety of different integrins was measured in cDNA samples derived from 12 canine mammary carcinoma cell lines. Three of them had high ligand-independent Wnt activity, 4 moderate ligand-dependent Wnt activity and 5 absent basal Wnt activity. mRNA expression is depicted as $\Delta\Delta CT$ difference from the mean expression levels (figure 2).

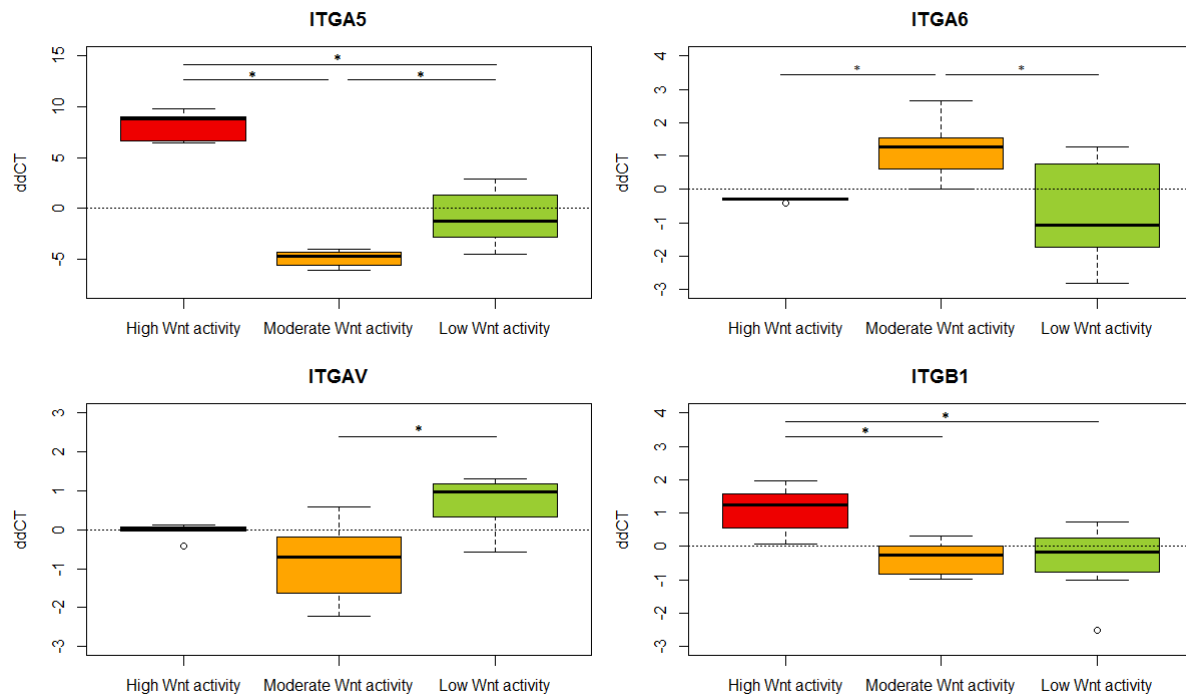


Figure 2 mRNA expression of integrins was not linearly related to Wnt activity in an panel of 12 CMT cell lines. Comparison of $\Delta\Delta CT$ of integrin $\alpha 5$, integrin $\alpha 6$, integrin αv , integrin $\beta 1$, integrin $\beta 3$, integrin $\beta 4$ and integrin $\beta 6$ in canine mammary tumor cell lines with high, moderate and low Wnt activity. Each cell line was sampled once at 2 different passages. Experiment was performed once. $^{\circ}$ represents outliers in data. * indicates $p < 0.05$. Continued on next page.

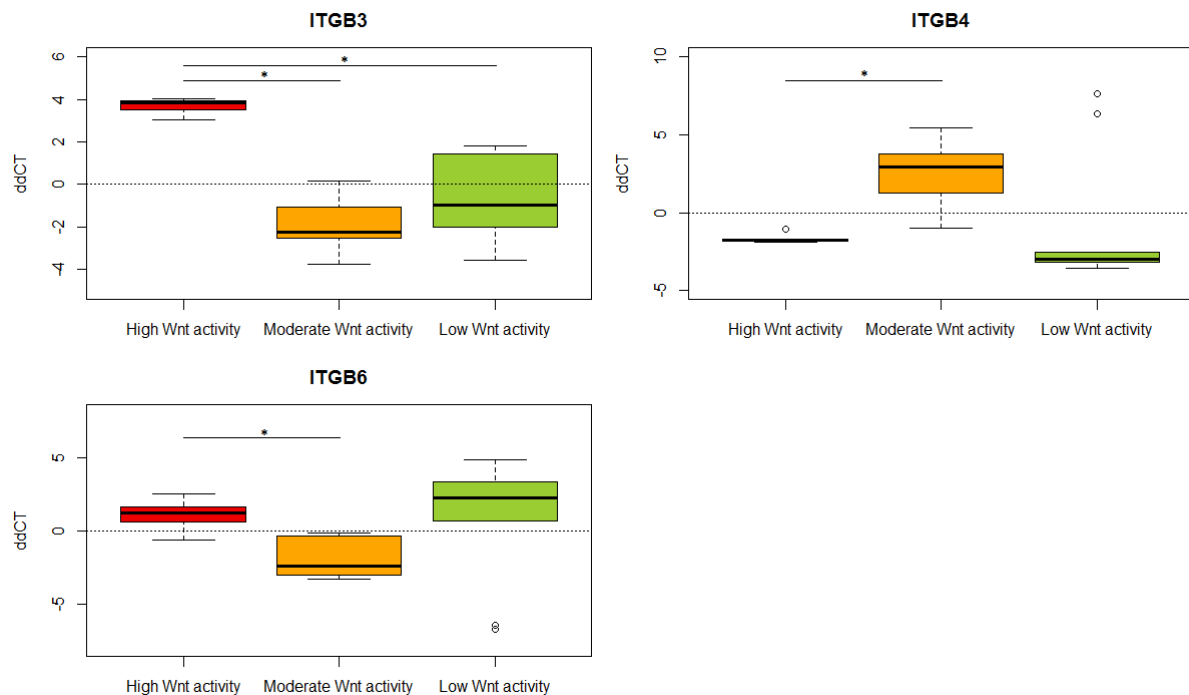


Figure 2 mRNA expression of integrins was not linearly related to Wnt activity in an panel of 12 CMT cell lines. Comparison of $\Delta\Delta CT$ of integrin $\alpha 5$, integrin $\alpha 6$, integrin αv , integrin $\beta 1$, integrin $\beta 3$, integrin $\beta 4$ and integrin $\beta 6$ in canine mammary tumor cell lines with high, moderate and low Wnt activity. Each cell line was sampled once at 2 different passages. Experiment was performed once. $^{\circ}$ represents outliers in data. * indicates $p < 0.05$.

None of the integrins tested showed an expression linearly related to the level of Wnt activity, i.e. with the moderate Wnt active lines between high- and absent basal Wnt activity. With respect to the cell lines with greatly enhanced basal Wnt activity, however, significant reduced expression was found for *ITGA5* (CD49e; $p < 0.002$ compared to moderate Wnt active lines, $p < 0.001$ compared to absent Wnt activity lines) with a 208 fold decreased expression, *ITGB1* (CD29; $p < 0.004$ compared to moderate Wnt active lines, $p < 0.009$ compared to absent Wnt activity lines) with a 1.9 fold decrease; and *ITGB3* (CD61; $p < 0.002$ compared to moderate Wnt active lines, $p < 0.008$ compared to absent Wnt activity lines) with a 12.7 fold decreased expression compared to the mean of all measurements. *ITGA6* (CD49f) expression in cell lines with enhanced basal Wnt activity was higher compared to in moderate Wnt active lines ($p < 0.002$) with a 1.2 fold increase compared to the mean of all measurements, but did not differ compared to absent Wnt activity lines. Other statistical differences are depicted in figure 2. Individual data per cell line are given in supplement 3.

Flow cytometry analysis of PE anti-CD49f labeled CMT1, CMT-U27, CMT9 and CIPp cell lines

To study the variation of CD49f protein expression in high and low Wnt activity cell lines on the level of the individual cell, five different cell lines were incubated with PE-labeled anti-CD49f and subsequently analyzed by fluorescence activated cell sorting (FACS) using the appropriate isotype controls (figures 3-6). The proportion of CD49f⁺ cells was expected to be higher in the cell lines with highly activated Wnt signaling.

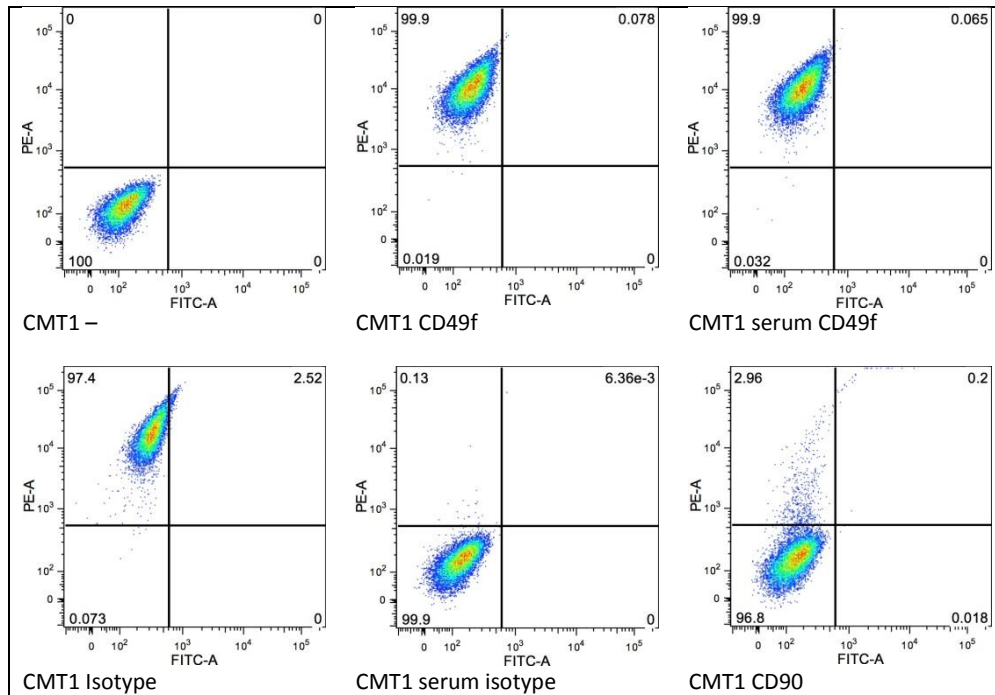


Figure 3 Flow cytometry results of CMT1 cell line unlabeled, PE anti-CD49f labeled, PE anti-CD49f labeled with normal rat serum blocking step, PE rat isotype, PE rat isotype with normal rat serum blocking step and PE anti-CD90. CD49f⁺ and CD49f⁻ gates were drawn based on unlabeled sample. Results from 1 experiment are shown.

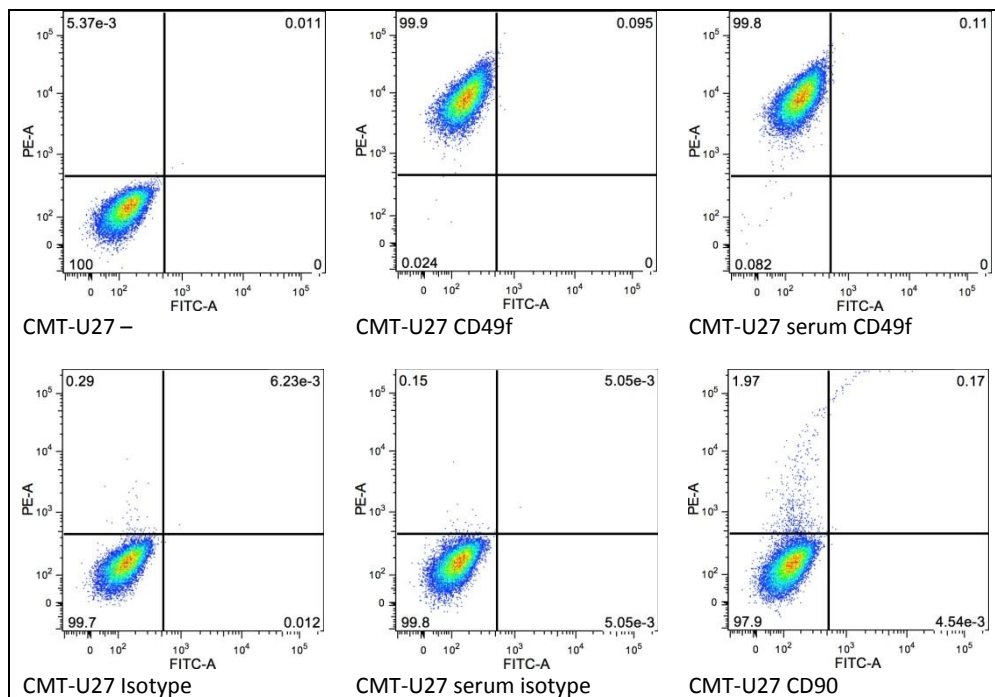


Figure 4 Flow cytometry results of CMT-U27 cell line unlabeled, PE anti-CD49f labeled, PE anti-CD49f labeled with normal rat serum blocking step, PE rat isotype, PE rat isotype with normal rat serum blocking step and PE anti-CD90. CD49f⁺ and CD49f⁻ gates were drawn based on unlabeled sample. Results from 1 experiment are shown.

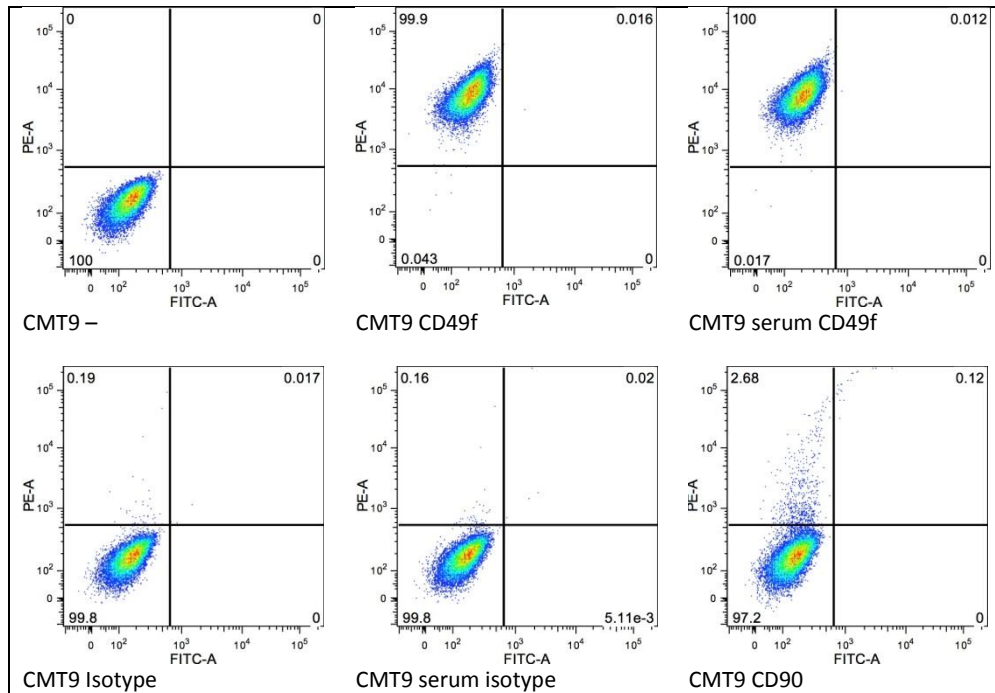


Figure 5 Flow cytometry results of CMT9 cell line unlabeled, PE anti-CD49f labeled, PE anti-CD49f labeled with normal rat serum blocking step, PE rat isotype, PE rat isotype with normal rat serum blocking step and PE anti-CD90. CD49f⁺ and CD49f⁻ gates were drawn based on unlabeled sample. Results from 1 experiment are shown.

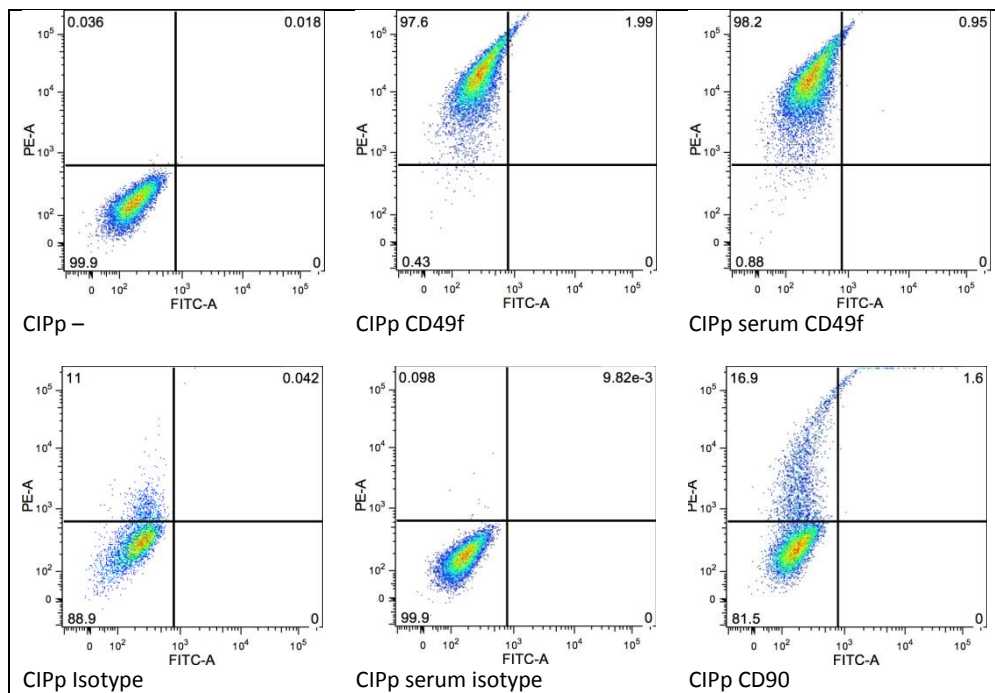


Figure 6 Flow cytometry results of CIPp cell line unlabeled, PE anti-CD49f labeled, PE anti-CD49f labeled with normal rat serum blocking step, PE rat isotype, PE rat isotype with normal rat serum blocking step and PE anti-CD90. CD49f⁺ and CD49f⁻ gates were drawn based on unlabeled sample. Results from 1 experiment are shown.

In CMT1, CMT-U27, CMT9 and CIPp cell lines nearly 100% of PE anti-CD49f labeled cells were PE-positive. Blocking aspecific binding of PE anti-CD49f with normal rat serum did not substantially change this (99.9% versus 99.9% PE-positive in CMT1, 99.9% versus 99.8% PE-positive in CMT-U27, 99.9% versus 100% PE-positive in CMT9, 97.6% versus 98.2% PE-positive in CIPp). Samples of CIPm cell line were of poor quality, but data from the flow cytometry experiment to sort cells into CD49f^{high} and CD49f^{low} populations (below) show equivalent results to the other cell lines (data in supplement 4). In CMT1 cell line 99.9% of PE rat isotype labeled cells were PE-positive. In CIPp cell line, this was 11%. Blocking aspecific binding of PE rat isotype with rat serum lowered the percentage of PE-positive cells to 0.13% in CMT1 and 0.098% in CIPp. CMT-U27 and CMT9 cells labeled with PE rat isotype did not show substantial positive cell populations (0.19% and 0.29% respectively). A PE anti-

CD90 labeled sample was included for each cell line as a control for the labeling procedure, seeing as our group has previous experience using this antibody in flow cytometry analysis of these cell lines. The percentages of PE positive PE anti-CD90 labeled cells reported here are equivalent to previous results (unpublished data).

Comparison of Wnt activity in relation to level of CD49f expression

As nearly 100% of CMT1, CMT-U27, CMT9 and CIPp cell lines were PE-CD49f positive, comparison of Wnt activity between integrin $\alpha 6$ positive and negative cells was not possible using this method. As an alternative Wnt-activity of CD49f^{high} and CD49f^{low} cells from CMT-U27 and CIPm cell lines was compared to see if the level of CD49f expression is related to the level of Wnt activity. TCF/LEF reporter assay was used to compare Wnt activity of integrin $\alpha 6$ ^{high} and integrin $\alpha 6$ ^{low} cells from CMT-U27 and CIPm cell lines sorted by flow cytometry. Wnt activity was expected to be higher in integrin $\alpha 6$ ^{high} cells.

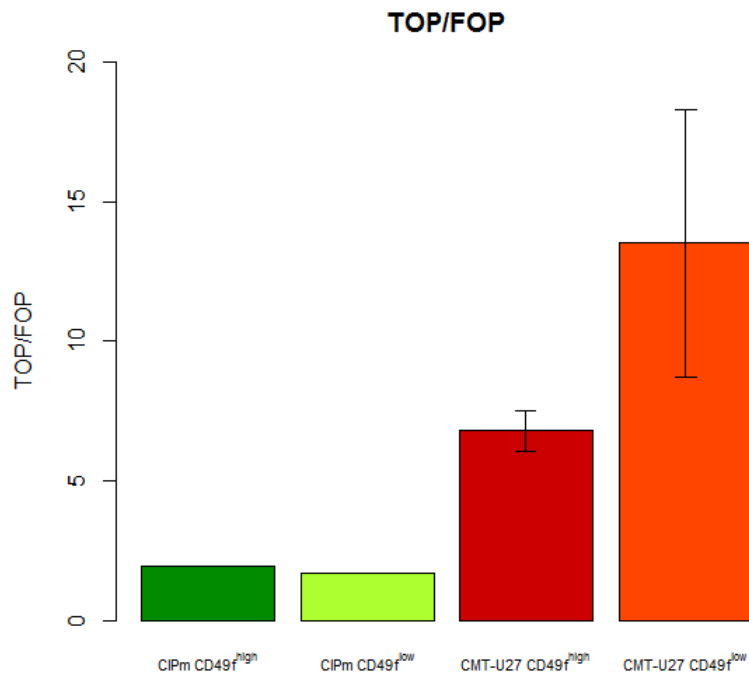


Figure 7 TOP/FOP ratios of CD49f^{high} and CD49f^{low} cells from CIPm and CMT-U27 cell lines. Cells were first transfected with TOP or FOP plasmid and Renilla plasmid, labeled with PE anti-CD49f and sorted by flow cytometry into CD49f^{high} and CD49f^{low} populations. Subsequently TCF/LEF reporter assay was performed and TOP/FOP ratios were calculated. For CIPm samples, TCF/LEF reporter assay was performed with 2 technical replicates. For CMT-U27 samples, TCF/LEF reporter assay was performed with 3 technical replicates. Experiment was performed once. Error bars represent standard deviation (SD).

Mean TOP/FOP ratios of CIPm CD49f^{high} and CD49f^{low} samples were 1.977 and 1.727 respectively. Mean TOP/FOP ratios of CMT-U27 CD49f^{high} and CD49f^{low} were 6.800 ± 0.714 and 13.524 ± 4.791 respectively and did not test significantly different ($p = 0.25$).

Extracellular matrix culture

Although the high basal Wnt active cell lines had considerable lower mRNA expression of various integrins they were still positive for CD49f in the FACS analysis. CD49f could therefore be a possible mediator of enhanced Wnt activity after activation by extracellular matrix proteins. We decided to analyze the effect of culturing cells on uncoated control plastic with the culture on a variety of extracellular matrices to determine if activated integrins enhance Wnt activity.

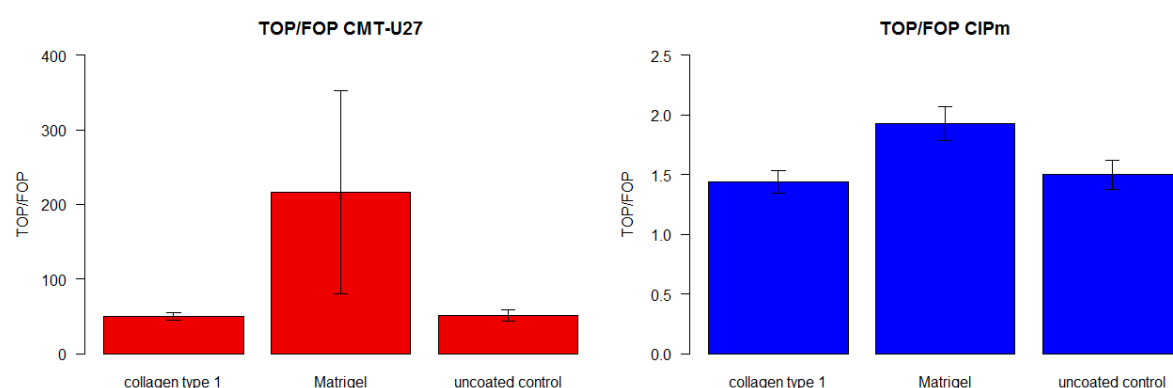


Figure 8 Effect of Matrigel and collagen type 1 on Wnt activity in CMT-U27 and CIPm cell lines. Mean TOP/FOP ratios of CMT-U27 and CIPm cultured on collagen type 1-coated, Matrigel-coated and uncoated plates are shown. 3 replicates of each sample were included. Experiment was performed once. Error bars represent SD.

Mean TOP/FOP ratio of CMT-U27 cultured on a Matrigel-coated plate increased from 52 in uncoated conditions to 216 fold. However the Matrigel data showed a large variation with a SD 136, therefore the difference in the mean TOP/FOP ratio of CMT-U27 Matrigel and CMT-U27 uncoated control was not statistically significant. In CIPm the mean TOP/FOP ratio of Matrigel culture was 1.9 compared to 1.5 in control. This difference in mean was not statistically significant. Culture on collagen type 1 did not significantly affect TOP/FOP ratio compared to control in both CMT-U27 and CIPm.

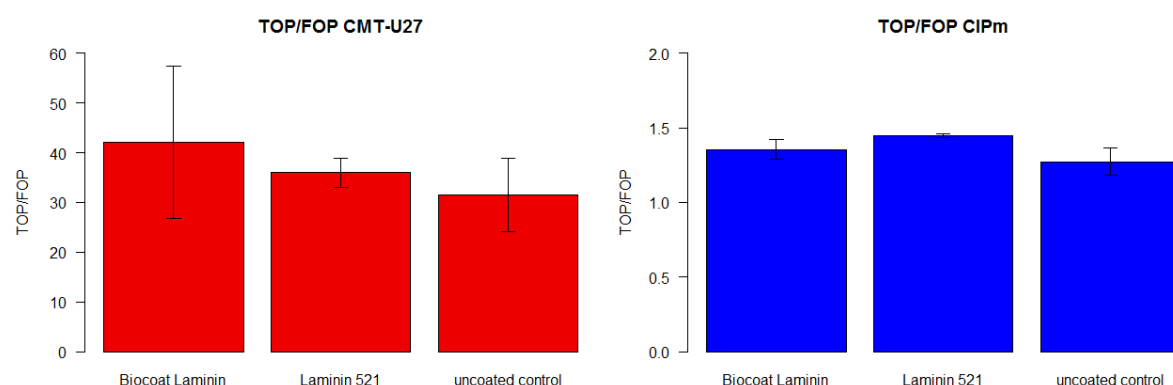


Figure 9 Effect of laminins on Wnt activity in CMT-U27 and CIPm cell lines. Mean TOP/FOP ratios of CMT-U27 and CIPm cell lines cultured on Biocoat Laminin-coated, Laminin 521-coated and uncoated plates are shown. 3 replicates of each sample were included. Experiment was performed once. Error bars represent SD.

Neither culture on Biocoat Laminin or Laminin 521 had a significant effect on mean TOP/FOP ratio of CMT-U27 and CIPm compared to uncoated controls.

Discussion

None of the integrins tested showed an expression linearly related to Wnt activity in a panel of 12 canine mammary tumor cell lines. Although both integrins and the Wnt pathway have been implicated as functional contributors to cancer progression and cancer stemness, the qPCR results of this study do not indicate that integrin mRNA expression is directly regulated by the Wnt pathway, or vice versa. Additionally, expression varied greatly within groups for some integrins, with both samples with positive and negative $\Delta\Delta CT$ values present within a group. This lack of uniformity within groups further indicates the presence of a more complex regulation of integrin expression than simple direct regulation by the Wnt pathway. As we were mainly interested in the three CMT cell lines with high Wnt activity, qPCR results of the high Wnt activity group will be discussed in detail.

Expression of integrin $\alpha 5$ was significantly lower in the high Wnt activity group compared to both the low and moderate Wnt activity groups. The contribution of integrin $\alpha 5$ to breast cancer is somewhat controversial. A study of 3 mouse mammary carcinoma cell lines found integrin $\alpha 5$ expression to be highest in the cell line with the lowest metastatic potential. Overexpression of integrin $\alpha 5$ inhibited cell proliferation, migration and invasion (68). However, a study using 2 steroid receptor co-activator-1 expressing mouse mammary carcinoma cell lines found that *ITGA5* silencing reduces cell migration. In human breast cancer cell line MDA-MB-231, cells with high cell surface integrin $\alpha 5$ expression had enhanced cell invasion (69). Furthermore, a study of microarray data of 295 patients found a significant association between high integrin $\alpha 5$ expression and reduced survival (70). They found a relationship between integrin $\alpha 5$ expression, malignancy and apoptotic resistance in mammary epithelial cells cultured in 3D (70). Additionally, the study measured integrin $\alpha 5\beta 1$ expression in several breast cancer cell lines. Interestingly, high integrin $\alpha 5\beta 1$ expression was present in highly aggressive breast cancer cell lines with a basal molecular phenotype, but not in highly aggressive breast cancer cell lines with a luminal molecular phenotype, indicating that perhaps the role of integrin $\alpha 5$ in breast cancer is dependent on the molecular subtype of the tumor (70). If this is the case, it would indicate that the 3 CMT cell lines with high Wnt activity are of the luminal molecular subtype.

The $\alpha v\beta 3$ and $\alpha v\beta 6$ heterodimers have been implicated to contribute to cancer progression. Expression of integrin αv in the high Wnt activity group was not significantly different from moderate and low Wnt activity groups, a finding that does not support the hypothesis that integrin αv is a specific marker for cells with high Wnt activity. Integrin $\beta 3$ expression was significantly lower in the high Wnt activity group compared to both the moderate and low Wnt activity groups. However, as integrin $\beta 3$ may also dimerize with integrin $\alpha 1b$ and integrin αv with integrins $\beta 1$, $\beta 5$, $\beta 6$, $\beta 6$, conclusions on the expression of integrin $\alpha v\beta 3$ cannot be drawn (42). Integrin $\beta 6$ exclusively dimerizes with integrin αv , therefore its expression may give some indication of $\alpha v\beta 6$ dimer expression (42). Integrin $\alpha v\beta 6$ has been implicated in epithelial-mesenchymal transition-like changes in breast cancer cells (71). Expression of integrin $\beta 6$ was lower in the high Wnt activity group when compared to the moderate, but not the low Wnt activity group, leaving its relation to Wnt activity unclear.

Interestingly, integrin $\beta 1$ expression was significantly lower in the high Wnt activity group compared to both the moderate and low Wnt activity groups. Integrin $\beta 1$ is thought to be a normal mammary stem cell marker (41,43). Its role in cancer progression is not quite clear: Integrin $\beta 1$ has been implicated in both pro-invasion/pro-metastatic and anti-invasion/anti-metastatic (53-57) and studies using integrin $\beta 1$ expression as a prognostic marker have produced conflicting results (58-60). Integrin $\beta 1$ is able to partner with 12 different integrin α subunits, forming a variety of collagen receptors, laminin receptors and RGD receptors (42), making it tempting to speculate that the role of

integrin $\beta 1$ in breast cancer is dependent on its dimerization partner. Therefore, the implication of low integrin $\beta 1$ expression in the cell lines with high Wnt activity is difficult to assess.

Integrin $\alpha 6$ has been reported to be a CSC marker (47,48,72). However, all 12 CMT cell lines had integrin $\alpha 6$ mRNA expression. Although expression of integrin $\alpha 6$ was significantly higher in the high Wnt activity group, the group expected to be enriched for CSCs, compared to the moderate Wnt activity group, the fold increase compared to the mean of all samples was only 1.2. Moreover, multiple samples in the low Wnt activity group had higher expression (supplement 3). These findings do not appear to support the hypothesis that the two supposed CSC markers, high Wnt activity and integrin $\alpha 6$, exclusively mark the same cells. However, the qPCR results do not exclude the existence of a small subset of integrin $\alpha 6^+$ cells within the high Wnt activity cell lines that is enriched for CSCs, as the cells used for qPCR were not subjected to any selection. If most cells present in a cell line had low expression, this could mask the high expression of a small subset of cells. Integrin $\alpha 6$ has two known heterodimerization partners: integrin $\beta 1$ and integrin $\beta 4$. Knockdown of both integrin $\alpha 6$ and integrin $\beta 1$ in CD24⁺CD29⁺ CSCs isolated from mammary tumors of a *Brca1* mouse model profoundly decreased cell migration (72). Integrin $\beta 4$ forms dimers exclusively with integrin $\alpha 6$ (42). It appears to play a role in HER2-driven mammary tumorigenesis (51). Integrin $\beta 4$ expression has been associated with the basal-like molecular subtype (73). Furthermore, integrin $\alpha 6\beta 4$ has been implicated in a signaling pathway that contributes to cancer stem cell properties in 2 basal-like breast cancer cell lines (74). Integrin $\beta 4$ expression was significantly higher in the high Wnt activity group compared to the moderate, but not the low Wnt activity group. If integrin $\beta 4$ and Wnt activity are related, it is likely not by a direct feedback mechanism.

It should be noted that mRNA expression does not always directly translate to protein expression due to post-translational modifications. As literature indicated integrin $\alpha 6$ to be a promising CSC marker, flow cytometry experiments with PE anti-CD49f were performed. Flow cytometry analysis of PE anti-CD49f labeled cells from CMT1, CMT-U27, CMT9 and CIPp cell lines showed approximately 100% of cells to be PE-positive. In all cell lines, <1% of cells was PE-negative. Aspecific binding was checked with an isotype antibody and corrected by including a blocking step with normal rat serum in the labeling protocol. PE anti-CD90 labeled cells served as a control for the execution of the labeling protocol. PE anti-CD90 results were in line with previous observations. Three theories may explain these results. One, integrin $\alpha 6$ is not a CSC marker in dogs, therefore it cannot be used as a marker to enrich for CSCs. However, in a canine prostate adenocarcinoma cell line, integrin $\alpha 6$ mRNA expression was increased in spheroid-forming cells compared to adherent cells (75). The sphere-forming assay is commonly used to evaluate cancer stemness (8). Furthermore, stem-like cells from a clone of CMT-U229 cell line were integrin $\alpha 6^+$ (76). Two, PE anti-CD49f does not specifically bind to canine integrin $\alpha 6$, but binds to other canine integrins and/or cell surface receptors. According to the manufacturer, the antibody was tested on dogs in development. Additionally, the same clone of anti-CD49f without a PE-label from the same manufacturer has been used in an indirect labeling protocol to characterize stem-like cells from a clone of CMT-U229 isolated by side population analyses (76). Three, integrin $\alpha 6$ is present on all cells, but is highly expressed on CSCs. To test the latter hypothesis, Wnt activity was compared with a TCF/LEF reporter assay between CD49f^{high} and CD49f^{low} cells from CMT-U27 and CIPm cell lines. No significant difference in Wnt activity was found. Although the sample size of this experiment was small (n=3), a relation between high integrin $\alpha 6$ expression and high Wnt activity appears less likely.

Recognizing the integrins' function as cell-ECM receptors, it was tested if culturing CMT-U27 and CIPm cell lines on various ECM substrates affected Wnt activity. Collagen is a substrate for $\alpha 1\beta 1$, $\alpha 2\beta 1$, $\alpha 10\beta 1$ and $\alpha 11\beta 1$ integrins (42). Matrigel was included as it is designed to mimic the basal membrane, which is part of the breast stem cell niche *in vivo*. It is a mixture of laminin, collagen IV, nidogen and proteoglycan. As such, it should provide substrate for integrin dimers that function as collagen receptors, laminin receptors or RGD receptors such as integrins $\alpha v\beta 3$ and $\alpha v\beta 6$ (42). An

additional experiment with 2 types of laminin was performed, as both know integrin $\alpha 6$ dimers (integrins $\alpha 6\beta 1$ and $\alpha 6\beta 4$) are laminin receptors (42), and integrin $\alpha 6$ was the main receptor of interest. No significant effect of any ECM substrate on Wnt activity was found in both CMT-U27 and CIPm, indicating integrin ligand-binding does not regulate Wnt activity in these CMT cell lines.

In conclusion

This study was designed on the premise that the activity of the Wnt pathway is indicative of CSC properties. Follow up experiments were designed to gather results that could either support or reject this premise. As results of the first experiments did not allow the comparison between cells with high Wnt activity and cells with low Wnt activity, the results of this study cannot be used to make claims about the relevance of the Wnt pathway to CSC properties. What can be concluded, is that integrin $\alpha 6$ is not the exclusive markers of a small subset of cells that the preliminary lyoplate experiments made it seem. The anti-CD49f antibody used in the lyoplate experiments is of the same clone and manufacturer as the PE anti-CD49f used in flow cytometry, leaving little more than speculation to explain the lack of correspondence between the lyoplate results and the flow cytometry results. For future research, it would be interesting to test for the presence of other CSC-markers in the CMT cell lines with high Wnt activity.

In contrast to our hypothesis the cell lines with the high basal Wnt activity showed not a direct but rather an inverse relation to the expression of various integrins, especially *ITGA5*, *ITGB1* and *ITGB3*. This may question either the stemness of these cells, or whether the integrins are reliable stem cell markers for these canine mammary carcinoma cell lines. Recent qPCR analyses of the panel of 12 CMT cell lines has shown that CMT1, CMT-U27 and CMT9 cell lines have mRNA expression of other stem cell markers, Aldehyde dehydrogenase 1A1 (*ALDH1A1*) and Leucine-rich-repeat-containing G-protein-coupled receptor 5 (*LGR5*) (supplement 5). ALDH activity is a commonly used CSC marker in research using human or mouse material (77) and has been used to enrich for CSCs in canine mammary carcinoma cell lines (78). LGR5 is a CSC marker in colorectal cancer (79) and an enhancer of Wnt signaling (80). These markers may enrich for CSCs, and combining them with the TCF/LEF assay could help decipher the relationship between high Wnt activity and cancer stemness in CMT cell lines.

Chapter III: Neither integrin adaptor expression levels, nor a mutation in the integrin adaptor P140CAP are clearly associated with high basal Wnt activity in 3 canine mammary tumor cell lines

Summary

The integrin adaptors P130CAS and P140CAP and associated regulatory protein CSK are known to regulate cSRC activity. Seeing as high basal Wnt activity in 3 canine mammary tumor cell lines (CMT cell lines) is known to be dependent on cSRC activity, it was investigated whether changes in integrin adaptor proteins are responsible. qPCR of P130CAS, P140CAP, CSK and a third integrin adaptor family known as the integrin-linked kinase (ILK)-PINCH-PARVIN complex (IPP complex) did not indicate expression levels to be the cause. Exome sequencing data revealed a G → C substitution exclusive to the 3 CMT cell lines with high basal Wnt activity at location 23658581, which according to the NCBI database is located in an exon in 5/8 transcript variants. Exon status of the region surrounding location 23658581 was confirmed by PCR and gel electrophoresis. P140CAP is known to be a negative regulator of cSRC activity; the mutation could be responsible for cSRC-dependent Wnt activity if it caused a loss of function. Conversely, introducing full length wild type P140CAP expression into these cell lines should lower Wnt activity. This was tested by transfecting cells with mouse P140CAP-pcDNA3.1 and TOPFLASH/FOPFLASH + Renilla to allow Wnt activity measurement by TCF/LEF reporter assay. This method, however, produced unreliable results. As an alternative, a Wnt target gene qPCR was developed. *AXIN 2*, a commonly used Wnt target gene, and *MUC1*, a gene of interest of our group, showed responsiveness to Wnt-3A stimulation and CSRC-mediated inhibition. P140CAP-transfected conditions differed neither in *AXIN 2* nor in *MUC1* expression compared to conditions transfected with the empty pcDNA3.1 vector. Metastasis of P140CAP-transfected CMT-U27 dsRed, one of the CMT cell lines with high Wnt activity, did not differ from control pcDNA3.1-transfected CMT-U27 dsRed. It is concluded that neither integrin adaptor expression levels, nor a mutation in the integrin adaptor P140CAP appear to be associated with high basal Wnt activity.

Introduction

Neither integrin expression nor function appeared to be related to Wnt activity in canine mammary tumor cell lines (Chapter II). These unexpected findings prompted us to look downstream in the integrin signaling pathway to investigate whether changes in integrin adaptor proteins could explain the cSRC-dependent basal Wnt activation in some canine mammary carcinoma cell lines. Integrin adaptors are intracellular proteins that assemble in complex molecular signaling hubs (81). They integrate signals, received from both integrin receptors and receptor tyrosine kinases (RTKs) in response to extracellular cues, to recruit adaptor proteins, which in turn activate intracellular cell signaling pathways (81). This enables the cell to respond appropriately to the extracellular cues. Several families of integrin adaptors have been described.

The CAS family has been studied the most. P130 Crk-associated substrate (*P130CAS* also known as *BCAR1*) and neural precursor cell expressed, developmentally down-regulated 9 (*NEDD9*, also known as *HEF1*) are the most widely expressed CAS family members (82,83). P130CAS or NEDD9 is tyrosine phosphorylated by activated integrin receptors and RTKs through focal adhesion kinase (FAK) and cSRC (82). This leads to recruitment of various adaptor proteins that activate cell signaling pathways involved in cell survival, cell transformation, cell invasion and cell migration (82,83). Additionally, in response to transforming growth factor β -signaling, NEDD9 appears to switch cell motility from collective to single cell motility (84). In breast cancer, prognostic studies of human breast cancer,

mouse models and functional studies of human breast cancer cells have indicated P130CAS to contribute to HER2-driven breast cancer (85-87). In ER+ breast cancer, P130CAS expression has been linked to intrinsic tamoxifen resistance and poor prognosis (88-90).

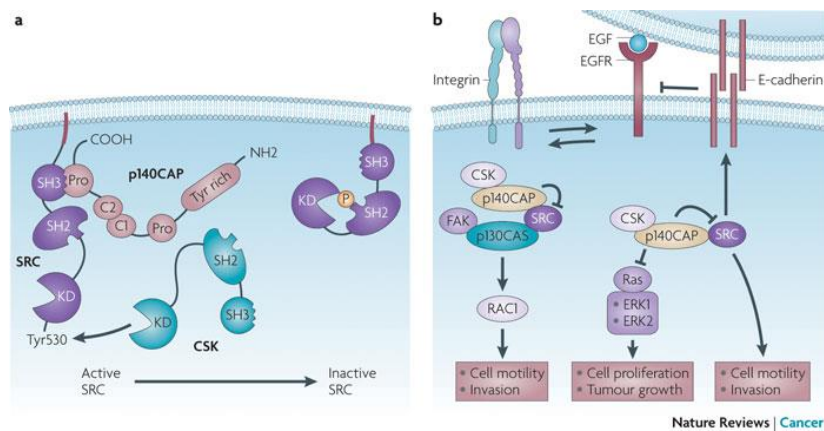
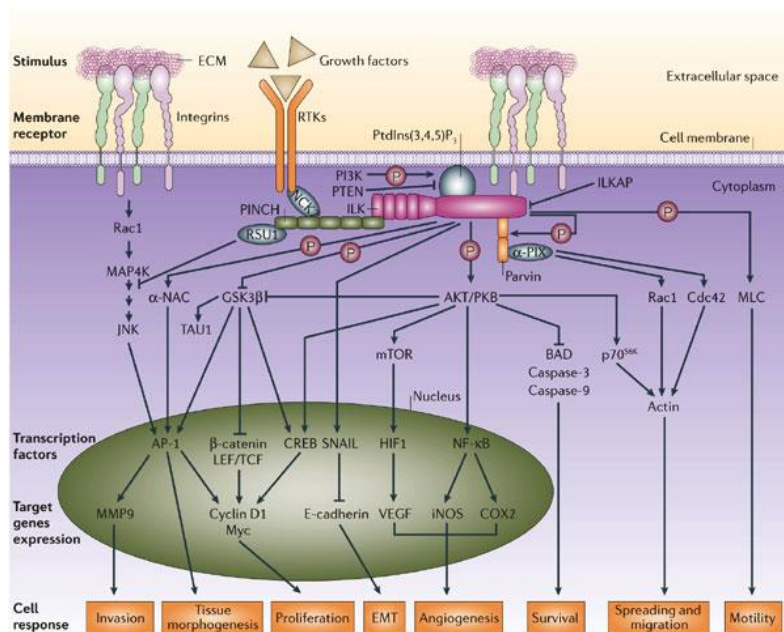


Figure 10 Interactions of P140CAP and P130CAS with SRC signaling. From Cabodi et al, *Nature Reviews Cancer*, 10, 858-870, 2010 (81).

A related family of integrin adaptors is the Cap family (Cas-associated protein), consisting of P140CAP and sickle-tail (SKT) (81). P140CAP (also known as SNIP) was identified in 2004 as a P130CAS-associated protein that is tyrosine-phosphorylated upon integrin adhesion to ECM and in response to EGF signaling (91). It is encoded by the *SRCIN1* gene (SRC kinase signaling inhibitor 1). Protein expression in the mouse was detected in brain, testis and epithelial-rich organs, including the mammary gland (91). A study of P140CAP mRNA expression in breast cancer biopsies and normal breast tissue found no expression in normal breast tissue (92). Furthermore, P140CAP expression was associated with poor prognosis (92). In contrast, a later study of P140CAP protein expression in human breast cancer biopsies found a loss of P140CAP protein expression was correlated with a more aggressive tumor type (93). P140CAP has been shown to be a regulator of cell spreading in MCF7 breast carcinoma cells, as silencing of P140CAP expression increased cell migration, and re-expressing P140CAP reduced migration to control levels (94). Moreover, P140CAP was shown to be a negative regulator of cell spreading in the early stages of cell adhesion (94). Silencing of P140CAP expression led to increased cSRC activation and sustained Rac GTPase activity upon cell adhesion (94). Conversely, overexpression of P140CAP reduced cell spreading and cell migration and inhibited integrin-dependent cSRC-, FAK- and P130CAS/Rac signaling (94). The P140CAP carboxy-terminal proline rich region was shown to directly associate with cSRC SH3 domain (cSRC tyrosine kinase) (94). P140CAP inhibits cSRC activity by binding to and activating Csk (cSRC tyrosine kinase) (94). Activated CSK phosphorylates the negative regulatory tyrosine 527 of cSRC, causing cSRC to fold into an inactive conformation (94). Subcutaneous injection of P140CAP-overexpressing MDA-MB-231 breast cancer cells into SCID mice did not give rise to tumors, unlike injection with control MDA-MB-231 (94). Furthermore, P140CAP-overexpression was shown to strongly reduce anchorage-independent growth, indicating it is a negative regulator of tumorigenic properties (94).

P140CAP co-localizes with E-Cadherin and EGFR at cell-cell contacts. P140CAP stabilizes E-cadherin at the cell membrane through cSRC activity inhibition, promoting cell attachment (93). E-cadherin mediated cell attachment is essential for P140CAP mediated EGFR inactivation. Additionally, P140CAP inhibits EGF-signaling by directly inhibiting Ras activation (93).

A third family of integrin adaptors is the integrin-linked kinase (ILK)-PINCH-PARVIN complex (IPP complex) (81). The IPP complex has both a structural and a functional role: the ILK component binds integrin $\beta 1$ with the actin cytoskeleton and relays integrin signaling, the PINCH component binds indirectly to RTKs and relays RTK signaling, the PARVIN component binds directly or indirectly to the actin cytoskeleton (81,95). ILK's kinase activity appears to depend on the PARVIN variant present in the IPP complex (96,97). This may explain why ILK has been implicated both as a tumor suppressor and as a proto-oncogene (81).



Copyright © 2006 Nature Publishing Group
Nature Reviews | Molecular Cell Biology

Figure 11 The ILK-PINCH-PARVIN complex in relation to integrin and growth factor signaling. From Legate et al, *Nature Reviews Molecular Cell Biology* 7, 20-31, 2006 (132).

The high Wnt activity in CMT1, CMT-U27 and CMT9 cell lines has previously been demonstrated to be dependent on cSRC activity (24). As P140CAP is a negative regulator of cSRC activity, loss of P140CAP function could explain the high Wnt activity in 3 CMT cell lines. To test this hypothesis, mRNA expression of P140CAP and other integrin adaptors was evaluated. Furthermore, exome sequencing data was checked for potentially deleterious mutations in P140CAP. It was attempted to test the effect of P140CAP overexpression on Wnt activity with a TCF/LEF reporter assay. When this technique did not produce reliable data, an alternative approach using Wnt target gene qPCR was developed.

Materials & methods

qPCR of integrin adaptors and CSK

qPCR of integrin adaptors and CSK was performed and analyzed as described in chapter 1 for the qPCR of integrins using the target- and reference gene primers included in table 2. Reference gene rank, stability graph and variance graph are included in supplement 1.

Gene	Product length	Tm (°C)	Forward/Reverse	Sequence 5'→3'
<i>BCAR1</i>	127	66.5	Forward	AGT-ATG-GCC-AAG-AGG-TAT-ATG-AC
			Reverse	GTG-GTG-GTT-AGT-CAA-CGG
<i>NEDD9</i>	168	62	Forward	ACC-TAC-AGG-GTA-AGG-AGG-AG
			Reverse	GGC-TTC-CAC-TTT-GAG-ATG-TC
<i>SRCIN1</i>	136	61	Forward	CCT-TCA-TCA-AGA-AAG-CCG-A
			Reverse	ATC-GTC-CTC-ATC-TTT-GAT-GG
<i>ILK</i>	197	64	Forward	AAA-GCA-GGG-ACT-TCA-ATG-AGG-A
			Reverse	ACT-TCA-CAG-CTT-GGC-TCT-GG
<i>PINCH1</i>	167	63	Forward	TCA-GAT-GCT-CTT-TGC-TCC
			Reverse	CGA-CAT-AGA-TGT-CTC-CCA-G
<i>PINCH2</i>	168	61.5	Forward	TAC-AAC-CAG-CTC-TTT-GGG
			Reverse	ACA-CGG-GCT-TCA-TGT-C
<i>Parvin α</i>	127	61.5	Forward	TCT-GTT-CAT-GCC-AAG-AGC
			Reverse	CCT-TCT-CGT-TTC-TGG-ACC
<i>Parvin β</i>	166	62	Forward	TTG-TCA-AGG-TTC-TCA-TCG-AC
			Reverse	GCC-TAT-CTT-AGA-CTG-TGT-CAC
<i>CSK</i>	134	61	Forward	CAT-TGG-GAA-GGG-GGA-GTT-TGG-AGA
			Reverse	TGC-CGA-AGT-TGC-GTC-ATC-ACA-GAG
<i>HMBS</i>	112	61	Forward	TCA-CCA-TCG-GAG-CCA-TCT
			Reverse	GTT-CCC-ACC-ACG-CTC-TTC-T
<i>RPS5</i>	141	62.5	Forward	TCA-CTG-GTG-AGA-ACC-CCC-T
			Reverse	CCT-GAT-TCA-CAC-GGC-GTA-G
<i>RPS19</i>	95	62	Forward	CCT-TCC-TCA-AAA-AGT-CTG-GG
			Reverse	GTT-CTC-ATC-GTA-GGG-AGC-AAG
<i>TBP</i>	56	57	Forward	CTA-TTT-CTT-GGT-GTG-CAT-GAG-G
			Reverse	CCT-CGG-CAT-TCA-GTC-TTT-TC
<i>GAPDH</i>	100	58	Forward	TGT-CCC-CAC-CCC-CAA-TGT-ATC
			Reverse	CTC-CGA-TGC-CTG-CTT-CAC-TAC-CTT

Table 2 Target and reference gene primers for integrin adaptor qPCR.

Exome sequencing of P140CAP in canine mammary tumor cell lines

The complete exome of eight canine mammary cell lines (CMT1, CMT-U27, CMT9, P114, CHMm, CNMm, CIPm and CIPp) was sequenced at Nijmegen University. Data were annotated in comparison to the canine genome (CanFam 3.1) and presented as mutations per cell line (data not shown).

PCR and gel electrophoresis of P140CAP

Canine *SRCIN1* for sequence analysis was amplified from cDNA derived from CMT1, CMT-U27, CMT9 and CMT-U335 cell lines as well as from normal canine pituitary and mammary gland tissue, made using RNeasy mini kit and iScript cDNA synthesis kit according to manufacturer's protocol. Primers were developed to amplify the region 3995-4763 (*SRCIN1* transcript variant 1; XM_014116609.1) surrounding the found mutation. Q5 hot start high-fidelity DNA polymerase (New England BioLabs,

Ipswich, USA) was used with or without a specific enhancer due to the high GC content of the amplicon, forward primer 5'-AGTGGGAGGGGCTGTGATGGT and reversed primer 5'-GAGTTGGGGGCGGGGAAGTGTG. After initial denaturation for 30 sec at 98°C PCR product was generated in 40 cycles of 10 sec denaturation at 98°C, annealing for 30 sec at 65°C, elongation at 72°C for 30 sec and final extension for 10 min at 72°C in a Bio-Rad C1000 Thermal Cycler (Bio-Rad). Product were analyzed on a 0.8% agarose submarine gel (Promega) containing EtBr (Promega) for detection. A DNA ladder of 100 bp between 100 and 1000 bp was used as marker (Promega).

Transfection with P140CAP-pcDNA3.1 for protein isolation and western blotting

CMT1, CMT-U27 and CMT9 were seeded at a density of 600.000 cells/well in Primaria 6-wells plates in DMEM:F12 + 10% FCS + 1% P/S. CIPm and CIPp were seeded at a density of 330.000 cells/well. For each cell line, the following conditions were included: untransfected control and P140CAP transfected. Full length murine P140CAP cDNA cloned into pcDNA3.1 (gift from dr. Paola Defilippi) was used for P140CAP transfection. Transfection was performed using optimized transfection conditions mentioned in TCF/LEF reporter assay method, scaled up to 6-well format. Cells were washed in HBSS and 1.2 ml DMEM:F12 was added to each well. For each well, 10 µl Lipofectamine 2000 was combined with 150 µl DMEM:F12 and incubated for 5 minutes at RT. It was subsequently added to 2 µg DNA in 150 µl DMEM:F12. The combined Lipofectamine 2000 + DNA mixture was incubated for 20 minutes at RT and added to each well. Protein was isolated at 24h, 48h and 72h. First, medium was removed, cells were washed using HBSS and placed on ice. To each well, 250 µl RIPA buffer + 0.03% Aprotinin + 0.01% PMSF + 0.01% NaVO₄ (all Sigma-Aldrich) was added, cells were scraped with cell scrapers (Greiner Bio-one) and transferred to 1.5 ml tubes on ice. Samples were rotated at 4 °C for 30 minutes and subsequently centrifuged at 18.000 rpm at 4 °C for 30 minutes. Supernatant was frozen at -20 °C. Protein concentration of supernatant was measured using DC protein assay (Bio-Rad) according to manufacturer's protocol. Each sample was diluted to 2µg/µl in sample buffer (0.125 M Tris-HCL ph 6.8, 2.5% SDS, 0.0075% bromophenolblue, 35% glycerol (all Sigma-Aldrich)). 10 µg protein per sample was used in electrophoresis with 7.5 % SDS-PAGE gel and Precision Plus Protein WesternC blotting standard (both Bio-Rad) and blotted for 1h on a nitrocellulose membrane (Bio-Rad). Membrane was blocked for 60 minutes in TBS + 0.1% Tween (TBST) + 4% Blocking (ECL, Amersham, GE Healthcare, Eindhoven, The Netherlands). Primary antibody used was monoclonal mouse anti-human P140CAP (kind gift from dr. Paola Defilippi), which also cross reacts with mouse and zebrafish P140CAP (personal communication with dr. Paola Defilippi), 0.5 µg/µl diluted 1:500 in TBST + 4% BSA. This was incubated overnight at 4 °C. Membrane was subsequently washed 3 times for 5 minutes in TBST and incubated for 60 minutes with the secondary antibody: goat anti-rabbit horse radish peroxidase (HRP) conjugated (HAF008; R&D Systems, Abingdon, UK) diluted 1:20.000 in TBST + 4% BSA. Membrane was washed 3 times for 5 minutes in TBST and HRP- signal was visualized using Advance TM_Enhanced chemiluminescence (ECL) in a GelDoc 2000 (Bio-Rad). Protein isolation was performed by the author, Western blotting was performed by dr. Ir. J.A. Mol.

Co-transfection with P140CAP-pcDNA3.1, TOP or FOP and Renilla plasmids and TCF/LEF reporter assay

In 3 preliminary experiments, CMT-U27 and CIPm were transiently transfected in using the method for 24 wells plates described in chapter 1. To assess the effect of P140CAP on Wnt activity, P140CAP cDNA-pcDNA3.1 vector was co-transfected with TOPFLASH- or FOPFLASH- pGL4 vector and Renilla. Other conditions included TOP/FOP transfected as a control, pcDNA3.1 + TOP/FOP transfected as a control for co-transfection effects and pGL4 + P140CAP (experiment 180316) or pGL3 + P140CAP (experiment 010416) as a control for background luciferase activity of TOP/FOP pGL4 vector. Briefly, 100.000 cells/well for CMT-U27 and 70.000 cells/well for CIPm were seeded in DMEM:F12 + 10% FCS + 1% P/S and allowed to adhere for 24h. After 24h, medium was replaced with DMEM:F12. In 3 preliminary experiments, each well was transfected by combining 3 µl Lipofectamine 2000 in 50 µl

DMEM:F12 with 0.8 µg total DNA + 0.5 ng Renilla in 50 µl DMEM:F12 and adding this to the well. In the TOP or FOP transfected conditions, 0.8 µg TOP or FOP pGL4 vector was used. In the P140CAP + TOP/FOP, pcDNA3.1 + TOP/FOP and pGL4/pGL3 + P140CAP transfected conditions, DNA was added in a 1:1 ratio making up 0.8 µg DNA total. In experiment 110316, TOP/FOP and P140CAP + TOP/FOP conditions were included with n = 3. In experiment 180316, conditions included TOP/FOP (n = 2), P140CAP + TOP/FOP (n = 6), pGL4 + P140CAP (n = 4). 1 well was transfected with pcDNA3.1 + TOP, however it must be noted only 0.012 µg pcDNA3.1 was available. In experiment 010416, conditions included TOP/FOP (n = 2), P140CAP + TOP/FOP (n = 4), pcDNA3.1 + TOP/FOP (n = 3), pGL4 + P140CAP (n = 4) and pGL3 + P140CAP (n = 2). In all experiments, transfection was stopped after 5h by adding an equal volume DMEM:F12 + 20% FCS. After 48h, TCF/LEF reporter assay was performed and data was normalized as described in chapter 1. Seeing as preliminary experiments did not provide reliable results, an optimization of transfection conditions was performed. Briefly, CMT-U27 was transfected with varying amounts of pcDNA3.1 (0 µg, 0.4 µg, 0.8 µg and 1.2 µg), varying amounts of Lipofectamine 2000 (2 µl or 3 µl per well) and varying amounts of Renilla (0.5 ng or 1 ng). 2 µl Lipofectamine 2000, 0.4 µg total DNA and 1 ng Renilla was found optimal (results included as supplement 6). A follow up experiment using the optimized transfection conditions was performed with CMT1, CMT-U27, CMT9, CIPm and CIPp cell lines. Additionally, CIPm and CIPp were seeded at 55.000 cells/well instead of 70.000 cells/well to achieve confluency closer to 80%. Ratios of DNA in co-transfection were 1:1, as in the preliminary experiments. For each cell line, the following conditions were included: TOP/FOP (n = 2), TOP/FOP + 20 µM Dasatinib (n = 2), TOP/FOP + 50 ng/ml Wnt3A (TOP n = 2, FOP n = 1), P140CAP + TOP/FOP (n = 4), P140CAP + TOP/FOP + 20 µM Dasatinib (n = 2), P140CAP + TOP/FOP + 50 ng/ml Wnt3A (n = 2), pcDNA3.1 + TOP/FOP (n = 3) and pGL3 + P140CAP (n = 3). Wnt3A (gift from dr. Bas Brinkhof) and Dasatinib (Sellekchem, Munich, Germany) were added 5h after transfection in DMEM:F12 + 20% FCS. Wnt3A was added to stimulate Wnt activity. Dasatinib is a cSRC inhibitor that has been shown to inhibit cSRC activity by the previous HP student. TCF/LEF reporter assay was performed and data was normalized as described in chapter 1.

Culture of P140CAP-pcDNA3.1 transfected and untransfected CMT-U27 and CIPm with and without Wnt pathway stimulation for Wnt target gene qPCR

100.000 cells/well for CMT-U27 and 55.000 cells/well for CIPm were seeded in DMEM:F12 + 10% FCS + 1% P/S and allowed to adhere for 24h. Transfection was performed using the optimized conditions of 2 µl Lipofectamine 2000 and 0.4 µg total DNA. Conditions included untransfected control, untransfected control + 50 ng/ml Wnt3a, P140CAP, P140CAP + 50 ng/ml Wnt3A, pcDNA3.1, pcDNA3.1 + 50 ng/ml Wnt3A, untransfected + 20 µM Dasatinib, untransfected + 20 µM Dasatinib + 50 ng/ml Wnt3A. Material for RNA isolation was gathered at 24h, 48h and 72h for all conditions by removing medium and adding 100 µl RLT (Qiagen) + 0.01% β-mercaptoethanol (Sigma-Aldrich).

RNA isolation, cDNA synthesis and qPCR of Wnt target genes

RNA was isolated from pooled material of 2 wells, making n = 3, using RNeasy mini kit (Qiagen) according to manufacturer's protocol. RNA concentration was measured on a NanoDrop 1000 (NanoDrop, Wilmington, USA). 500 ng RNA per sample was used in 20 µl reactions of iScript cDNA synthesis kit according to manufacturer's protocol. Quantitative PCR of Wnt target genes and 5 reference genes was performed in duplicate using IQ SYBR green master mix in a CFX384 Touch Real-Time PCR System (Bio-Rad) according to manufacturer's protocol. Putative Wnt target genes were selected from literature (98,99) and the Wnt homepage of the Nusse labs (wnt.stanford.edu). Primer sequences of target and reference genes are listed in table 3. Stability of reference genes was tested using Genorm method in Rstudio software (results included in supplement 7). Relative gene expression was calculated using the $\Delta\Delta CT$ -method (66).

Gene	Product length	Tm	Forward/Reverse	Sequence 5'->3'
<i>ALDH1A2</i>	194	66.5	Forward	AGG-AGT-GTT-GAA-CGG-GCT-AAA-AAG
			Reverse	AAC-GGT-GGG-CTG-GAT-GAA-GAA
<i>LBH</i>	175	66.5	Forward	TGG-AGG-CAG-GCG-TGG-GAA-AGG-AC
			Reverse	CAA-AGG-GTG-GGG-GTG-AGG-GGT-AAA
<i>FOSL1</i>	154	66.5	Forward	TCC-TCG-GGG-CCT-GTG-CTT-GAA-C
			Reverse	CCG-CTG-CTG-CTG-CTG-CTC-CTG
<i>AXIN 2</i>	141	60	Forward	GGA-CAA-ATG-CGT-GGA-TAC-CT
			Reverse	TGC-TTG-GAG-ACA-ATG-CTG-TT
<i>HER3</i>	103	70	Forward	TAG-TGG-TGA-AGG-ACA-ACG-GCA-G
			Reverse	GGT-CTT-GGT-CAA-TGT-CTG-GCA-G
<i>LEF1</i>	137	60	Forward	AGA-CAT-CCT-CCA-GCT-CCT-GA
			Reverse	GAT-GGA-TAG-GGT-TGC-CTG-AA
<i>SURVIVIN</i>	121	58	Forward	CCT-GGC-AGC-TCT-ACC-TCA-AG
			Reverse	TCA-GTG-GGA-CAG-TGG-ATG-AA
<i>EGFR</i>	107	53	Forward	CTG-GAG-CAT-TCG-GCA
			Reverse	TGG-CTT-TGG-GAG-ACG
<i>MUC1</i>	173	62	Forward	CTA-TGA-GGA-GGT-TTC-TGC-AG
			Reverse	GAA-CAC-AGT-TGA-GAG-GAG-AG
<i>ID2</i>	114	60.5	Forward	GCT-GAA-TAA-ATG-GTG-TTC-GTG
			Reverse	GTT-GTT-CTC-CTT-GTG-AAA-TGG
<i>HMBS</i>	112	61	Forward	TCA-CCA-TCG-GAG-CCA-TCT
			Reverse	GTT-CCC-ACC-ACG-CTC-TTC-T
<i>RPS5</i>	141	62.5	Forward	TCA-CTG-GTG-AGA-ACC-CCC-T
			Reverse	CCT-GAT-TCA-CAC-GGC-GTA-G
<i>RPS19</i>	95	62	Forward	CCT-TCC-TCA-AAA-AGT-CTG-GG
			Reverse	GTT-CTC-ATC-GTA-GGG-AGC-AAG
<i>TBP</i>	56	57	Forward	CTA-TTT-CTT-GGT-GTG-CAT-GAG-G
			Reverse	CCT-CGG-CAT-TCA-GTC-TTT-TC
<i>GAPDH</i>	100	58	Forward	TGT-CCC-CAC-CCC-CAA-TGT-ATC
			Reverse	CTC-CGA-TGC-CTG-CTT-CAC-TAC-CTT

Table 3 Target and reference gene primers for Wnt target qPCR.

Transfection of CMT-U27 dsRED with P140CAP-pcDNA3.1 and subsequent injection into zebrafish embryos to study metastasis

CMT-U27 dsRed was cultured in selection medium consisting of DMEM:F12 + 10% FCS + 1% P/S + 0.03% Puromycin (Thermo Fisher Scientific). Cells were seeded on Primaria 6-well plates at 500.000 cells/well and transfected using the method described under protein isolation. 24h after transfection, cells were washed with HBSS, detached using TrypLE Express and pooled in HBSS. Cells were counted with 0.40% trypan blue dye on a Bio-Rad TC20 automated cell counter and strained through a 100 µM cell strainer if needed. Cells were centrifuged at 1300 rpm for 3 minutes at RT in a Hettich Zentrifugen Rotofix 32A (Hettich Lab Technology, Tuttlingen, Germany). Supernatant was carefully discarded and pellet was resuspended in HBSS + 2% PVP40 (Sigma-Aldrich) to a concentration of 200 cells/nl. Cells were kept on ice until injection into the yolk sac of 2 dpf (days post fertilization) zebrafish embryos by experienced technician A. Slob. After 5 days, zebrafish embryos were fixed in 100 µl formaldehyde for 24h. After 24h, formaldehyde was replaced with 70% ethanol and zebrafish embryos were scored for tumor formation using fluorescence microscopy on an Olympus IMT-2

(Olympus, Zoeterwoude, the Netherlands). This experiment was performed twice. In the first experiment, zebrafish embryos were scored for tumor formation by both A. Slob and the author. In the second experiment, zebrafish embryos were scored only by the author.

Statistics

Analysis of qPCR results of integrin adaptors and CSK in the panel of CMT cell lines was performed as previously described (Chapter II). Results of Wnt target qPCR were analyzed across all timepoints with unpaired Mann Whitney U test with Bonferroni correction. Frequency data of zebrafish injections were analyzed with Fisher's exact test. All statistical analysis was performed in RStudio 0.99.902. Results were considered significant at (corrected) $p < 0.05$.

Results

qPCR of integrin adaptors

To determine if there is a relation between Wnt activity and integrin adaptor mRNA expression, the expression of the mRNAs encoding integrin adaptors was measured in cDNA samples derived from 12 canine mammary carcinoma cell lines by quantitative RT-PCR. Three of them had high ligand-independent Wnt activity, 4 moderate ligand-dependent Wnt activity and 5 absent basal Wnt activity. Data of individual cell lines is shown as fold change compare to mean expression of all samples. Data grouped according to the level of Wnt activity of the cell lines is shown as $\Delta\Delta CT$ compared to mean expression of all samples (figures 12-17).

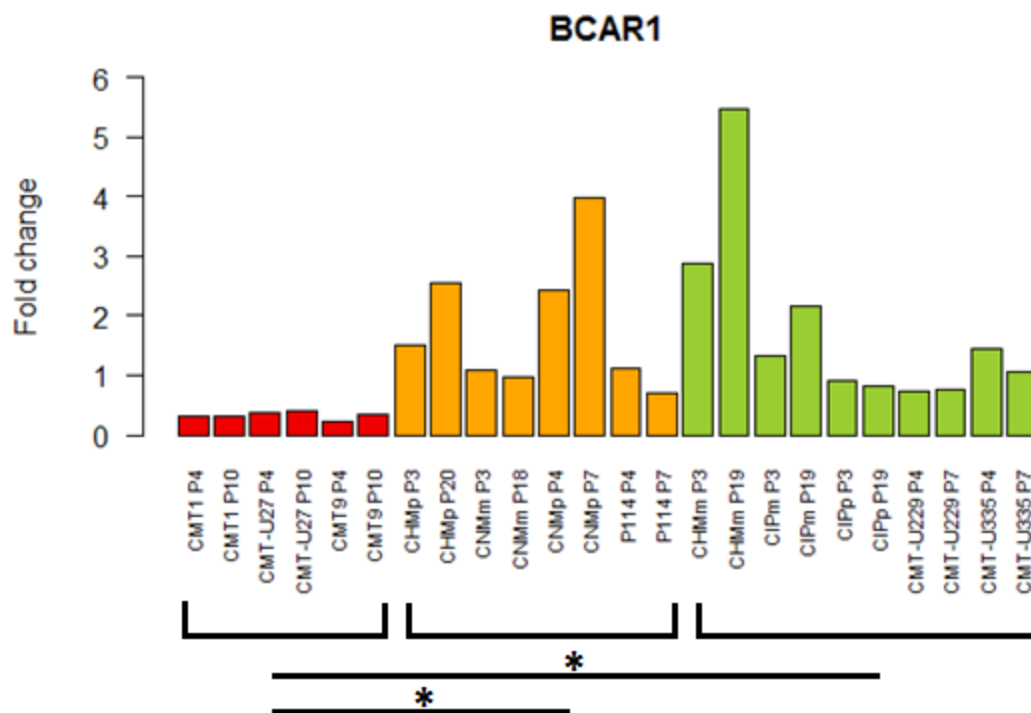


Figure 12 mRNA expression of BCAR1, the gene encoding P130CAS, in a panel of 12 canine mammary tumor cell lines. Each cell line was sampled at 2 passages. Cell lines with high Wnt activity have red bars, cell lines with moderate Wnt activity have orange bars and cell lines with low Wnt activity have green bars. mRNA expression is expressed as fold change compared to mean expression of all samples. Each cell line was sampled once at 2 different passages. Experiment was performed once. * indicates $p < 0.05$.

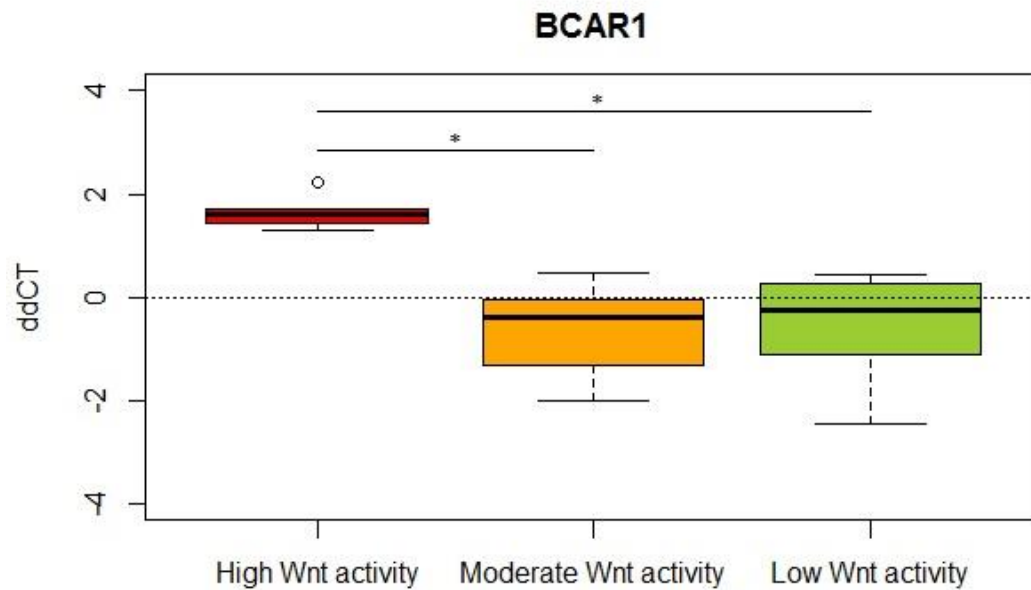


Figure 13 Boxplot of *BCAR1* mRNA expression in 12 canine mammary tumor cell lines sampled at 2 passages, grouped according to the level of Wnt activity of the cell line. mRNA expression is expressed here in $\Delta\Delta CT$ values, as using fold change values would result in skewed plots. Dotted line at a $\Delta\Delta CT$ value of 0 represents mean expression of all cell lines. Negative $\Delta\Delta CT$ values correspond with increased mRNA expression, positive $\Delta\Delta CT$ values correspond with decreased mRNA expression. Each cell line was sampled once at 2 different passages. Experiment was performed once. ^o represents outliers in data. * indicates $p < 0.05$.

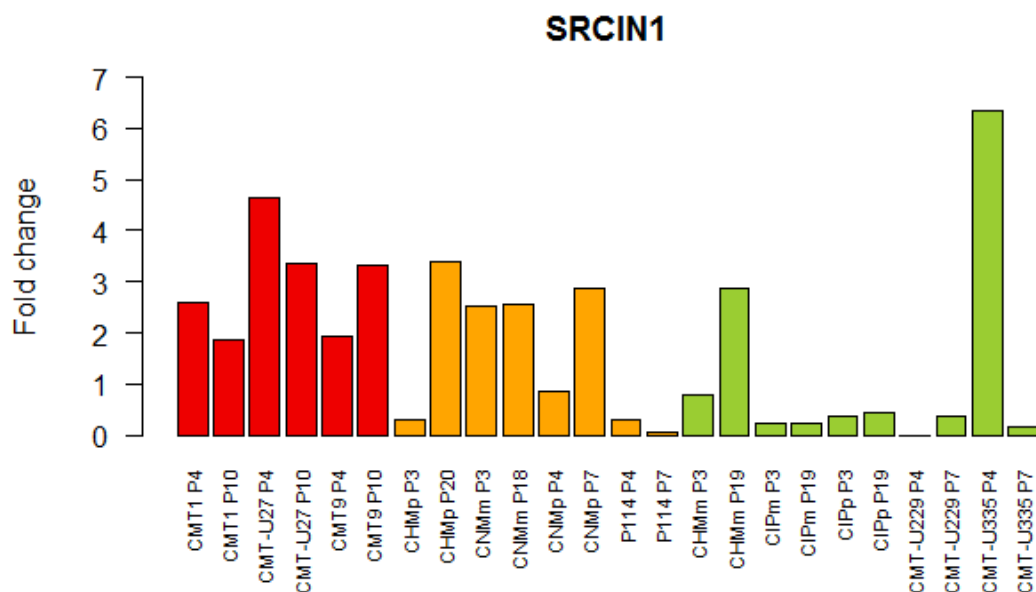


Figure 14 mRNA expression of *SRCIN1*, the gene encoding P140CAP, in a panel of 12 canine mammary tumor cell lines. Refer to figure 12 for details.

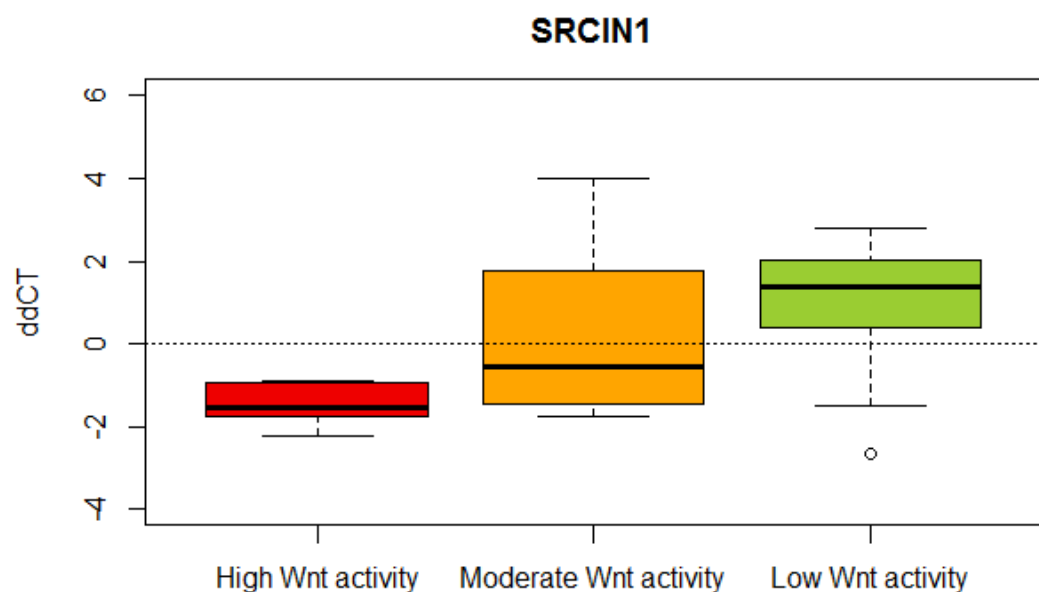


Figure 15 Boxplot of SRCIN1 mRNA expression in 12 canine mammary tumor cell lines sampled at 2 passages, grouped according to the level of Wnt activity of the cell line. For details, refer to figure 13.

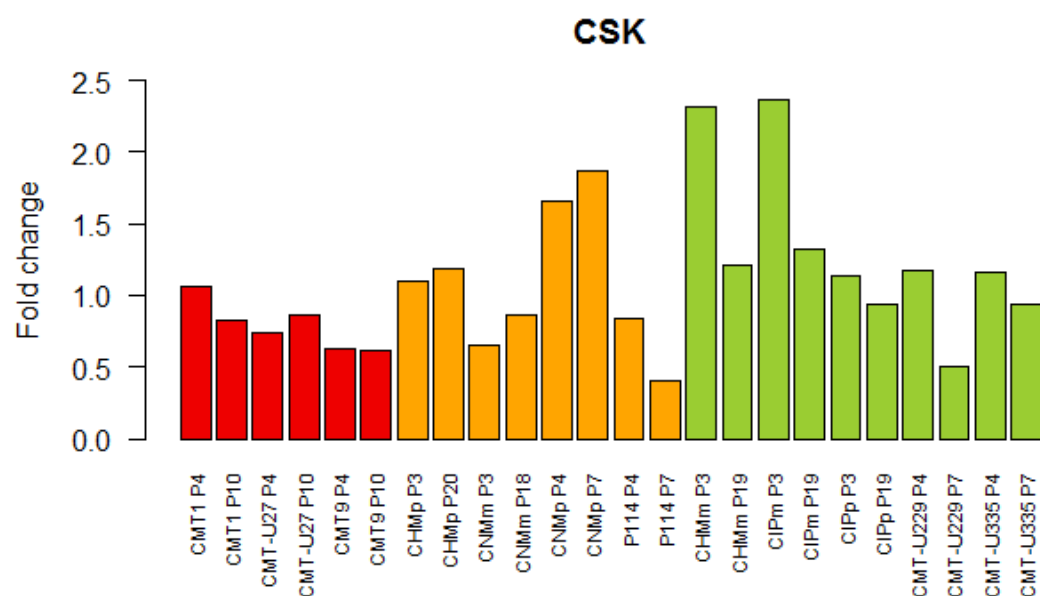


Figure 16 mRNA expression of CSK in a panel of 12 canine mammary tumor cell lines. Each cell line was sampled at 2 passages. For details, refer to figure 12.

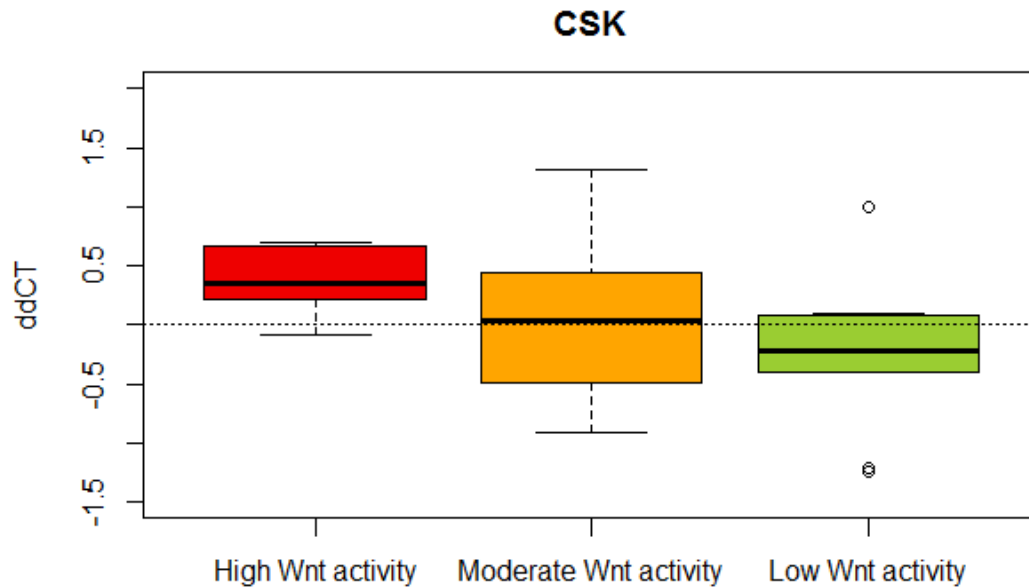


Figure 17 Boxplot of *CSK* mRNA expression in 12 canine mammary tumor cell lines sampled at 2 passages, grouped according to the level of Wnt activity of the cell line. For details, refer to figure 13.

As literature has shown P130CAS, P140CAP and CSK to interact and regulate cSRC activity, data for the corresponding genes will be discussed in detail. mRNA expression of *NEDD9* and the *IPP*-complex is included in supplement 8. Expression of *BCAR1*, the gene encoding P130CAS, was significantly lower in high Wnt activity group (mean $\Delta\Delta\text{CT}$ 1.65 ± 0.32) compared to the moderate Wnt activity group (mean $\Delta\Delta\text{CT}$ -0.62 ± 0.79) and the low Wnt activity group (mean $\Delta\Delta\text{CT}$ -0.49 ± 0.95), with p-values of 0.002 and < 0.001 respectively. *BCAR1* expression in moderate and low Wnt activity groups showed considerable spread and did not differ significantly. *SRCIN1* mRNA expression was not significantly different in any group. However, the high Wnt activity group had consistently upregulated *SRCIN1* expression (mean $\Delta\Delta\text{CT}$ -1.48 ± 0.51), unlike the moderate and low Wnt activity group where samples showed both up- and downregulated expression (mean $\Delta\Delta\text{CT}$ 0.23 ± 1.39 and mean $\Delta\Delta\text{CT}$ 0.79 ± 1.79 respectively). *CSK* expression did not show great variation across all samples. Mean $\Delta\Delta\text{CT}$ in High Wnt activity group was 0.37 ± 0.29 , which was not significantly different compared to the moderate Wnt activity with mean $\Delta\Delta\text{CT}$ 0.05 ± 0.57 . Mean $\Delta\Delta\text{CT}$ of moderate Wnt activity group was not significantly different from low Wnt activity group with mean $\Delta\Delta\text{CT}$ 0.26 ± 0.64 . Comparison of high Wnt activity group with low Wnt activity yielded a p-value just below significance threshold ($p = 0.048$).

Exome sequencing of *SRCIN1* in canine mammary tumor cell lines

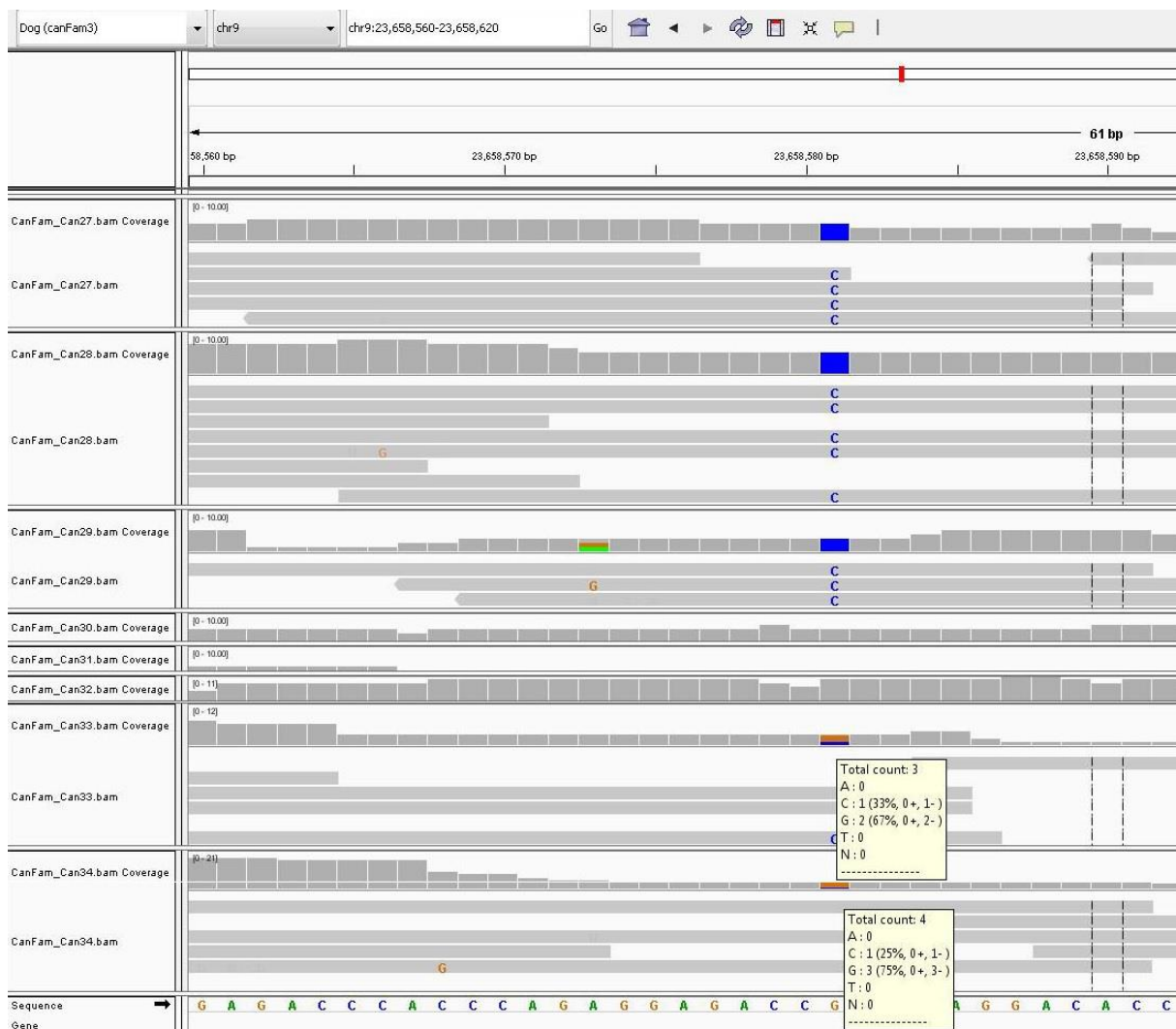


Figure 18 Exome sequencing data of *SRCIN1* in 8 CMT cell line revealed a mutation unique to the 3 CMT cell lines with high Wnt activity. CanFam_27 = CMT1, 28 = CMT-U27, 29 = CMT9, 30 = P114, 31 = CHMm, 32 = CNMm, 33 = CIPm and 34 = CIPp. At location 23658581 there is G -> C substitution exclusive to CMT1, CMT-U27 and CMT9 present in all reads covering this location. In CanFam_33 the G -> C substitution is present in 1 read, but absent from 2 other reads covering the location. In CanFam_34 the G -> C substitution is present in 1 read, but absent from 3 other reads covering the location.

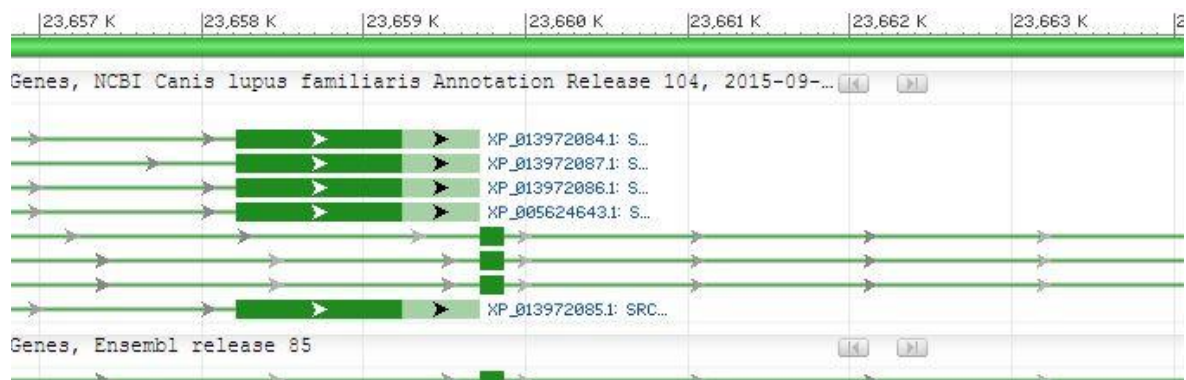


Figure 19 The exon-intron structure of the canine *SRCIN1* gene in NCBI gene. In the NCBI database, location 23658581 is located in an exon in 5/8 transcript variants. In the Ensembl database, location 23658581 is located in an intron.

As qPCR did not provide evidence of a relation between integrin adaptor expression and Wnt activity it was investigated if mutations were present in *SRCIN1*. *SRCIN1* was chosen due to its regulatory activity on cSRC activity. A mutation resulting in a loss of function in *SRCIN1* could therefore be the cause of cSRC-dependent high Wnt activity. The canine *SRCIN1* gene is located on chromosome 9 (23599926-23666314) and has 8 predicted transcript variants according to NCBI nucleotide database. 8 CMT cell lines were previously exome sequenced. This data was evaluated for mutations in *SRCIN1*, exclusive to the 3 CMT cell lines with high Wnt activity, CMT1, CMT-U27 and CMT9. A G → C substitution was found at location 23658581. In CMT1, this substitution was present in 4/4 reads covering the location, in CMT-U27 it was present in 5/5 reads and in CMT9 it was present in 3/3

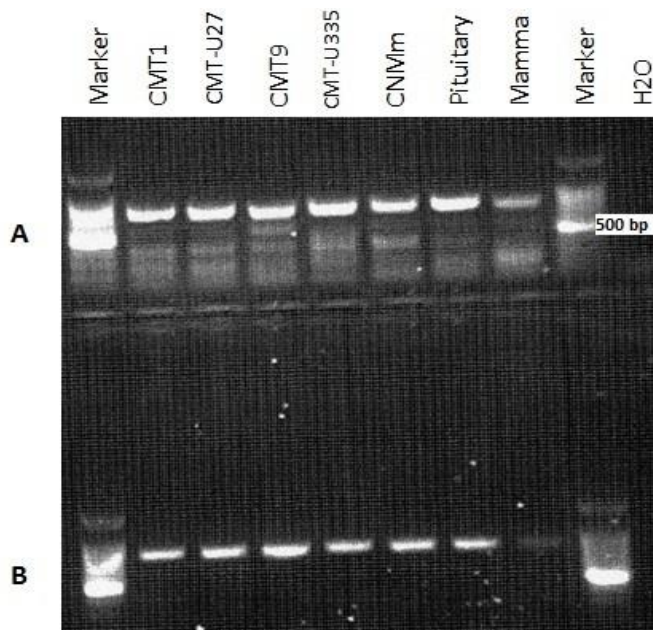


Figure 20 PCR of canine *SRCIN1* cDNA derived from various mammary cell lines, pituitary and mammary gland confirms location 23658581 is located in an exon. Shown is amplification of a product which corresponds to the expected size of 769 bp. Panel A amplification without, and B with enhancer solution (see M&M).

normal pituitary and mammary gland tissue. By using an enhancer solution for GC-rich products, a single product with a size around the expected length of 769 bp was amplified in all samples (figure 20).

reads. A G → C substitution at location 23658581 was also present in CIPm and CIPp, but only in 1/3 reads and 1/4 reads respectively. The G → C substitution would result in an Alanine → Proline amino acid substitution as shown by the translation into protein. The NCBI gene database showed location 23658581 to be located in an exon in 5/8 *SRCIN1* mRNA transcript variants, namely X1 (XM_014116609.1), X2 (XM_014116610.1), X3 (XM_005624586.2), X4 (XM_014116611.1) and X5 (XM_014116612.1). However, in Ensembl database, location 23658581 was located in an intron of the *SRCIN1* gene (figure 19). To confirm location 23658581 is located in an exon, PCR of the region surrounding location 23658581 was performed on cDNA of a panel of 5 CMT cell lines, including the 3 CMT cell lines with high Wnt activity, and on cDNA of

Western blot of P140CAP transfected cells

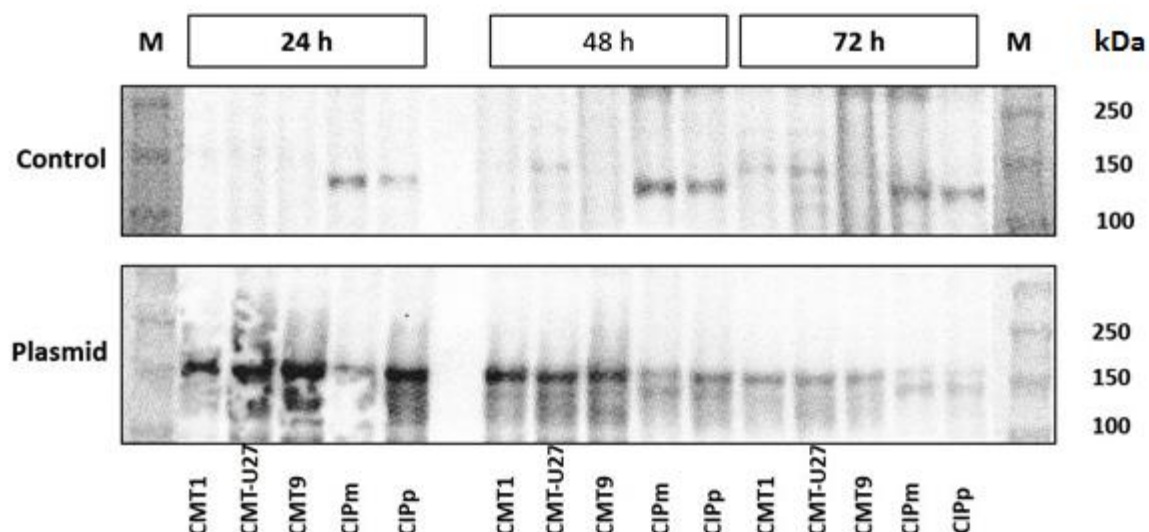


Figure 21 Western blot results of control and P140CAP-transfected CMT1, CMT-U27, CMT9, CIPm and CIPp probed with rabbit anti-human P140CAP antibody confirm transfection with the P140CAP expression plasmid results in P140CAP overexpression. In samples transfected with P140CAP expression plasmid a distinct band is visible around 150 kDa. Experiment was performed once with 1 technical replicate of each sample.

To confirm transfection of CMT cell lines with murine P140CAP expression plasmid results in P140CAP overexpression, protein from P140CAP transfected and control samples of CMT1, CMT-U27, CMT9, CIPm and CIPp was used in a Western blot with rabbit anti-human P140CAP antibody. A distinct band around 150 kDa was exclusively present in the samples transfected with the P140CAP expression plasmid (figure 21). P140CAP has a molecular weight around 140kDa.

The effect of transfection with murine P140CAP expression plasmid on Wnt activity

The mutation in P140CAP is potentially deleterious for the function. As P140CAP is thought to inhibit cSRC activity, loss-of-function would result in enhanced cSRC activity. Restoring wild type P140CAP expression would reverse this and lower cSRC-dependent Wnt activity. We therefore introduced an expression plasmid encoding P140CAP in CMT-U27 and CIPm cell lines to investigate the effect on Wnt activity as measured with TCF/LEF reporter assay. pcDNA3.1 transfected samples served as a control for aspecific transfection effects.

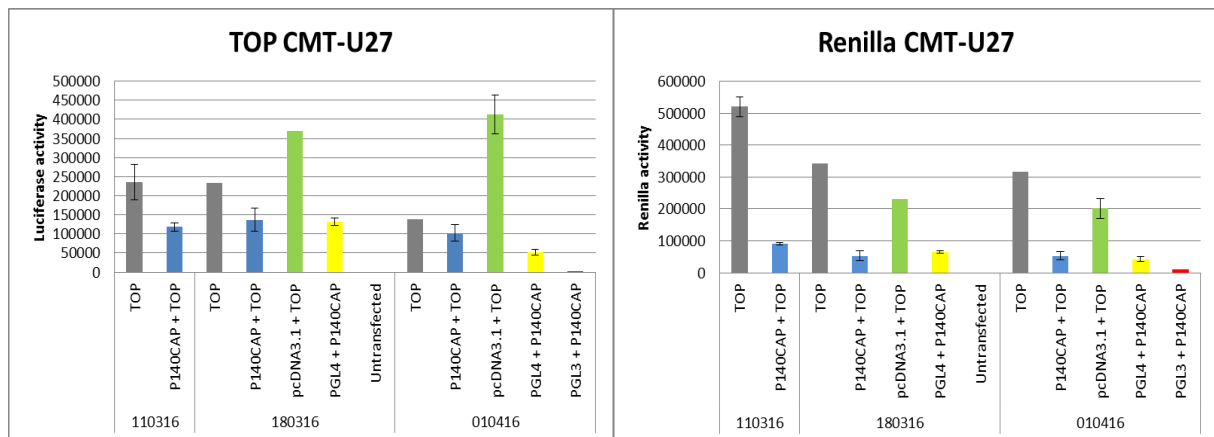


Figure 22 Mean luciferase (left) and Renilla (right) activity of TOPFLASH- and Renilla-transfected CMT-U27 cells show decreased Renilla activity in P140CAP and pcDNA3.1 transfected samples. In addition to control, cells were transfected with the P140CAP expression plasmid. As an additional control empty pcDNA3.1 plasmid was used. In experiment 110316, for all conditions $n = 3$. In experiment 180316, TOP $n = 2$, P140CAP + TOP $n = 6$, pGL4 + P140CAP $n = 4$, untransfected $n = 3$. For pcDNA3.1 + TOP $n = 1$, and only 0.012 μg pcDNA3.1 was added instead of 0.04 μg . In experiment 010416, TOP $n = 2$, P140CAP + TOP $n = 4$, pcDNA3.1 + TOP $n = 3$, PGL4 + P140CAP $n = 4$, PGL3 + P140CAP $n = 2$. Results are presented per individually performed experiment. Error bars represent SD.

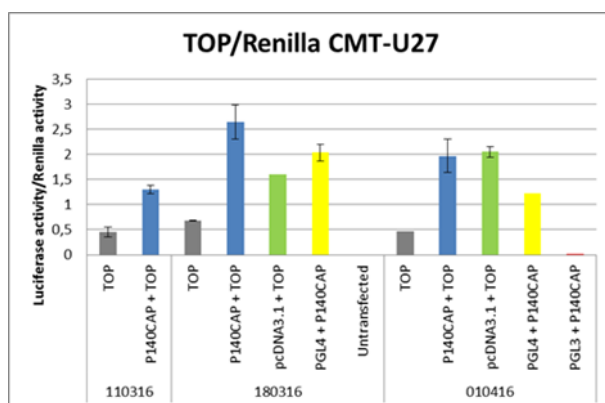


Figure 23 Mean normalized Luciferase activity of TOP-transfected conditions. Results are presented per individually performed experiment. Error bars represent SD.

Co-transfection of the TOPFLASH reporter with the P140CAP expression plasmid appeared to result in lower luciferase activity (figure 22). However, a strong decrease in Renilla activity was also noticed resulting in increased TOPFLASH/Renilla (figure 23). Addition of empty pcDNA3.1 vector showed a less pronounced decrease in Renilla activity.

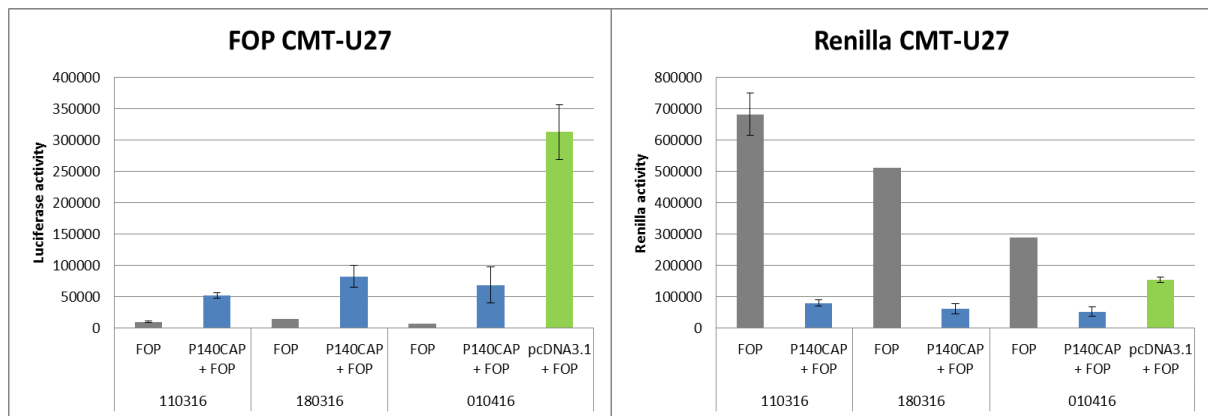


Figure 24 Mean luciferase (left) and Renilla (right) activity of FOPFLASH- and Renilla-transfected CMT-U27 cells show increased luciferase activity and decreased Renilla activity in P140CAP and pcDNA3.1 transfected samples. Results are presented per individually performed experiment. Error bars represent SD. For further details see legend to figure 22.

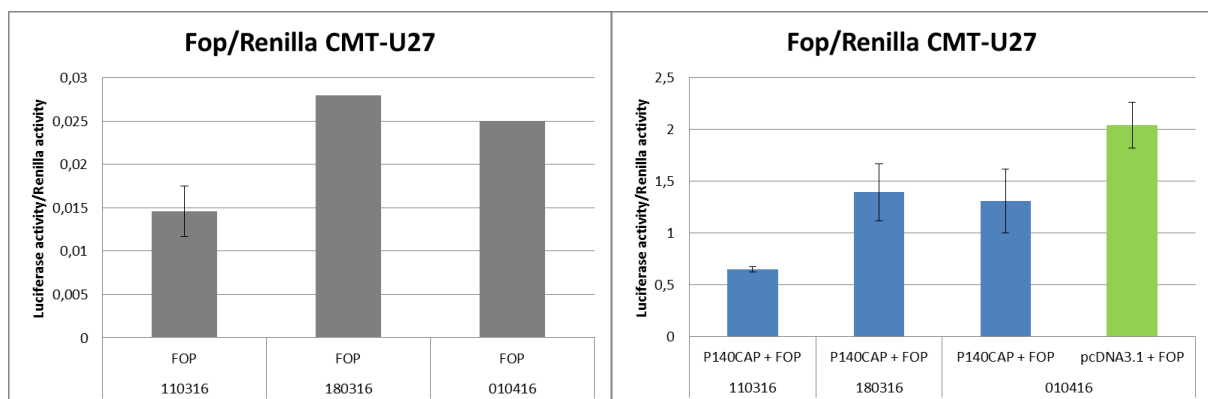


Figure 25 Mean normalized luciferase activity of FOP-transfected conditions from 3 individual preliminary experiments. In experiment 110316, for all conditions n = 3. In experiment 180316, FOP n = 2, P140CAP + FOP n = 6. In experiment 010416, FOP n = 2, P140CAP + FOP n = 4, pcDNA3.1 + FOP n = 3. Results are presented per individually performed experiment. Error bars represent SD.

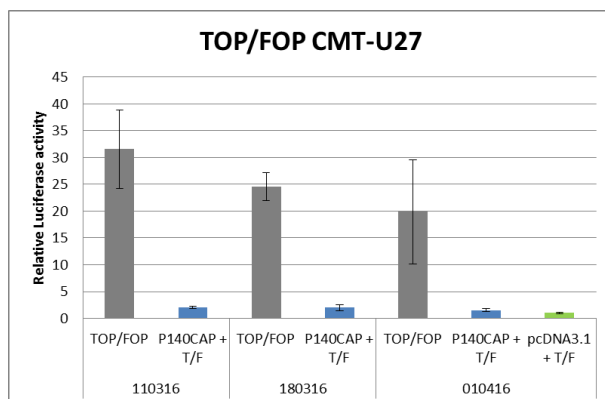


Figure 26 Mean relative luciferase activity of TOP/FOP-transfected, P140CAP + T/F transfected and pcDNA3.1 + T/F transfected conditions from 3 individual experiments. Results are presented per individually performed experiment. Error bars represent SD.

Calculation of relative luciferase activity as TOP/FOP ratios as a measure of Wnt activity showed a strong inhibition after transfection with the P140CAP expression plasmid (figure 26). However, also the empty vector showed identical decreases questioning the validity of these results. Data of CIPm showed similar, though less pronounced results (supplement 9). Therefore an optimization of the

transfection protocol was performed in order to remedy these technical difficulties. Transfection optimization showed transfection with 2 μ l Lipofectamine 2000, 0.4 μ g total DNA and 1 ng Renilla per 80% confluent well of a 24 well plate to be optimal (data included as supplement 6).

A follow up experiment using the optimized transfection conditions was performed on 3 CMT cell lines with high Wnt activity (CMT1, CMT-U27 and CMT9) and 2 CMT cell lines with low Wnt activity (CIPm and CIPp). Conditions included TOP/FOP transfected, P140CAP + TOP/FOP transfected and pcDNA3.1 transfected. Additionally, stimulation of Wnt activity with Wnt3A and inhibition of Wnt activity with Dasatinib, a cSRC inhibitor, was performed on TOP/FOP transfected and P140CAP + TOP/FOP transfected cells from all 5 cell lines. Normalized TOP luciferase activity after transfection with the P140CAP expression plasmid or the empty vector pcDNA3.1 control was higher mainly due to a decreased Renilla activity (figure 27, left). In FOP + P140CAP and FOP + pcDNA3.1 transfected samples, increased FOP luciferase activity was observed in addition to decreased Renilla activity (figure 27, right). FOP luciferase activity of samples transfected with P140CAP + FOP was increased 7-9 fold in CMT cell lines with high Wnt activity and 2 fold in CMT cell lines with low Wnt activity compared to FOP transfected control. Samples transfected with pcDNA3.1 + FOP had a fold increase of 22-23 in cell lines with high Wnt activity and a fold increase of 7 in cell lines with low Wnt activity. Normalizing the data with the Renilla activity increased the fold changes: normalized FOP luciferase activity of P140CAP + FOP and pcDNA3.1 + FOP transfected samples from cell lines with high Wnt activity was increased 20-30 fold compared to normalized luciferase activity of FOP transfected controls. As a result, TOP/FOP ratios of P140CAP and pcDNA3.1 transfected samples were substantially decreased compared to TOP/FOP controls (figure 28). Relative luciferase activity of TOP/FOP control of all cell lines corresponded with earlier reported data (23). In CIPm and CIPp this effect was not as pronounced, however the basal TOP/FOP ratios in these cell lines are already low. These results are in line with observations of the preliminary experiments.

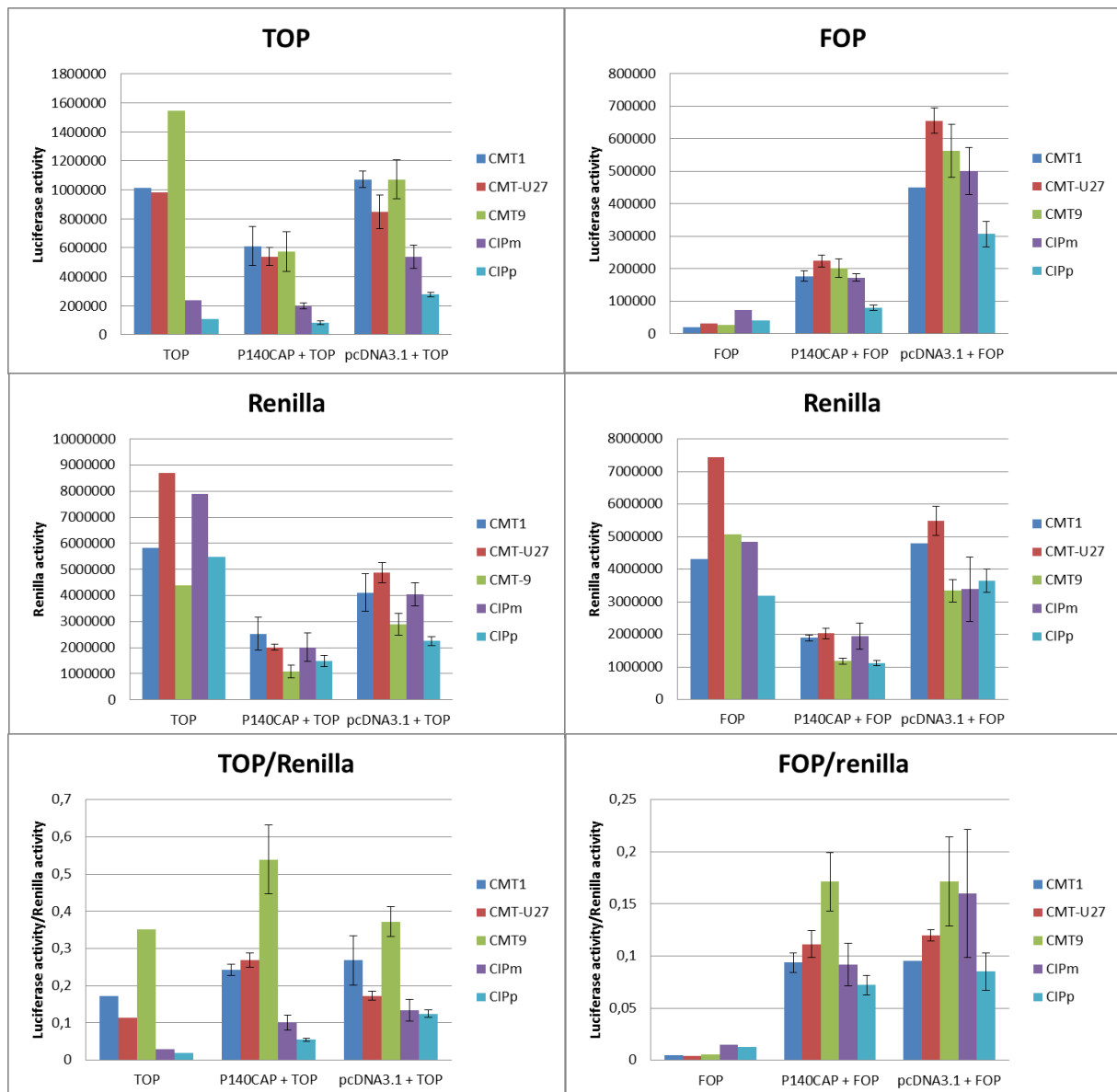


Figure 27 Luciferase activity, Renilla activity and normalized Luciferase activity of TOPFLASH (left) or FOPFLASH (right), in mammary carcinoma cell lines CMT1, CMT-U27, CMT9, CIPm and CIPp co-transfected with a P140CAP expression plasmid or an empty vector show similar results as preliminary experiments. For each cell line, TOP/FOP $n = 2$, P140CAP + TOP/FOP $n = 4$, pcDNA3.1 + TOP/FOP $n = 3$. Data represents replicates from 1 experiment. Error bars represent SD.

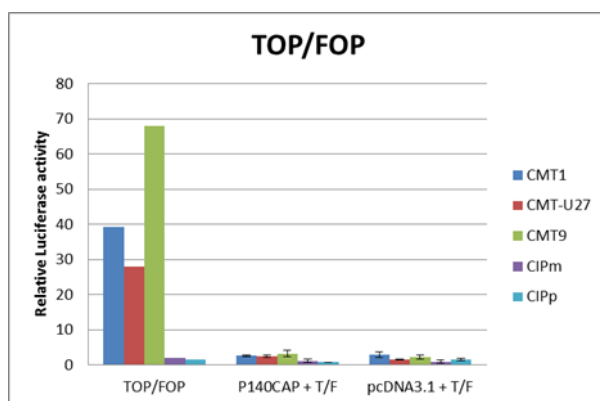


Figure 28 Relative luciferase activity of CMT1, CMT-U27, CMT9, CIPm and CIPp transfected with TOP/FOP-FLASH reporters and the effect of co-transfection with P140CAP or empty pcDNA3.1 vector shows similar results as preliminary experiments. For each cell line, TOP/FOP $n = 2$, P140CAP + TOP/FOP $n = 4$, pcDNA3.1 + TOP/FOP $n = 3$. Data represents replicates from 1 experiment. Error bars represent SD.

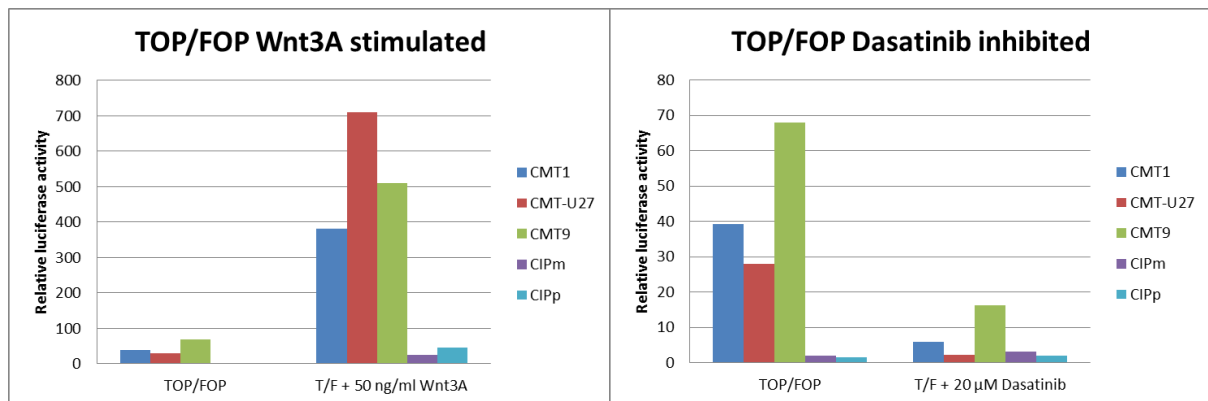


Figure 29 Relative luciferase activity of TOP/FOP without and with 50 ng/ml Wnt3A stimulation (left) or without and with 20 μ M Dasatinib (right) shows luciferase activity in TOP/FOP controls is responsive to Wnt stimulation and inhibition. For all samples, $n = 2$, except for FOP + Wnt3A $n = 1$.

Relative luciferase activity of TOP/FOP controls could be stimulated with Wnt3A, and inhibited with Dasatinib, a cSRC inhibitor, in CMT1, CMT-U27 and CMT9 (figure 29). Attenuation of Wnt activity in these cells lines with a cSRC inhibitor has been previously reported (24).

qPCR of Wnt target genes

Seeing as co-transfection with the expression vector gave unreliable results of the measurement of Wnt activity we had to search for a different way to quantify the Wnt activity. qPCR of putative Wnt target genes *AXIN 2*, *FOSL1*, *LBH*, *ID2* and *SURVIVIN* was performed on CMT-U27 and CIPm control, 20 μ M Dasatinib inhibited, P140CAP transfected and pcDNA3.1 transfected control. Each condition was measured unstimulated and Wnt3A stimulated. Additionally, qPCR of genes of interest *ALDH*, *HER3*, *LEF1*, *EGFR* and *MUC1* was performed to see if expression of these genes is Wnt regulated. First, it was verified if the putative Wnt target genes indeed showed response to Wnt pathway stimulation and inhibition. Expression of Wnt3A stimulated control and Dasatinib inhibited control was normalized to unstimulated control at 24h, 48h and 72h. Data was first examined to see if expression of a putative Wnt target gene increased upon Wnt3A stimulation and decreased upon Dasatinib inhibition, or vice versa. Furthermore, the fold changes should be larger in CMT-U27 than in CIPm to correspond with the data from the TCF/LEF reporter assay. *AXIN 2* and *MUC1* appeared to be Wnt target genes by these criteria. *AXIN 2* expression increased upon Wnt3A stimulation in both CMT-U27 and CIPm (figure 30). This effect was most clearly present at 24h (supplement 10). Additionally, *AXIN 2* expression increased more in CMT-U27 than in CIPm, with mean fold changes of 4.54 and 2.00 at 24h respectively (supplement 10). Dasatinib inhibited *AXIN 2* expression most clearly at 24h and 72h. In CMT-U27, mean fold change of Dasatinib inhibited samples was 0.70 at 24h, 0.90 at 47h and 0.62 at 72h. In CIPm, mean fold change of Dasatinib inhibited samples 0.75 at 24h, 1.16 at 48h and 0.66 at 72h (supplement 10). Statistical analysis of controls vs. Wnt3A stimulated and controls vs. Dasatinib inhibited across all time points was significant in CMT-U27 (control vs. Wnt3A $p < 0.001$, control vs. Dasatinib $p = 0.022$) but not in CIPm. This may have been due to the smaller effect size observed in CIPm, which does correspond with TCF/LEF reporter assay data.

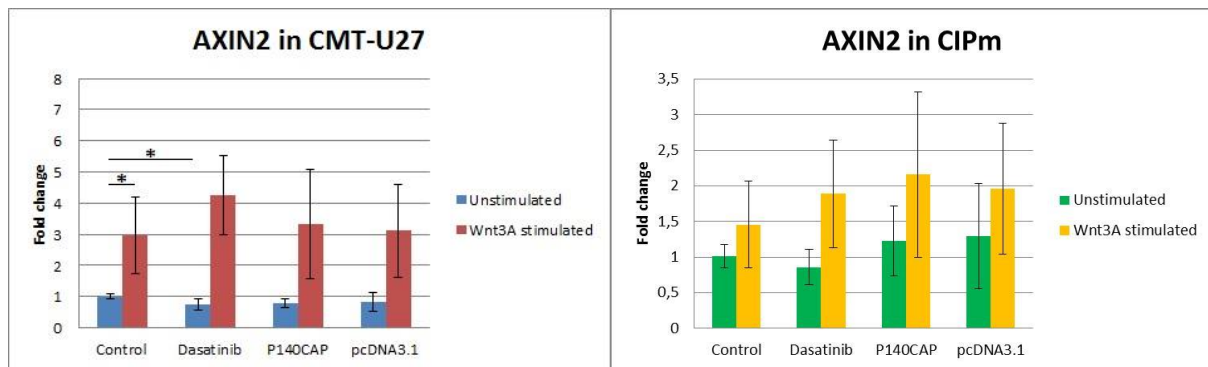


Figure 30 AXIN2 expression in 20 μ M Dasatinib inhibited, P140CAP transfected and pcDNA3.1 transfected samples of CMT-U27 and CIPm, both unstimulated and Wnt3A stimulated show AXIN2 expression is Wnt-responsive. Gene expression is normalized to unstimulated control of each timepoint. Left: Results for CMT-U27. Right: Results for CIPm. Results from 3 samples from 3 timepoints per condition are included, making $n = 9$. Experiment was performed once. Error bars represent SD. * indicates $p < 0.05$.

Interestingly, one of the genes of interest, *MUC1*, showed significantly increased expression upon Wnt3A stimulation in CMT-U27 ($p < 0.001$) and CIPm ($p = 0.032$) across all timepoints and a decreased expression upon Dasatinib inhibition in both CMT-U27 and CIPm ($p < 0.001$ and $p < 0.001$ respectively) across all timepoints (figure 31). Unlike *AXIN 2* expression, *MUC1* expression appeared to be inhibited by Dasatinib in Wnt3A stimulated controls. Expression of other putative Wnt target genes or genes of interest did not meet the criteria. Data of these genes was therefore not used to evaluate the effect of P140CAP transfection on Wnt activity. Results and analyses of all tested genes are available in supplement 10. In unstimulated samples of CMT-U27 and CIPm, neither *AXIN 2* expression nor *MUC1* expression differed between P140CAP transfected and pcDNA3.1 transfected samples at 24h, 48h and 72h. In Wnt3A stimulated samples, the same was observed. Interestingly, Wnt3A stimulation increased the expression of *AXIN 2* in Dasatinib treated CMT-U27 and CIPm samples compared to unstimulated Dasatinib samples, but this effect was not observed in *MUC1*.

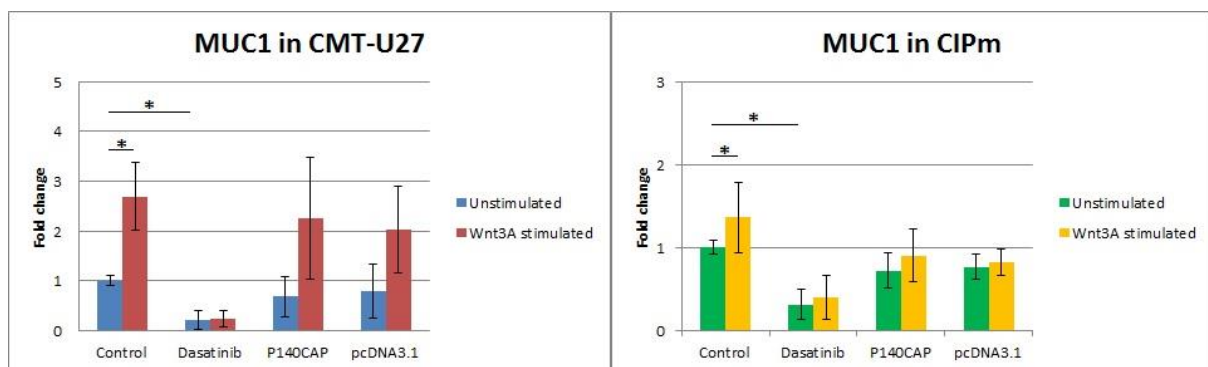


Figure 31 MUC1 expression in 20 μ M Dasatinib inhibited, P140CAP transfected and pcDNA3.1 transfected samples of CMT-U27 and CIPm, both unstimulated and Wnt3A stimulated show MUC1 expression is Wnt-responsive. Gene expression is normalized to unstimulated control of each timepoint. Left: Results for CMT-U27. right: Results for CIPm. Results from 3 samples from 3 timepoints per condition are included, making $n = 9$. Experiment was performed once. Error bars represent SD. * indicates $p < 0.05$.

Effect of P140CAP overexpression on metastasis of CMT-U27 dsRed in zebrafish

Experiment 130416	P140CAP transfected	pcDNA3.1 transfected	Experiment 200416	P140CAP transfected	pcDNA3.1 transfected
Tumor	9	8	Tumor	15	12
No tumor	29	19	No tumor	22	4
% tumor formation in P140CAP: 23.7% % tumor formation in pcDNA3.1: 29.6% Fisher's exact test p-value = 0.775			% tumor formation in P140CAP: 40.5% % tumor formation in pcDNA3.1: 75% Fisher's exact test p-value = 0.035		

Pooled data	P140CAP transfected	pcDNA3.1 transfected	<i>Table 4 Frequencies of tumor formation in zebrafish injected with P140CAP transfected CMT-U27 dsRed or pcDNA3.1 transfected CMT-U27 dsRed control. In experiment 130416, P140CAP group was injected with 93 cells/injection (n=38) and pcDNA3.1 control with 66 cells/injection (n=27). In experiment 200416, P140CAP group was injected with 400 cells/injection (n=37) and pcDNA3.1 control with 4.000 cells/injection (n=16). Results are given per individually performed experiment and as pooled data.</i>
Tumor	24	20	
No tumor	51	23	
% tumor formation in P140CAP: 32% % tumor formation in pcDNA3.1: 46.5% Fisher's exact test p-value = 0.166			

As P140CAP is thought to be a negative regulator of cell migration, P140CAP overexpression is expected to reduce cell migration. To evaluate the effect of P140CAP overexpression on metastasis *in vivo*, P140CAP transfected CMT-U27 dsRed was injected into the yolk sac of 2 dpf zebrafish embryos. pcDNA3.1 transfected CMT-U27 dsRed was used as a control. This experiment was performed twice. In experiment 130416, zebrafish in the P140CAP group were injected with 93 cells/injection (n=38). The pcDNA3.1 control group was injected with 66 cells/injection (n=27). In this experiment, zebrafish were scored for tumor formation by both experienced technician A. Slob and the author. 23.7% of P140CAP zebrafish embryos formed tumors compared to 29.6% in pcDNA3.1 controls. This effect was not statistically significant. In experiment 200416, the P140CAP group was injected with 400 cells/injection (n=37). pcDNA3.1 controls were injected with 4.000 cells/injection (n=16). This time, zebrafish were scored for tumor formation by the author only. 40.5% of P140CAP zebrafish embryos formed tumors compared to 75% in pcDNA3.1 control, with a p = 0.035. Pooled data of both experiments did not show a statistically significant effect of P140CAP on metastasis with p = 0.166.

Discussion

P140CAP and CSK are known to interact and regulate cSRC activity, and thereby also P130CAS activity. As the high Wnt/ β -catenin signaling in CMT1, CMT-U27 and CMT9 is known to be attenuated by cSRC-inhibition, mRNA expression of *P130CAS*, *P140CAP* and *CSK* was measured in a panel of 12 CMT cell lines grouped into 3 groups based on the activity of the Wnt pathway as previously determined by TCF/LEF reporter assay (23). P130CAS has been implicated as a contributor to cancer progression (81) and is activated by cSRC- and FAK-mediated phosphorylation (100). mRNA expression of *P130CAS* was lower in the high Wnt activity group compared to both the moderate and low Wnt activity groups, indicating high expression of *P130CAS*, a contributor to cancer progression, is not associated with high Wnt activity, another contributor to cancer progression. However, expression levels do not necessarily correspond with activity. P140CAP is a negative regulator of cSRC activity, and thereby P130CAS activity. *P140CAP* expression was not found to be significantly down- or upregulated in the high Wnt activity group compared to both the moderate and low Wnt activity groups. However, *P140CAP* expression was uniformly upregulated in the high Wnt activity group, indicating a loss of *P140CAP* expression is not the cause of cSRC-dependent high Wnt activity in this group. P140CAP inhibits cSRC activity directly by binding to SRC homology 3 domain of cSRC and indirectly by binding to and activating CSK, a cSRC inhibitor (81,94). Loss of *CSK* expression would therefore explain the contradictory finding of upregulated P140CAP expression in cells with SRC activity, yet a difference in *CSK* expression was only found between high and low Wnt activity groups at borderline significance level. Overall, qPCR results do not indicate a loss of *P140CAP* or *CSK* expression is the cause of cSRC-dependent high Wnt activity in CMT1, CMT-U27 and CMT9. Seeing as mRNA expression is not the only determinant of protein function, exome sequencing data was analyzed for mutations in *P140CAP* unique to the three CMT cell lines with high Wnt activity. An inactivating mutation in *P140CAP* could cause a loss of function irrespective of expression. At location 23658581 a G \rightarrow C substitution was found that was present in all reads of only CMT1, CMT-U27 and CMT9. Since NCBI database and Ensembl did not agree upon the intron/exon state of this region of DNA, PCR of cDNA of these cell lines and controls was performed using primers covering this region. Gel electrophoresis of PCR product showed 1 band at the expected length, but Sanger sequencing of the product to confirm the results of the exome sequencing was not managed.

If the G \rightarrow C substitution was deleterious for P140CAP function it could be the cause of high cSRC-dependent Wnt activity. Reconstituting wild type P140CAP expression would then reverse this. To test this hypothesis, wildtype murine P140CAP was overexpressed in the three CMT cell lines with high Wnt activity and in two CMT cell lines with low Wnt activity as a control by transient transfection with a P140CAP-pcDNA3.1 vector. Co-transfection of P140CAP-pcDNA3.1, TOP or FOP plasmid and Renilla plasmid was performed in order to assess the effect of P140CAP overexpression on Wnt activity using a TCF/LEF reporter assay. While relative luciferase activity, calculated as TOP/FOP ratio, appeared to be substantially lower in P140CAP + T/F transfected cells than in TOP/FOP transfected controls, relative luciferase activity of pcDNA3.1 + T/F transfected controls appeared similarly low. Inspection of the data of preliminary experiments revealed the low TOP/FOP ratio of P140CAP + T/F and pcDNA3.1 + T/F transfected cells was due to a high FOP luciferase activity and a low Renilla activity, not due to a high TOP luciferase activity. To remedy this, optimization of the transfected conditions was performed. However, results of the follow up experiment, which used the optimized transfection conditions, corresponded with results of preliminary experiments. Similar to the TOP vector, the FOP vector is a pGL4 vector onto which TCF/LEF binding sites have been cloned upstream of the luciferase reporter gene. In the FOP vector, the TCF/LEF binding sites have been mutated. As a result, luciferase transcription in FOP transfected samples is not responsive to Wnt/ β -catenin dependent TCF/LEF transcription factors. For this reason, FOP transfected samples may be used to correct data from TOP transfected samples for Wnt pathway independent luciferase transcription. Ideally, FOP luciferase activity is low and consistent across samples. The substantial

increases in luciferase activity of P140CAP + FOP and pcDNA3.1 + FOP transfected samples found here indicate co-transfection with a pcDNA3.1 vector stimulates Wnt pathway independent transcription of luciferase. It has been reported before that promoters of co-transfected plasmids may alter reporter gene expression (101). This may explain the substantial increase in luciferase activity of P140CAP + FOP and pcDNA3.1 + FOP transfected samples observed here. Furthermore, this implicates it is highly questionable if observed luciferase activity of P140CAP + TOP and pcDNA3.1 + TOP transfected samples has any correspondence with Wnt activity. It seems plausible that the transcriptional interference observed in P140CAP + FOP and pcDNA3.1 + FOP transfected samples is also present in P140CAP + TOP and pcDNA3.1 + TOP transfected samples, seeing as the TOP and FOP reporter plasmids are both based on the same pGL4 backbone. For these reasons, the data was deemed unreliable and was not statistically analyzed.

As an alternative to the TCF/LEF reporter assay, qPCR of putative Wnt reporter genes was performed on unstimulated and Wnt3A stimulated CMT-U27 and CIPm samples. Conditions included control, Dasatinib inhibited, P140CAP transfected and pcDNA3.1 transfected. Gene were verified for Wnt responsiveness by comparing Wnt3A stimulated control and Dasatinib inhibited control with unstimulated control. Surprisingly, expression of several putative Wnt target genes did not show responsiveness to Wnt pathway inhibition or stimulation. However, *AXIN 2*, a commonly used Wnt target gene (98), and gene of interest *MUC1* did show Wnt responsiveness. *MUC1* is a type I transmembrane protein that has been implicated to contribute to cancer progression. *MUC1* overexpression is a negative prognostic factor in both women and dogs (102,103). It is known to interact with EGFR, HER2 and other receptor tyrosine kinases (104). Furthermore, it has been shown play a role in cSRC-mediated tumor cell migration (103), Wnt pathway activation (104) and induction of ALDH expression (105). In these cell lines, *MUC1* expression was previously shown to increase in response to Wnt pathway activation mediated by PI3K/mTOR inhibitor (24). *AXIN 2* and *MUC1* expression did not differ between P140CAP and pcDNA3.1 samples in both CMT-U27 and CIPm, in both unstimulated and Wnt3As stimulated samples. These results do not support the hypothesis that P140CAP overexpression can decrease Wnt activity by inhibiting cSRC activity.

Overexpression of P140CAP did not inhibit metastasis of CMT-U27 dsRed in zebrafish in experiment 130416, yet experiment 200416 did show a significant inhibition. It must be noted that in experiment 130416, the number of cells per injection was 93 cells/injection in the P140CAP group and 66 cells/injection in the pcDNA3.1 group. In experiment 200416 the number of cells per injection was less comparable between groups, with 400 cells/injection in the P140CAP group and 4.000 cells/injection in the pcDNA3.1 group. The higher frequency of metastasis in the pcDNA3.1 group in experiment 200416 may therefore be the result of a 10-fold higher dose compared to the P140CAP group. Furthermore, experiment 200416 was scored by just the author, whose only previous experience of scoring for metastasis was scoring experiment 130416 under supervision of an experienced lab technician. This lack of experience may have led to bias. In light of these remarks, it is concluded that these experiments do not provide evidence that P140CAP inhibits metastasis of CMT-U27 dsred in vivo. This is in contrast to earlier reported findings in mice. Subcutaneous injection of P140CAP overexpressing MDA-MB-231, a human breast cancer cell line characterized as highly aggressive, into SCID mice did not give rise to tumors, whereas injection of controls did. In *Rag2^{-/-}γ^c^{-/-}* mice injected with EGFR overexpressing rat mammary adenocarcinoma MTLn3 cells into the mammary fat pad, P140CAP overexpression did not prevent tumor formation or reduce tumor volume, but it did decrease lung metastasis by 80% (106).

In conclusion

Neither integrin adaptor mRNA expression levels, nor a mutation in *P140CAP* appear to be associated with cSRC-dependent high basal Wnt activity in 3 CMT cell lines. As for the therapeutic benefit of P140CAP, the zebrafish metastasis experiments would need to be repeated in a more standardized manner to gather more reliable data. Wnt target qPCR showed that one gene of interest, *MUC1*, was

Wnt-responsive, a finding which has been previously reported for these CMT cell lines. Seeing as MUC1 has been implicated as a prognostic factor in both women and dogs, and has been associated with cSRC, ALDH and β -catenin, it seems advisable to shed light on its function in these CMT cell lines, for instance by performing gain and loss of function studies.

Chapter IV: Attempts at long-term 3D canine mammary organoid culture

Summary

Long-term 3D organoid culture system is one of the most promising scientific advancements in recent years, but it has never been described for the mammary gland. Here it was attempted to culture organoids from mammary duct pieces isolated from mammary gland tissue of intact female dogs. 2 experiments were overgrown with fibroblasts, limiting organoid growth. 1 experiment was cultured with DMEM/F12 + P/S + ITS + 3 μ M CHIR, resulting in growth of spherical and irregularly shaped cell structures. The 4th experiment was cultured with mini-gut organoid growth medium, which has been used for long-term culture of a large variety of epithelial tissues. Here, it resulted in spherical structures and budded, lobular structures. Based on the structure of the mammary gland *in vivo*, it is argued that the cell structures grown here are not quite 'mini-mamma's' yet. In light of the numerous practical and technical difficulties, it is recommended to further optimize the isolation protocol and culture conditions using mammary tissue from a more readily available species. It is briefly discussed how, once established, the 3D mammary organoid culture system can be verified and how it may be used in future research.

Introduction

Studies of stem cells were in the past limited by the inability to culture them *in vitro*. However, in recent years, advances in 3D culture systems have made it possible to imitate the stem cell niche *in vitro*, enabling stem cells to self-renew and give rise to 3D cell complexes that closely mimic the tissue architecture *in vivo*. These aptly named 'organoids' (resembling an organ) can now be cultured from an increasing variety of tissues, including gut (107), liver (108), pancreas (109), kidney (110), brain (111) and retina (112). The term 'organoid' has been used throughout the years for various 3D organ-like structures generated using different methods. In the years 1965-1985, the term 'organoid' referred to structures resulting from dissociation and reaggregation of cells (113). Although these studies revealed the ability of a certain tissue to self-organize, they did not specifically use stem cells to achieve this. From 2009 onwards, the term 'organoid' refers to 3D organ-like cell structures derived from pluripotent stem cells (both embryo-derived and synthetically induced) or adult organ-specific tissue stem cells (114). These organoids are grown in a gel-like substance that contains extracellular matrix proteins, and with a culture medium that contains growth factors and signaling molecules that promote stemness. Lancaster and Knoblich have defined the organoid as follows: 'A collection of organ-specific cell types that develops from stem cells or organ progenitors and self-organizes through cell-sorting and spatially restricted lineage commitment in a manner similar to *in vivo*' (113). Additionally, they have defined 3 criteria of organoids. First, an organoid consists of multiple organ-specific cell types. Second, an organoid can in some form simulate a specific function of the organ *in vivo*, such as excretion of certain substances, filtration or contraction. Third, the cells of an organoid are grouped together and spatially organized similar to the tissue architecture *in vivo* (113).

Due to these unique properties, 3D organoid culture has been seen as the bridge between 2D cell culture and *in vivo* experiments. 2D cell culture has been an indispensable technique in experimental research for years, yet it has its limitations. 2D cell culture commonly uses cell lines that have been naturally or experimentally immortalized to enable indefinite growth on plastic culture ware. These conditions are less similar to the *in vivo* cellular environment. Primary 2D cell culture overcomes some of these limitations, but may select for cell types which grow well under the culture conditions (115). This limitation could also apply to 3D organoid culture, yet as conditions more closely

resemble the *in vivo* environment, this limitation could be less great than in 2D culture. 3D mammary organoid culture is not a complete substitute for *in vivo* experiments, as organoid culture lacks supportive tissue such as blood vessels and neurons. However, organoids are more accessible for experimental manipulation and monitoring than cells *in vivo*, meaning a wider range of techniques may be used.

To date, no long-term culture method of mammary organoids has been published, although branched structures with alveoli-like buds at the tips have been cultured for 2-3 passages in collagen gels in the presence of a Rho-associated kinase inhibitor (116). We established a collaboration with the van Amerongen lab of the University of Amsterdam, who have been working on short term murine mammary organoid culture. The resident organoid technician, A.L. Zeeman BA, kindly agreed to isolate and culture organoids from a canine mammary gland using the murine mammary organoid protocol. She allowed us to observe the isolation and shared her isolation and culture protocols. After a few unsuccessful attempts to culture canine mammary organoids long-term using the van Amerongen lab protocols, we substituted the culture medium with the culture medium used for long-term colon organoid culture at the Hubrecht institute (117). This medium, with some adaptations, has been successfully used for long-term culture of adult stem cell-derived organoids from a wide range of epithelial tissues (114).

Materials & methods

Canine mammary gland tissue

Mammary gland tissue was excised from euthanized intact female Beagle mixed breed dogs aged 19-20 months, weighing 22-24 kg. These animals were euthanized for the purpose of other experiments, mostly heart function studies. The dogs were otherwise healthy at the time of euthanasia. No reproductive history was available for any of the dogs. Most dogs enter puberty between 8-12 months of age (range 4-22 months) (118), with smaller breeds entering puberty sooner than larger breeds (119). It appears likely that the dogs from which mammary tissue was collected had entered puberty at the time of euthanasia. Additionally, blood progesterone level at time of euthanasia was measured for some dogs. Due to practical limitations a blood sample could not be obtained of all dogs. Details of the individual animals can be found in table 7.

Isolation of mammary organoids

All reagent solutions were prepared on the day of isolation and filtered through sterile 0.22 μ M filters (Millipore). Components of collagenase solution can be found in table 5. DNase solution for 1 cm^3 tissue was 5 ml DMEM/F12 with 100 units DNase (Sigma-A3059, Sigma-Aldrich). BSA solution was 25 mg/ml dissolved in HBSS. This was used to coat all culture ware used after the collagenase tissue digestion step.

Collagenase solution for 1 cm^3 tissue		
Reagent	Manufacturer	Amount
DMEM/F12	Thermo Fisher Scientific	9.5 ml
FBS	Thermo Fisher Scientific	0.5 ml
Gentamycin	Thermo Fisher Scientific	10 μ l
Insulin (2 mg/ml stock)	Thermo Fisher Scientific	5 μ l
TrypLE Select 10x	Thermo Fisher Scientific	0.5 ml
Collagenase IV	Sigma-Aldrich	0.02 g

Table 5 Components of collagenase solution used for mammary organoid isolation.

After being excised from the animal, mammary glands were kept on ice and transported to a sterile cell culture flow hood. Mammary gland tissue was cut into small clumps with sterile surgical scissors. 1 cm^3 of cut tissue was added per 10 ml collagenase solution in a 15 ml cell culture tube. This was incubated at 37 °C on a rotating unit in an incubator until the solution became cloudy (20-25 minutes). The digested tissue was subsequently centrifuged at 1500 rpm for 10 minutes at RT. After centrifugation, 3 layers were present: a pellet of epithelium at the bottom, an aqueous layer in the middle and a fatty layer on top. In all experiments except experiment 080616, the aqueous layer and fatty layer were removed, resuspended, centrifuged a second time at 1500 rpm for 10 minutes at RT and recombined with the epithelial pellet in 10 ml DMEM/F12. After finding in literature that the supernatant may contain mammary fibroblasts, it was decided to not use the aqueous and fatty layer in experiment 080616 (120). Combined suspension, or epithelial pellet with 10 ml DMEM/F12 in experiment 080616 was resuspended and centrifuged at 1500 rpm for 10 minutes at RT. Supernatant was removed and 5 ml DNase solution was added. The suspension was kept in continuous motion for 5 minutes by gently tilting the closed tube by hand. After this incubation, 6 ml DMEM/F12 was added, the suspension was resuspended and centrifuged for at 1500 rpm for 10 minutes at RT.

Supernatant was removed, the pellet was resuspended in 10 ml DMEM/F12 and strained through a 100 μ m and a 70 μ m cell strainer (both Greiner Bio-one). Subsequently differential centrifugation was performed to isolate the ductal epithelium from the fibroblast and other stromal components. Suspension was centrifuged by pulsing to 1500 rpm at RT, supernatant was removed and pellet was resuspended in 10 ml DMEM/F12. This was repeated until the supernatant did not contain any single cells (4-6 times). The resulting pellet was resuspended in Matrigel and plated on Millicell glass slides (Millipore BV, Amsterdam, the Netherlands) (experiments 301115, 090216, 030516) or Greiner 24 well plates (experiment 080616). The plates were incubated for 20 minutes at 37 °C to solidify the Matrigel before adding the culture medium.

Organoid culture method and culture media

In all experiments, organoids were cultured at 37 °C with 5% CO₂. Medium was replaced every two days. Van Amerongen basic organoid growth medium consisted of DMEM/F12 + 1% P/S + 1% Insulin-transferrin-sodium selenite (ITS) (all Thermo Fisher Scientific). Additives used included 3 μ M CHIR (Stemgent, Germany) (a small molecule GSK3 inhibitor that functions as a Wnt pathway activator), EGF = human epidermal growth factor (Thermo Fisher Scientific), B27 = B27 without vitamin A (a cocktail supplement that supports proliferation of stem cells) (Thermo Fisher Scientific), Cortisol = hydrocortisone (Sigma-Aldrich) dissolved to a 100x stock in ethanol, MPA = medroxyprogesterone acetate (Sigma-Aldrich) dissolved to a 1000x stock in ethanol. Mini-gut organoid growth medium consisted of Advanced DMEM/F12 (Thermo Fisher Scientific) with the additives shown in table 6 (117). It is a combination of Wnt pathway activation (RSPO1, Wnt3A), tyrosine kinase receptor signaling activation (hEGF, FGF10) and BMP/TGF- β signaling inhibition (hNoggin, A83-01) (117). Nicotinamide was required for long-term culture of human small intestine and colon tissues (117). GH may stimulate stem/progenitors to enter the cell cycle (121), but it has not been previously used in long-term 3D organoid culture.

Reagent name	Supplier	Cat No.	Solvent	Stock concentration	Final concentration
Glutamax	Thermo Fisher Scientific	35050-079		10000 U/ml	100 U/ml
HEPES	Thermo Fisher Scientific	15630106			1.5%
Pen/Strep	Thermo Fisher Scientific	15140-122		10000/10000U/ml	100/100 U/ml
B27 supplement	Thermo Fisher Scientific	17504-044		50x	1x
hNoggin	Preprotech	120-10c	HBSS/0,1%BSA	100 ug/ml	100 ng/ml
hEGF	Invitrogen	PHG0313	HBSS/0,1%BSA	100 ug/ml	50 ng/ml
RSPO1	Thermo Fisher Scientific	11083-H08H-5	HBSS/0,1%BSA	1 mg/ml	1 ug/ml
Prostaglandin E2	Tocris	2296	DMSO	100 mM	1 uM
A83-01	Tocris	2939	DMSO	50 mM	0.5 uM
Wnt3a	R&D	5036-WN-010	HBSS	10 ug/ml	100 ng/ml
GH	Pharmacy of companion animals UU	N/A	HBSS	2.5 mg/ml	100 ng/ml
Y-27632/ROCK inhibitor	Sigma-Aldrich	Y0503	HBSS	10 mM	10 uM
FGF10	Preprotech	100-26-100ug	HBSS/0,1%BSA	100 ug/ml	100 ng/ml
Nicotinamide	Sigma-Aldrich	N0636	MQ	100 M	1 M

Table 6 Additives added to Advance DMEM/F12 to recreate mini-gut organoid growth medium (117).

Passaging of canine mammary organoids

In experiment 080616, organoids were passaged weekly. Medium was removed from wells. Either specific organoids were picked out using a pipet tip, or the whole well was harvested by adding ice cold Advanced DMEM/F12 and pipetting and scraping vigorously. Organoids were collected in a 15 ml cell culture tube and washed with 15 ml ice cold Advanced DMEM/F12. After shaking the tube 3-5 times it was centrifuged at 1500 rpm for 5 minutes at 4 °C. Supernatant was removed and washing and centrifugation steps were repeated 2 times. If organoids needed to be broken up, this was done after the first centrifugation step by pipetting the organoid pellet 40 times with a FCS-coated 200 µl pipet tip. Organoid pellet was resuspended 3:7 in Matrigel and plated onto 24 well plates. Plates were incubated for 20 minutes at 37 °C before adding mini-gut organoid growth medium with all additives.

Results

Summarizing table of individual dog records, conditions and results

Date of isolation	Date of birth of dog	Dog ID number	Body weight in kg	Blood progesterone level	Medium + additives used	Results
30-11-2015*	30-3-2014	967459	24 kg	15.2 ng/ml	Van Amerongen medium with: 3 μ M CHIR FGF DMSO	Chir gives concentration dependent growth. 7 DPI culture was overgrown with fibroblasts.
9-2-2016	30-7-2014	975257	28 kg	0.1 ng/ml	Van Amerongen medium with: 3 μ M CHIR	Growth did not occur on all slides. Growing organoids exhibited 2 different morphologies: spheres and irregular shapes. Growth could not be maintained for a prolonged period of time.
3-5-2016	15-10-2014	981851	22 kg	Not available	Van Amerongen medium with: 50 ng/ml EGF + 1x B27 + 5 μ g/ml Cortisol 50 ng/ml EGF + 1x B27 + 100 nM MPA	Large number of organoids, but a lot of debris and fibroblasts, resulting in fibroblast overgrowth 6 DPI.
8-6-2016	4-9-2014	977721	21 kg	15.1 ng/ml	Mini-gut organoid growth medium (table 6)	A lot of fibroblasts present. Both spheres and more lobular structures grew. Could be passaged, but not expanded.

Table 7 Individual dog records, culture conditions and summarized results from organoid isolation and culture. *Isolation and subsequent culture kindly performed by A.L. Zeeman BA at the van Amerongen labs.

Isolation of mammary organoids

The isolation protocol yielded variable results, both between and within experiments. Isolated pieces of mammary duct 1 DPI (days post isolation) from experiment 030516 can be seen in figure 32 on the left as the budded, irregular structures. Figure 32 on the right is an image from the same isolation experiment. Aside from pieces of mammary duct, a large amount debris can be seen. This debris appeared to be pieces of supporting tissue such as muscle fibers and nerve bundles. The number of mammary duct pieces and the ratio of mammary duct pieces to debris as approximated by visual inspection varied considerably between experiments and between wells from the same experiment. As a consequence, starting conditions for culture experiments were variable.

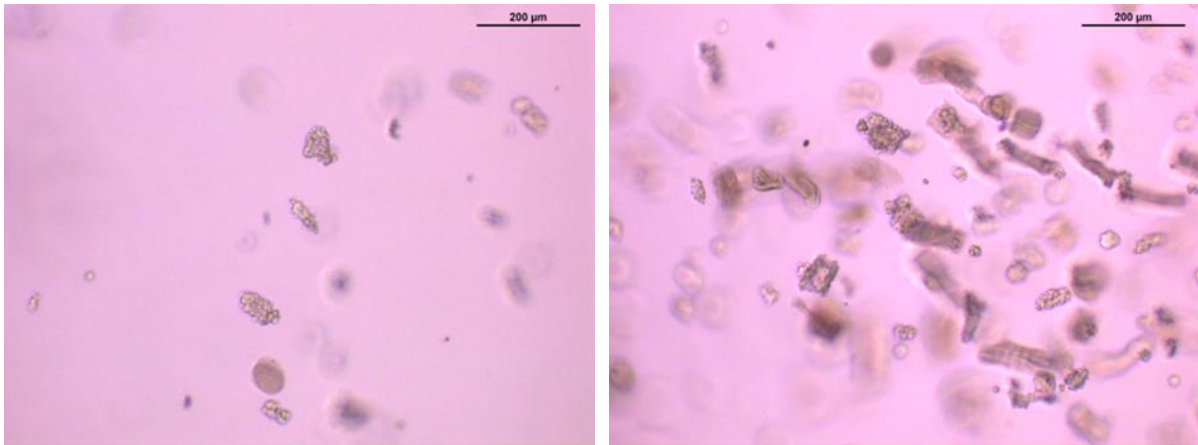


Figure 32 Experiment 030516 1 DPI cultured with van Amerongen medium + EGF + B27 + Cortisol yielded variable isolates. Left: isolated pieces of mammary duct can be seen as budded, irregular structures. Right: in a different well from the same experiment, a large amount of debris is present.

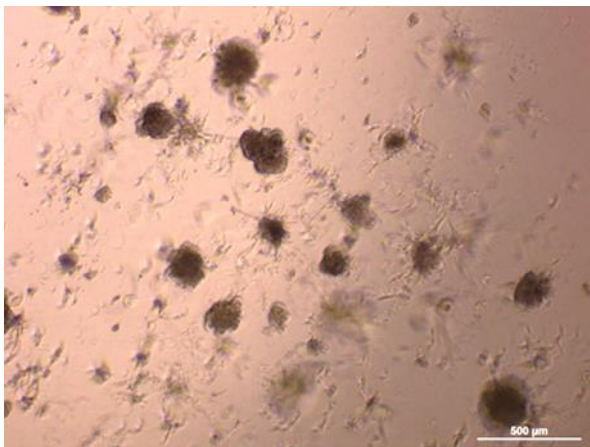


Figure 33 Experiment 080616 5 DPI cultured with mini-gut organoid growth medium showed infiltrative fibroblast growth. The fibroblasts can be seen as narrow cells that infiltrate the larger, darker, spherical organoids.

In experiment 301115, 030516 and 080616 fibroblasts were present in the isolated material. These fibroblasts grew quickly and infiltrated the organoids within 7 DPI. An example of infiltrative fibroblast growth can be found in figure 33. In experiments 301115 and 030516, the fibroblast growth rendered the culture useless. In experiment 080616, some organoids without fibroblast infiltration were present. These were used in subsequent culture.

Organoid culture with the van Amerongen medium + 3 μ M CHIR

In experiment 090216, organoids were plated in Matrigel on 4 Millicell 8 well slides with the van Amerongen medium + 3 μ M CHIR. On 1 slide organoids showed growth. From 6 DPI onwards, 2 morphologies were observed: dense spheres with a layered structure and more irregular shapes (figure 34).

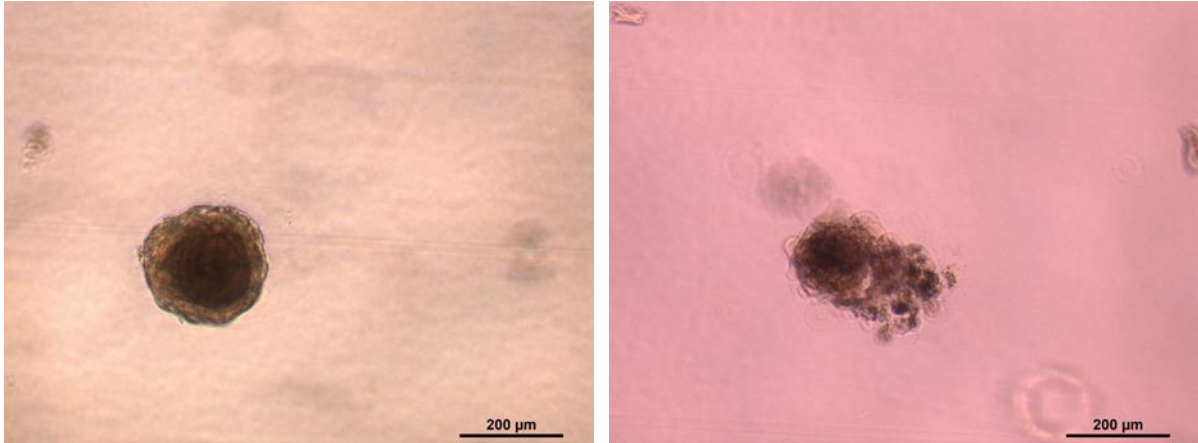


Figure 34 Experiment 090216 cultured with van Amerongen medium + 3 μ M Chir resulted in organoids with 2 morphologies. Left: organoid with sphere morphology at 10 DPI. Right: organoid with irregular morphology at 15 DPI.

Organoid culture with the mini-gut organoid growth medium

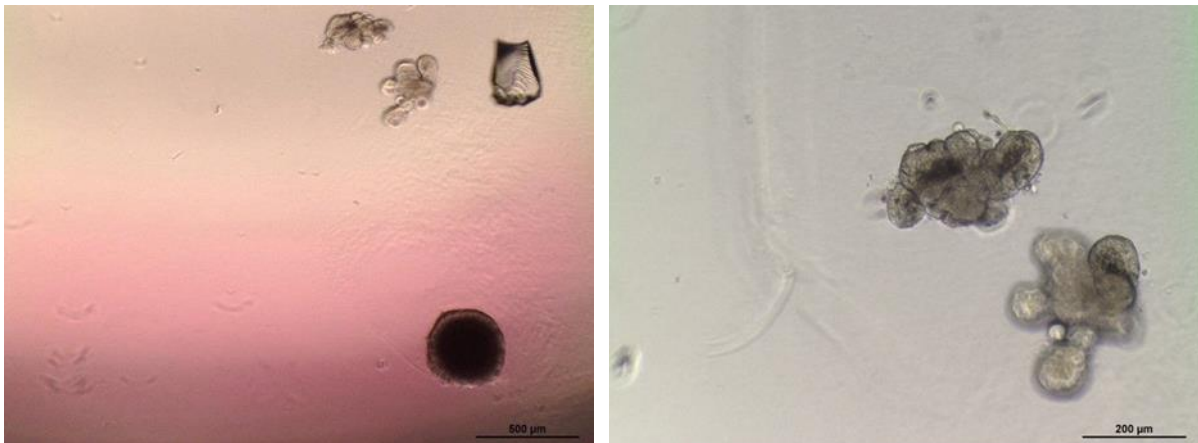


Figure 35 Experiment 080616 P3 with mini-gut organoid growth medium resulted in a budded morphology not seen with van Amerongen medium. Left: 27 DPI, 2 organoids with a lobular, budded morphology (top left and middle), 1 organoid with a sphere morphology (bottom) and a scrape in the Matrigel (top right). Right: 28 DPI, detail of the same 2 organoids with lobular, budded morphology.

Experiment 080616 showed some infiltrative fibroblast growth. Organoids without fibroblast infiltration were picked out and used for subsequent culture. Organoids were passaged weekly. It must be noted this technique still needs refinement. There was difficulty with breaking up the organoids into smaller pieces and removing the old Matrigel. Additionally, organoids were lost during passaging. In addition to the spherical and irregular morphologies observed with the van Amerongen medium, with the mini-gut medium 2 organoids with a lobular, budded morphology were observed (figure 35). At the time of writing, organoids are still kept in culture, but it has not been managed to expand the number of organoids.

Discussion

From a morphological point of view, the canine mammary cell structures grown here do not quite resemble the branched, 2 layered-epithelial structure with terminal end buds that is present in the *in vivo* mammary gland. Cell structures grown in the van Amerongen medium had a spherical, smooth, multilayered morphology. Some of the cell structures grown in the mini-gut organoid growth medium had a more budded morphology, indicating the components of the mini-gut organoid growth medium somewhat promote the maintenance of normal tissue architecture. However, none of the organoids had a branched structure, indicating the current medium does not provide all the cues necessary for *in vivo* tissue architecture maintenance. The cell structures grown thus far are not quite 'mini-mamma's' yet. An earlier reported short term culture protocol using free-floating collagen gels and a medium with only a ROCK-inhibitor and forskolin generated branched structures with budded tips, resembling terminal ductulo-lobular units (116). These cell structures displayed basal and luminal markers at the same positions as *in vivo* and showed contractility (116). Perhaps combining elements of this protocol with the mini-gut medium would result in a protocol for long-term culture of mammary organoids that meet all of the criteria defined by Lancaster and Knoblich (113).

The development of a 3D culture system of canine mammary organoids was limited by numerous factors. One of the most profound limitations is the lack of a steady supply of canine mammary tissue. Currently, all tissue is sourced from euthanized dogs that have been used in other scientific experiments of the department of companion animals of the faculty of veterinary medicine of Utrecht University or from experiments of the University Medical Center Utrecht (UMCU). The number of dog studies taking place is not very large and varies from year to year. Additionally, not all dogs used in animal studies are female, and many are too old at the time of euthanasia to be used for mammary organoid culture. In the period November 2015 – June 2016, only 4 animals were euthanized that met the criteria. From a technical point of view, the high variability and poor reproducibility of the results of the isolation protocol, both within experiments and between subsequent experiments, is challenging. When examined directly after isolation, wells containing material isolated from the same animal in the same experiment differed profoundly in the number of organoids present, the amount of debris present, the ratio organoid: debris and the amount of fibroblasts present. Additionally, organoids within a well vary greatly in size. These highly variable starting conditions combined with an often low organoid yield meant it was not possible to compare the effect of different media compositions on organoid growth. The organoid growth medium could therefore not be optimized. Ambitions were reduced to simply keeping the organoids alive and growing. Any supplement or growth factor that literature showed potentially beneficial was therefore included. Once the organoids could be successfully expanded, large enough groups could be created to evaluate the effect of each individual additive. Unfortunately, the required expansion was not achieved. As no long-term culture of mammary organoids has yet been described, it was challenging to evaluate if the organoids were developing well. Unlike cells, where a small fraction can be stained for cell viability, there is no simple method to determine organoid viability that does not require sacrificing the organoids.

Combined with the suboptimal morphologies observed, it appears necessary to optimize the organoid protocol and culture medium. In light of the scarcity of canine material, the lack of expertise and the absence of a specific protocol for mammary glands, it seems advisable to find an alternative, steady source of material to allow isolations to be performed more frequently. This would likely require a temporary switch to a more commonly euthanized animal such as mice. Once an optimal protocol has been established and adapted to the canine mammary gland, it should be verified that the grown structures resemble the *in vivo* mammary tissue. A suggested approach is to divide any used mammary gland into two parts: one part from which organoids may be isolated, one

part to fix and process for histological staining. Organoids could then be fixed and stained at various passages and compared to the mammary gland tissue. Points of comparison could include general tissue architecture and presence and distribution of different cell types by staining for proliferation markers, hormone receptors, stem cell markers and basal/luminal markers. An overview of suitable marker combinations can be found in the excellent review by Tornillo and Smalley (122). Aside from morphological similarity, organoids should have some organ-specific function in common with the *in vivo* tissue. Mammary gland-specific functions include contractility of myoepithelial cells and milk production. A method to determine contractility of mammary organoids has been described (116). The organoids were cultured in free floating gels. After adding a contraction-stimulating agent, the size of the gel and the individual cells was monitored.

Once it has been verified that the mammary organoids are a faithful representation of *in vivo* mammary tissue they may be used in various applications. It would be interesting to determine which cell type(s) is/are able to initiate organoid formation, as this capability is expected to be limited to stem/progenitor cells. For this, the mammary tissue would need to be digested to a single cell suspension, sorted into subpopulations with flow cytometry and brought into 3D culture. The mammary organoids could potentially bridge a gap in a longstanding area of interest of the CTO research group: progesterone-induced growth hormone production in the mammary gland (123,124). This has been known for many years to occur *in vivo* in the dog, yet 2D cultured canine mammary cells could never be stimulated to do so (unpublished observations), indicating they are missing some vital signaling cue in 2D culture. Mammary cells may be stimulated to produce growth hormone in the more *in vivo*-like conditions of 3D organoid culture. This would be an accessible method to study the functional significance of growth hormone production in mammary development and mammary tumorigenesis. Aside from developmental studies, the 3D mammary organoid system could be adapted to culture mammary tumor samples. This system would need additional verification to ensure no selective pressure is present that influences the cell composition of the tumor organoids. Once the system has been verified, it could be used to start a canine mammary tumor organoid biobank, as has been described for human colorectal cancer (125). The mammary tumor organoids could be used as a screening tool for experimental cancer treatments. With the consent of the owner, treatments that were effective on the patient-derived mammary tumor organoids could then be tested on the patient itself. The data derived from these trials could provide important clues for personalized cancer treatment in women with breast cancer.

Chapter V: General discussion

This honours program research project made little progress towards finding the cause of high basal Wnt activity in 3 canine mammary tumor cell lines. It did exclude integrin receptors and the integrin adaptor P140CAP as players in high Wnt activity, but it provided no deeper understanding of the signaling mechanisms driving these cell lines. The project did not go according to plan. The original plan, to compare Wnt activity between integrin-positive and – negative cells, came to an early halt as the premise of the plan turned out to be false. An alternative plan was conceived – different target, largely the same methods. A mutation in the integrin adaptor P140CAP, unique to the three CMT cell lines with high Wnt activity, was found. This mutation appeared to be a plausible cause of the high Wnt activity, seeing as P140CAP is known to negatively regulate cSRC activity (94), and the Wnt activity in these cell lines is known to depend on cSRC activity (24). Conversely, introducing wildtype P140CAP overexpression in these cell lines should have lowered Wnt activity and potentially reduced invasiveness. The combined results from the Wnt reporter qPCR and the zebrafish injections showed no effect of wildtype P140CAP overexpression on Wnt activity or metastasis, suggesting the mutation in P140CAP is not the cause of high Wnt activity in these cell lines.

Not all experiments described in the research plan were performed. Due to the change of subject and subsequent technical difficulties with the TCF/LEF Wnt reporter assay there was insufficient time to perform the P140CAP & CSK siRNA experiment, to perform the scratch assays and to culture mammospheres. Additionally, developing a working 3D mammary organoid culture system was given priority over culturing mammospheres. Although technical skills have increased and some progress has been made towards finding the right culture conditions, the 3D mammary organoid culture system must still be substantially optimized and verified before it can be used in research. In hindsight, it was perhaps unrealistic to think this novel culture system could be set up within in a year as a side project to the Wnt-related research.

As for future research, it is tempting to look in literature for another cell signaling molecule that is in some way implicated in Wnt signaling, cSRC activity or stem cell maintenance. Alternatively, the research strategy could be reconsidered. The current line of thought is that there is one cause of high Wnt activity, that this cause is the same in all 3 CMT cell lines. Using the simplest explanation is attractive, as simpler hypotheses are easier to test than more complex ones. Indeed, the 3 CMT cell lines with high Wnt activity are morphologically similar, and in their expression of various target genes tested throughout this year they were remarkably consistent. However, the simplest theory is not in principal the most likely to be true. Considering the cause of high Wnt activity may be multifactorial and therefore more complex to test, the question arises if finding the cause of high Wnt activity should be given the highest priority. Cancer cell lines are a simplified model of cancer *in vivo*: they consist of one cell type and are grown 2-dimensionally on plastic cell culture ware without interaction with a tumor microenvironment. Similar to non-malignant cells, cancer cells interact with their environment through integrin- and focal adhesion-signaling (126). Components of the tumor microenvironment such as extracellular matrix proteins, cancer-associated fibroblasts, immune cells and endothelial cells have long been known to influence cancer behavior, both positively and negatively (127). 3-dimensionality also appears to influence cancer cell behavior: 3D cancer models have shown that cell signaling can differ between 2D or 3D cultures of the same cell line (126). Furthermore, they have revealed cellular structures only present in 3D culture and *in vivo* (126). With regard to the 3 CMT cell lines with high Wnt activity, these findings implicate that the activity of their internal signaling pathways and thereby their behavior may differ in a 3D tumor microenvironment. How would these cell lines behave when transplanted *in vivo*? Do they show aggressive, infiltrative growth, are they able to metastasize and resist therapy more easily than the other CMT cell lines? Is the Wnt pathway still activated and does it contribute to cancer progression?

Currently, there is no data to directly answer any of these questions. There is, however, some data that supports the interest in these cell lines. In addition to high Wnt activity, they have uniquely high mRNA expression of 2 other stem cells markers: *LGR5*, which has been used to isolate stem cells for organoid culture in a range of epithelial tissues (114), and *ALDH* (77,78). Normal tissue stem cells *in vivo* are tightly regulated by the stem cell niche (128). Pluripotent mammary stem cells reside in the basal layer between the basement membrane and the luminal layer. Mammary stem cells themselves are hormone receptor negative; it is thought hormone receptor positive luminal cells relay hormonal signals to the mammary stem cells by local second messages (129). It is not quite clear if a similar niche exists for cancer stem cells. Traditionally, cancer cells were thought of as cells that had gained the ability to survive without cell-cell contact and become insensitive to inhibitory signaling from the micro-environment. However, given the contribution of the tumor micro-environment to cancer progression, the existence of a cancer stem cell niche has become accepted in recent years (130). If such a niche exists for breast cancer stem cells it appears unlikely that the 3 CMT cell lines with high Wnt activity are true cancer stem cells, as they are cultured without niche components such as ECM proteins or stromal cells.

Even if these cell lines do have cancer stem cell characteristics or highly malignant behavior, it does not necessarily mean that they are clinically relevant. Perhaps these cell lines contain mutations and alterations which are rarely seen in the tumors of canine patients. Moreover, it remains to be seen if the specific alterations which cause the high Wnt activity are also a common cause of high Wnt activity in human breast cancer. The primary aim of this research is not developing better treatments for canine patients, as castration after the first estrus is a much more effective and affordable method to prevent canine mammary tumors in female pet dogs (given the owner does not intend to use the dog for breeding) (15). This research uses canine mammary tumors as a model for human breast cancer. The ultimate goal is to benefit the health of women, not bitches. No model is perfect. There must be strong benefits to using the model to justify not studying the disease in humans directly. The research presented here is strictly preclinical, using only cell lines. It seems challenging to see the additional value of using canine cell lines instead of human ones. The additional value can be found in the clinical setting. Canine mammary tumors are common, naturally occurring tumors in pet dogs (12-14). Moreover, pet dogs share the environment of their owners, meaning they are exposed to the same risk factors. With the consent of the owners, the pet dog population could help test new breast cancer treatments.

Naturally, this approach would only make sense if canine mammary tumors indeed resemble human breast cancer. The way to prove this similarity is not, however, to study cell lines. All major cell signaling pathways have been conserved in evolution, therefore canine and human cells share the same cellular mechanisms (131). Mutations or other alterations in these cell signaling pathway are an important component of tumorigenesis. Cancer is a highly heterogeneous disease, meaning that within a tumor, different cells have different alterations. By chance, there will be a canine mammary tumor cell which has a pathway activated that has previously been observed in human breast cancer. That does not automatically mean that canine mammary cancer as a systemic disease resembles human breast cancer. In this light, developing the 3D mammary organoid culture and adapting it to grow mammary tumors seems vital, as the tumor cell variety, tumor cell-tumor cell dynamics and ECM interactions present *in vivo* can be imitated. This will allow for a more accurate comparison between canine mammary tumors and human breast cancer subtypes, although it must be noted that tumor-associated cells and vasculature are still missing from this model. Once it has been established for which subtype of breast cancer canine mammary tumors are a good model, previous experience with Wnt-related research can be applied to the organoids. This may lead to new therapeutic targets which could be tested in canine patients. Positive results in canine patients may provide an incentive to test the treatment in women, making dogs ‘woman’s best friend’.

References

- (1) Globocan. Globocan 2012: Estimated Cancer Incidence, Mortality and Prevalence Worldwide in 2012. 2012; Available at: http://globocan.iarc.fr/Pages/fact_sheets_cancer.aspx. Accessed 03/05, 2016.
- (2) Coleman MP, Quaresma M, Berrino F, Lutz J, De Angelis R, Capocaccia R, et al. Cancer survival in five continents: a worldwide population-based study (CONCORD). *The Lancet Oncology* 2008 8;9(8):730-756.
- (3) Clarke R, Tyson JJ, Dixon JM. Endocrine resistance in breast cancer – An overview and update. *Mol Cell Endocrinol* 2015 12/15;418, Part 3:220-234.
- (4) Maximiano S, Magalhaes P, Guerreiro MP, Morgado M. Trastuzumab in the Treatment of Breast Cancer. *BioDrugs* 2016 Apr;30(2):75-86.
- (5) Puglisi F, Fontanella C, Amoroso V, Bianchi GV, Bisagni G, Falci C, et al. Current challenges in HER2-positive breast cancer. *Crit Rev Oncol* 2016 2;98:211-221.
- (6) Dawood S. Triple-Negative Breast Cancer. *Drugs* 2010;70(17):2247-2258.
- (7) Marmé F, Schneeweiss A. Targeted Therapies in Triple-Negative Breast Cancer. *Breast Care* 2015;10(3):159-166.
- (8) Charafe-Jauffret E, Monville F, Ginestier C, Dontu G, Birnbaum D, Wicha MS. Cancer Stem Cells in Breast: Current Opinion and Future Challenges. *Pathobiology* 2008;75(2):75-84.
- (9) Visvader J, Lindeman G. Cancer Stem Cells: Current Status and Evolving Complexities. *Cell Stem Cell* 2012 6/14;10(6):717-728.
- (10) Nowell PC. The clonal evolution of tumor cell populations. *Science* 1976 Oct 1;194(4260):23-28.
- (11) Kelly PN, Dakic A, Adams JM, Nutt SL, Strasser A. Tumor growth need not be driven by rare cancer stem cells. *Science* 2007 Jul 20;317(5836):337.
- (12) Dobson JM, Samuel S, Milstein H, Rogers K, Wood JL. Canine neoplasia in the UK: estimates of incidence rates from a population of insured dogs. *J Small Anim Pract* 2002 Jun;43(6):240-246.
- (13) Merlo DF, Rossi L, Pellegrino C, Ceppi M, Cardellino U, Capurro C, et al. Cancer incidence in pet dogs: findings of the Animal Tumor Registry of Genoa, Italy. *J Vet Intern Med* 2008 Jul-Aug;22(4):976-984.
- (14) Vascellari M, Capello K, Carminato A, Zanardello C, Baioni E, Mutinelli F. Incidence of mammary tumors in the canine population living in the Veneto region (Northeastern Italy): Risk factors and similarities to human breast cancer. *Prev Vet Med* 2016 Apr 1;126:183-189.
- (15) Schneider R, Dorn CR, Taylor DON. Factors Influencing Canine Mammary Cancer Development and Postsurgical Survival. *Journal of the National Cancer Institute* 1969 December 01;43(6):1249-1261.

- (16) Sleenckx N, de Rooster H, Veldhuis Kroeze E, Van Ginneken C, Van Brantegem L. Canine Mammary Tumours, an Overview. *Reproduction in Domestic Animals* 2011;46(6):1112-1131.
- (17) Liu D, Xiong H, Ellis AE, Northrup NC, Rodriguez CO, O'Regan RM, et al. Molecular Homology and Difference between Spontaneous Canine Mammary Cancer and Human Breast Cancer. *Cancer Res* 2014 09/15;74(18):5045-5056.
- (18) Uva P, Aurisicchio L, Watters J, Loboda A, Kulkarni A, Castle J, et al. Comparative expression pathway analysis of human and canine mammary tumors. *BMC Genomics* 2009;10(1):1-20.
- (19) Rivera P, von Euler H. Molecular Biological Aspects on Canine and Human Mammary Tumors. *Veterinary Pathology Online* 2011 January 01;48(1):132-146.
- (20) Araújo MR, Campos LC, Damasceno KA, Gamba CO, Ferreira E, Cassali GD. HER-2, EGFR, Cox-2 and Ki67 expression in lymph node metastasis of canine mammary carcinomas: Association with clinical-pathological parameters and overall survival. *Res Vet Sci* 2016 6;106:121-130.
- (21) Hsu W, Huang H, Liao J, Wong M, Chang S. Increased survival in dogs with malignant mammary tumours overexpressing HER-2 protein and detection of a silent single nucleotide polymorphism in the canine HER-2 gene. *The Veterinary Journal* 2009 4;180(1):116-123.
- (22) Kim JH, Im KS, Kim NH, Yhee JY, Nho WG, Sur JH. Expression of HER-2 and nuclear localization of HER-3 protein in canine mammary tumors: Histopathological and immunohistochemical study. *The Veterinary Journal* 2011 9;189(3):318-322.
- (23) Gracanin A, Timmermans-Sprang E, van Wolferen ME, Rao NAS, Grizelj J, Vince S, et al. Ligand-Independent Canonical Wnt Activity in Canine Mammary Tumor Cell Lines Associated with Aberrant LEF1 Expression. *PLoS ONE* 2014 06/02;9(6):e98698.
- (24) Timmermans-Sprang EP, Gracanin A, Mol JA. High basal Wnt signaling is further induced by PI3K/mTor inhibition but sensitive to cSRC inhibition in mammary carcinoma cell lines with HER2/3 overexpression. *BMC Cancer* 2015 Jul 25;15:545-015-1544-y.
- (25) Kahn M. Can we safely target the WNT pathway? *Nat Rev Drug Discov* 2014 print;13(7):513-532.
- (26) van Amerongen R, Mikels A, Nusse R. Alternative Wnt Signaling Is Initiated by Distinct Receptors. *Sci Signal* 2008 09/02;1(35):re9-re9.
- (27) Izrailit J, Reedijk M. Developmental pathways in breast cancer and breast tumor-initiating cells: Therapeutic implications. *Cancer Lett* 2012 4/28;317(2):115-126.
- (28) Duchartre Y, Kim Y, Kahn M. The Wnt signaling pathway in cancer. *Crit Rev Oncol* 2016 3;99:141-149.
- (29) Hatsell S, Rowlands T, Hiremath M, Cowin P. Beta-catenin and Tcfs in mammary development and cancer. *J Mammary Gland Biol Neoplasia* 2003 Apr;8(2):145-158.
- (30) Liu S, Dontu G, Wicha MS. Mammary stem cells, self-renewal pathways, and carcinogenesis. *Breast Cancer Res* 2005;7(3):86-95.

- (31) Brown AM. Wnt signaling in breast cancer: have we come full circle? *Breast Cancer Res* 2001;3(6):351-355.
- (32) Chu EY, Hens J, Andl T, Kairo A, Yamaguchi TP, Briskin C, et al. Canonical WNT signaling promotes mammary placode development and is essential for initiation of mammary gland morphogenesis. *Development* 2004 09/09;131(19):4819-4829.
- (33) Lindvall C, Evans NC, Zylstra CR, Li Y, Alexander CM, Williams BO. The Wnt Signaling Receptor Lrp5 Is Required for Mammary Ductal Stem Cell Activity and Wnt1-induced Tumorigenesis. *Journal of Biological Chemistry* 2006 November 17;281(46):35081-35087.
- (34) van Genderen C, Okamura RM, Fariñas I, Quo RG, Parslow TG, Bruhn L, et al. Development of several organs that require inductive epithelial-mesenchymal interactions is impaired in LEF-1-deficient mice. *Genes & Development* 1994 November 15;8(22):2691-2703.
- (35) Lindvall C, Bu W, Williams BO, Li Y. Wnt signaling, stem cells, and the cellular origin of breast cancer. *Stem Cell Rev* 2007 Jun;3(2):157-168.
- (36) Zeng YA, Nusse R. Wnt Proteins Are Self-Renewal Factors for Mammary Stem Cells and Promote Their Long-Term Expansion in Culture. *Cell Stem Cell* 2010 6/4;6(6):568-577.
- (37) Li Y, Hively WP, Varmus HE. Use of MMTV-Wnt-1 transgenic mice for studying the genetic basis of breast cancer. *Oncogene* 2000 Feb 21;19(8):1002-1009.
- (38) Li Y, Welm B, Podsypanina K, Huang S, Chamorro M, Zhang X, et al. Evidence that transgenes encoding components of the Wnt signaling pathway preferentially induce mammary cancers from progenitor cells. *Proc Natl Acad Sci U S A* 2003 Dec 23;100(26):15853-15858.
- (39) Incassati A, Chandramouli A, Eelkema R, Cowin P. Key signaling nodes in mammary gland development and cancer: beta-catenin. *Breast Cancer Res* 2010;12(6):213.
- (40) Khramtsov AI, Khramtsova GF, Tretiakova M, Huo D, Olopade OI, Goss KH. Wnt/beta-catenin pathway activation is enriched in basal-like breast cancers and predicts poor outcome. *Am J Pathol* 2010 Jun;176(6):2911-2920.
- (41) Desgrosellier JS, Cheresch DA. Integrins in cancer: biological implications and therapeutic opportunities. *Nat Rev Cancer* 2010 print;10(1):9-22.
- (42) Hynes RO. Integrins: Bidirectional, Allosteric Signaling Machines. *Cell* 2002 9/20;110(6):673-687.
- (43) Taddei I, Deugnier MA, Faraldo MM, Petit V, Bouvard D, Medina D, et al. Beta1 integrin deletion from the basal compartment of the mammary epithelium affects stem cells. *Nat Cell Biol* 2008 Jun;10(6):716-722.
- (44) Shackleton M, Vaillant F, Simpson KJ, Stingl J, Smyth GK, Asselin-Labat M, et al. Generation of a functional mammary gland from a single stem cell. *Nature* 2006 01/05;439(7072):84-88.
- (45) Stingl J, Eirew P, Ricketson I, Shackleton M, Vaillant F, Choi D, et al. Purification and unique properties of mammary epithelial stem cells. *Nature* 2006 02/23;439(7079):993-997.

- (46) Seguin L, Desgrosellier JS, Weis SM, Cheresch DA. Integrins and cancer: regulators of cancer stemness, metastasis, and drug resistance. *Trends Cell Biol* 2015 Apr;25(4):234-240.
- (47) Ghebeh H, Sleiman GM, Manogaran PS, Al-Mazrou A, Barhoush E, Al-Mohanna F, et al. Profiling of normal and malignant breast tissue show CD44^{high}/CD24^{low} phenotype as a predominant stem/progenitor marker when used in combination with Ep-CAM/CD49f markers. *BMC Cancer* 2013;13(1):1-14.
- (48) Cariati M, Naderi A, Brown JP, Smalley MJ, Pinder SE, Caldas C, et al. Alpha-6 integrin is necessary for the tumorigenicity of a stem cell-like subpopulation within the MCF7 breast cancer cell line. *International Journal of Cancer* 2008;122(2):298-304.
- (49) Friedrichs K, Ruiz P, Franke F, Gille I, Terpe HJ, Imhof BA. High expression level of alpha 6 integrin in human breast carcinoma is correlated with reduced survival. *Cancer Res* 1995 Feb 15;55(4):901-906.
- (50) Ye F, Qiu Y, Li L, Yang L, Cheng F, Zhang H, et al. The Presence of EpCAM(-)/CD49f(+) Cells in Breast Cancer Is Associated with a Poor Clinical Outcome. *J Breast Cancer* 2015 Sep;18(3):242-248.
- (51) Nistico P, Di Modugno F, Spada S, Bissell MJ. Beta1 and Beta4 Integrins: from Breast Development to Clinical Practice. *Breast Cancer Res* 2014;16(5):459.
- (52) Vassilopoulos A, Wang RH, Petrovas C, Ambrozak D, Koup R, Deng CX. Identification and characterization of cancer initiating cells from BRCA1 related mammary tumors using markers for normal mammary stem cells. *Int J Biol Sci* 2008 May 4;4(3):133-142.
- (53) Arboleda MJ, Lyons JF, Kabbinavar FF, Bray MR, Snow BE, Ayala R, et al. Overexpression of AKT2/protein kinase Bbeta leads to up-regulation of beta1 integrins, increased invasion, and metastasis of human breast and ovarian cancer cells. *Cancer Res* 2003 Jan 1;63(1):196-206.
- (54) Chen IH, Chang FR, Wu YC, Kung PH, Wu CC. 3,4-Methylenedioxy-beta-nitrostyrene inhibits adhesion and migration of human triple-negative breast cancer cells by suppressing beta1 integrin function and surface protein disulfide isomerase. *Biochimie* 2015 Mar;110:81-92.
- (55) Truong HH, Xiong J, Ghotra VP, Nirmala E, Haazen L, Le Devedec SE, et al. beta1 integrin inhibition elicits a prometastatic switch through the TGFbeta-miR-200-ZEB network in E-cadherin-positive triple-negative breast cancer. *Sci Signal* 2014 Feb 11;7(312):ra15.
- (56) Xu Y, Zhang H, Lit LC, Grothey A, Athanasiadou M, Kiritsi M, et al. The kinase LMTK3 promotes invasion in breast cancer through GRB2-mediated induction of integrin beta(1). *Sci Signal* 2014 Jun 17;7(330):ra58.
- (57) Zhang Y, Gong Y, Hu D, Zhu P, Wang N, Zhang Q, et al. Nuclear SIPA1 activates integrin beta1 promoter and promotes invasion of breast cancer cells. *Oncogene* 2015 Mar 12;34(11):1451-1462.
- (58) Lanzafoame S, Emmanuele C, Torrisi A. Correlation of $\alpha 2\beta 1$ Integrin Expression with Histological Type and Hormonal Receptor Status in Breast Carcinomas. *Pathology - Research and Practice* 1996;192(10):1031-1038.

- (59) Yao ES, Zhang H, Chen Y, Lee B, Chew K, Moore D, et al. Increased $\beta 1$ Integrin Is Associated with Decreased Survival in Invasive Breast Cancer. *Cancer Res* 2007 American Association for Cancer Research;67(2):659-664.
- (60) Berry MG, Gui GPH, Wells CA, Carpenter R. Integrin expression and survival in human breast cancer. *European Journal of Surgical Oncology (EJSO)* 2004 6;30(5):484-489.
- (61) Wong NC, Mueller BM, Barbas CF, Ruminiski P, Quaranta V, Lin EC, et al. Alphav integrins mediate adhesion and migration of breast carcinoma cell lines. *Clin Exp Metastasis* 1998 Jan;16(1):50-61.
- (62) Takayama S, Ishii S, Ikeda T, Masamura S, Doi M, Kitajima M. The relationship between bone metastasis from human breast cancer and integrin alpha(v)beta3 expression. *Anticancer Res* 2005 Jan-Feb;25(1A):79-83.
- (63) Wu YJ, Muldoon LL, Gahramanov S, Kraemer DF, Marshall DJ, Neuwelt EA. Targeting alphaV-integrins decreased metastasis and increased survival in a nude rat breast cancer brain metastasis model. *J Neurooncol* 2012 Oct;110(1):27-36.
- (64) Li Y, Drabsch Y, Pujuguet P, Ren J, van Laar T, Zhang L, et al. Genetic depletion and pharmacological targeting of alphav integrin in breast cancer cells impairs metastasis in zebrafish and mouse xenograft models. *Breast Cancer Res* 2015 Feb 25;17:28-015-0537-8.
- (65) Desgrosellier J, Lesperance J, Seguin L, Gozo M, Kato S, Franovic A, et al. Integrin $\alpha v \beta 3$ Drives Slug Activation and Stemness in the Pregnant and Neoplastic Mammary Gland. *Developmental Cell* 2014 8/11;30(3):295-308.
- (66) Livak KJ, Schmittgen TD. Analysis of relative gene expression data using real-time quantitative PCR and the 2(-Delta Delta C(T)) Method. *Methods* 2001 Dec;25(4):402-408.
- (67) Doleschall M, Mayer B, Cervenak J, Cervenak L, Kacs Kovics I. Cloning, expression and characterization of the bovine p65 subunit of NFkB. *Developmental & Comparative Immunology* 2007;31(9):945-961.
- (68) Wang Y, Shenouda S, Baranwal S, Rathinam R, Jain P, Bao L, et al. Integrin subunits alpha5 and alpha6 regulate cell cycle by modulating the chk1 and Rb/E2F pathways to affect breast cancer metastasis. *Mol Cancer* 2011 Jul 13;10:84-4598-10-84.
- (69) Mierke CT, Frey B, Fellner M, Herrmann M, Fabry B. Integrin $\alpha 5 \beta 1$ facilitates cancer cell invasion through enhanced contractile forces. *J Cell Sci* 2011 The Company of Biologists Ltd;124(3):369-383.
- (70) Nam J, Onodera Y, Bissell MJ, Park CC. Breast Cancer Cells in Three-dimensional Culture Display an Enhanced Radioresponse after Coordinate Targeting of Integrin $\alpha 5 \beta 1$ and Fibronectin. *Cancer Res* 2010 American Association for Cancer Research;70(13):5238-5248.
- (71) Katoh D, Nagaharu K, Shimojo N, Hanamura N, Yamashita M, Kozuka Y, et al. Binding of alpha[vbeta]1 and alpha[vbeta]6 integrins to tenascin-C induces epithelial-mesenchymal transition-like change of breast cancer cells. *Oncogenesis* 2013 08/19;2:e65.
- (72) Vassilopoulos A, Chisholm C, Lahusen T, Zheng H, Deng C. A critical role of CD29 and CD49f in mediating metastasis for cancer-initiating cells isolated from a Brca1-associated mouse model of breast cancer. *Oncogene* 2014 11/20;33(47):5477-5482.

- (73) Lu S, Simin K, Khan A, Mercurio AM. Analysis of integrin beta4 expression in human breast cancer: association with basal-like tumors and prognostic significance. *Clin Cancer Res* 2008 Feb 15;14(4):1050-1058.
- (74) Vieira AF, Ribeiro AS, Dionisio MR, Sousa B, Nobre AR, Albergaria A, et al. P-cadherin signals through the laminin receptor alpha6beta4 integrin to induce stem cell and invasive properties in basal-like breast cancer cells. *Oncotarget* 2014 Feb 15;5(3):679-692.
- (75) Liu W, Moulay M, Willenbrock S, Roelf C, Junghanss C, Ngenazahayo A, et al. Comparative characterization of stem cell marker expression, metabolic activity and resistance to doxorubicin in adherent and spheroid cells derived from the canine prostate adenocarcinoma cell line CT1258. *Anticancer Res* 2015 Apr;35(4):1917-1927.
- (76) Ferletta M, Grawe J, Hellmen E. Canine mammary tumors contain cancer stem-like cells and form spheroids with an embryonic stem cell signature. *Int J Dev Biol* 2011;55(7-9):791-799.
- (77) Ginestier C, Hur MH, Charafe-Jauffret E, Monville F, Dutcher J, Brown M, et al. ALDH1 Is a Marker of Normal and Malignant Human Mammary Stem Cells and a Predictor of Poor Clinical Outcome. *Cell Stem Cell* 2007 11/15;1(5):555-567.
- (78) Michishita M, Akiyoshi R, Suemizu H, Nakagawa T, Sasaki N, Takemitsu H, et al. Aldehyde dehydrogenase activity in cancer stem cells from canine mammary carcinoma cell lines. *Vet J* 2012 Aug;193(2):508-513.
- (79) Hirsch D, Barker N, McNeil N, Hu Y, Camps J, McKinnon K, et al. LGR5 positivity defines stem-like cells in colorectal cancer. *Carcinogenesis* 2014 Apr;35(4):849-858.
- (80) de Lau W, Peng WC, Gros P, Clevers H. The R-spondin/Lgr5/Rnf43 module: regulator of Wnt signal strength. *Genes Dev* 2014 Feb 15;28(4):305-316.
- (81) Cabodi S, del Pilar Camacho-Leal M, Di Stefano P, Defilippi P. Integrin signalling adaptors: not only figurants in the cancer story. *Nat Rev Cancer* 2010 Dec;10(12):858-870.
- (82) Tikhmyanova N, Little JL, Golemis EA. CAS proteins in normal and pathological cell growth control. *Cell Mol Life Sci* 2010 Apr;67(7):1025-1048.
- (83) Defilippi P, Di Stefano P, Cabodi S. p130Cas: a versatile scaffold in signaling networks. *Trends Cell Biol* 2006 May;16(5):257-263.
- (84) Giampieri S, Manning C, Hooper S, Jones L, Hill CS, Sahai E. Localized and reversible TGFbeta signalling switches breast cancer cells from cohesive to single cell motility. *Nat Cell Biol* 2009 Nov;11(11):1287-1296.
- (85) Cabodi S, Tinnirello A, Bisaro B, Tornillo G, del Pilar Camacho-Leal M, Forni G, et al. p130Cas is an essential transducer element in ErbB2 transformation. *FASEB J* 2010 Oct;24(10):3796-3808.
- (86) Tornillo G, Bisaro B, Camacho-Leal Mdel P, Galie M, Provero P, Di Stefano P, et al. p130Cas promotes invasiveness of three-dimensional ErbB2-transformed mammary acinar structures by enhanced activation of mTOR/p70S6K and Rac1. *Eur J Cell Biol* 2011 Feb-Mar;90(2-3):237-248.

- (87) Cabodi S, Tinnirello A, Di Stefano P, Bisaro B, Ambrosino E, Castellano I, et al. p130Cas as a new regulator of mammary epithelial cell proliferation, survival, and HER2-neu oncogene-dependent breast tumorigenesis. *Cancer Res* 2006 May 1;66(9):4672-4680.
- (88) Brinkman A, van der Flier S, Kok EM, Dorssers LC. BCAR1, a human homologue of the adapter protein p130Cas, and antiestrogen resistance in breast cancer cells. *J Natl Cancer Inst* 2000 Jan 19;92(2):112-120.
- (89) Dorssers LC, Grebenchtchikov N, Brinkman A, Look MP, van Broekhoven SP, de Jong D, et al. The prognostic value of BCAR1 in patients with primary breast cancer. *Clin Cancer Res* 2004 Sep 15;10(18 Pt 1):6194-6202.
- (90) van der Flier S, Brinkman A, Look MP, Kok EM, Meijer-van Gelder ME, Klijn JG, et al. Bcar1/p130Cas protein and primary breast cancer: prognosis and response to tamoxifen treatment. *J Natl Cancer Inst* 2000 Jan 19;92(2):120-127.
- (91) Di Stefano P, Cabodi S, Boeri Erba E, Margaria V, Bergatto E, Giuffrida MG, et al. P130Cas-associated protein (p140Cap) as a new tyrosine-phosphorylated protein involved in cell spreading. *Mol Biol Cell* 2004 Feb;15(2):787-800.
- (92) Kennedy S, Clynes M, Doolan P, Mehta JP, Rani S, Crown J, et al. SNIP/p140Cap mRNA expression is an unfavourable prognostic factor in breast cancer and is not expressed in normal breast tissue. *Br J Cancer* 2008 May 20;98(10):1641-1645.
- (93) Damiano L, Di Stefano P, Camacho Leal MP, Barba M, Mainiero F, Cabodi S, et al. p140Cap dual regulation of E-cadherin/EGFR cross-talk and Ras signalling in tumour cell scatter and proliferation. *Oncogene* 2010 Jun 24;29(25):3677-3690.
- (94) Di Stefano P, Damiano L, Cabodi S, Aramu S, Tordella L, Praduroux A, et al. p140Cap protein suppresses tumour cell properties, regulating Csk and Src kinase activity. *EMBO J* 2007 Jun 20;26(12):2843-2855.
- (95) Qin J, Wu C. ILK: a pseudokinase in the center stage of cell-matrix adhesion and signaling. *Curr Opin Cell Biol* 2012 Oct;24(5):607-613.
- (96) Mongroo PS, Johnstone CN, Naruszewicz I, Leung-Hagesteijn C, Sung RK, Carnio L, et al. Beta-parvin inhibits integrin-linked kinase signaling and is downregulated in breast cancer. *Oncogene* 2004 Nov 25;23(55):8959-8970.
- (97) Sepulveda JL, Wu C. The parvins. *Cell Mol Life Sci* 2006 Jan;63(1):25-35.
- (98) Christensen J, Bentz S, Sengstag T, Shastri VP, Anderle P. FOXQ1, a Novel Target of the Wnt Pathway and a New Marker for Activation of Wnt Signaling in Solid Tumors. *PLoS ONE* 2013 03/26;8(3):e60051.
- (99) Rieger ME, Sims AH, Coats ER, Clarke RB, Briegel KJ. The embryonic transcription cofactor LBH is a direct target of the Wnt signaling pathway in epithelial development and in aggressive basal subtype breast cancers. *Mol Cell Biol* 2010 Sep;30(17):4267-4279.

- (100) Di Stefano P, Leal MP, Tornillo G, Bisaro B, Repetto D, Pincini A, et al. The adaptor proteins p140CAP and p130CAS as molecular hubs in cell migration and invasion of cancer cells. *Am J Cancer Res* 2011;1(5):663-673.
- (101) Farr A, Roman A. A pitfall of using a second plasmid to determine transfection efficiency. *Nucleic Acids Res* 1992 Feb 25;20(4):920.
- (102) Campos LC, Silva JO, Santos FS, Araújo MR, Lavallo GE, Ferreira E, et al. Prognostic significance of tissue and serum HER2 and MUC1 in canine mammary cancer. *Journal of Veterinary Diagnostic Investigation* 2015 July 01;27(4):531-535.
- (103) Haddon L, Hugh J. MUC1-mediated motility in breast cancer: a review highlighting the role of the MUC1/ICAM-1/Src signaling triad. *Clin Exp Metastasis* 2015 Apr;32(4):393-403.
- (104) Kufe DW. MUC1-C oncoprotein as a target in breast cancer: activation of signaling pathways and therapeutic approaches. *Oncogene* 2013 Feb 28;32(9):1073-1081.
- (105) Alam M, Ahmad R, Rajabi H, Kharbanda A, Kufe D. MUC1-C oncoprotein activates ERK-->C/EBPbeta signaling and induction of aldehyde dehydrogenase 1A1 in breast cancer cells. *J Biol Chem* 2013 Oct 25;288(43):30892-30903.
- (106) Damiano L, Le Devedec SE, Di Stefano P, Repetto D, Lalai R, Truong H, et al. p140Cap suppresses the invasive properties of highly metastatic MTLn3-EGFR cells via impaired cortactin phosphorylation. *Oncogene* 2012 Feb 2;31(5):624-633.
- (107) Sato T, Clevers H. Growing Self-Organizing Mini-Guts from a Single Intestinal Stem Cell: Mechanism and Applications. *Science* 2013 06/06;340(6137):1190-1194.
- (108) Huch M, Dorrell C, Boj SF, van Es JH, Li VSW, van dW, et al. In vitro expansion of single Lgr5+ liver stem cells induced by Wnt-driven regeneration. *Nature* 2013 02/14;494(7436):247-250.
- (109) Huch M, Bonfanti P, Boj SF, Sato T, Loomans CJM, van dW, et al. Unlimited in vitro expansion of adult bi-potent pancreas progenitors through the Lgr5/R-spondin axis. *EMBO J* 2013 09/17;32(20):2708-2721.
- (110) Takasato M, Er PX, Chiu HS, Maier B, Baillie GJ, Ferguson C, et al. Kidney organoids from human iPS cells contain multiple lineages and model human nephrogenesis. *Nature* 2015 10/22;526(7574):564-568.
- (111) Lancaster MA, Renner M, Martin C, Wenzel D, Bicknell LS, Hurles ME, et al. Cerebral organoids model human brain development and microcephaly. *Nature* 2013 09/19;501(7467):373-379.
- (112) Nakano T, Ando S, Takata N, Kawada M, Muguruma K, Sekiguchi K, et al. Self-Formation of Optic Cups and Storable Stratified Neural Retina from Human ESCs. *Cell Stem Cell* 2012 /6/14;10(6):771-785.
- (113) Lancaster MA, Knoblich JA. Organogenesis in a dish: Modeling development and disease using organoid technologies. *Science* 2014 07/17;345(6194).
- (114) Clevers H. Modeling Development and Disease with Organoids. *Cell* 2016 6/16;165(7):1586-1597.

- (115) Schweiger PJ, Jensen KB. Modeling human disease using organotypic cultures. *Curr Opin Cell Biol* 2016 12;43:22-29.
- (116) Linnemann JR, Miura H, Meixner LK, Irmeler M, Kloos UJ, Hirschi B, et al. Quantification of regenerative potential in primary human mammary epithelial cells. *Development* 2015 09/22;142(18):3239-3251.
- (117) Sato T, Stange DE, Ferrante M, Vries RG, Van Es JH, Van den Brink S, et al. Long-term expansion of epithelial organoids from human colon, adenoma, adenocarcinoma, and Barrett's epithelium. *Gastroenterology* 2011 Nov;141(5):1762-1772.
- (118) Schafer-Somi S, Kaya D, Gultiken N, Aslan S. Suppression of fertility in pre-pubertal dogs and cats. *Reprod Domest Anim* 2014 Jun;49 Suppl 2:21-27.
- (119) Gobello C. Prepubertal and pubertal canine reproductive studies: conflicting aspects. *Reprod Domest Anim* 2014 Dec;49(6):e70-3.
- (120) Stingl J, Emmerman JT, Eaves CJ. Enzymatic dissociation and culture of normal human mammary tissue to detect progenitor activity. *Methods Mol Biol* 2005;290:249-263.
- (121) Lombardi S, Honeth G, Ginestier C, Shinomiya I, Marlow R, Buchupalli B, et al. Growth Hormone Is Secreted by Normal Breast Epithelium upon Progesterone Stimulation and Increases Proliferation of Stem/Progenitor Cells. *Stem Cell Reports* 2014 6/3;2(6):780-793.
- (122) Tornillo G, Smalley MJ. ERrrr... Where are the Progenitors? Hormone Receptors and Mammary Cell Heterogeneity. *J Mammary Gland Biol Neoplasia* 2015;20(1):63-73.
- (123) Mol JA, Lantinga-van Leeuwen IS, van Garderen E, Selman PJ, Oosterlaken-Dijksterhuis MA, Schalken JA, et al. Mammary growth hormone and tumorigenesis--lessons from the dog. *Vet Q* 1999 Oct;21(4):111-115.
- (124) Selman PJ, Mol JA, Rutteman GR, van Garderen E, Rijnberk A. Progestin-induced growth hormone excess in the dog originates in the mammary gland. *Endocrinology* 1994 Jan;134(1):287-292.
- (125) van de Wetering M, Francies H, Francis J, Bounova G, Iorio F, Pronk A, et al. Prospective Derivation of a Living Organoid Biobank of Colorectal Cancer Patients. *Cell* 2015 /5/7;161(4):933-945.
- (126) Herrmann D, Conway JR, Vennin C, Magenau A, Hughes WE, Morton JP, et al. Three-dimensional cancer models mimic cell-matrix interactions in the tumour microenvironment. *Carcinogenesis* 2014 Aug;35(8):1671-1679.
- (127) Egeblad M, Nakasone ES, Werb Z. Tumors as Organs: Complex Tissues that Interface with the Entire Organism. *Developmental Cell* 2010 6/15;18(6):884-901.
- (128) Jones DL, Wagers AJ. No place like home: anatomy and function of the stem cell niche. *Nat Rev Mol Cell Biol* 2008 print;9(1):11-21.
- (129) Joshi PA, Di Grappa MA, Khokha R. Active allies: hormones, stem cells and the niche in adult mammaryopoiesis. *Trends in Endocrinology & Metabolism* 2012 6;23(6):299-309.

(130) Ye J, Wu D, Wu P, Chen Z, Huang J. The cancer stem cell niche: cross talk between cancer stem cells and their microenvironment. *Tumor Biol* 2014;35(5):3945-3951.

(131) Gerhart J. 1998 warkany lecture: Signaling pathways in development. *Teratology* 1999;60(4):226-239.

(132) Legate KR, Montanez E, Kudlacek O, Fassler R. ILK, PINCH and parvin: the tIPP of integrin signalling. *Nat Rev Mol Cell Biol* 2006 Jan;7(1):20-31.

Acknowledgements

As my HP year comes to an end, I have quite a few people to thank.

First and foremost, my supervisors. Jan, thank you for your help with designing the experiments. You always had a plan B when things didn't work out quite as planned, and your critical comments really improved my work. Thank you also for your great sense of humor during the weekly group meetings. Elpetra, thank you for your patience when perfectly logical things made no sense to me. It might have taken me a while sometimes, but now that the year is over I can say I've learned many different lab techniques thanks to you. Aside from being an excellent teacher, you were very kind, always asking me what I did last weekend.

I would also like to thank my office mates and fellow CTO group members. Karin, you were both an example and very relatable at the same time. Yvet, it was great to see your familiar face appear from behind the computer screen several times a day. Sandra, I will miss our pointless Q-bit sessions and hot chocolate breaks. Jon San, I hope our endless chattering didn't distract you from your work too much. Sara, even though you were often in a hurry you always had time to be friendly. Adri, thank you for performing the zebrafish injections for me.

To all other employees and students at the JDV: thank you for the countless nice conversations during lunch. I've felt welcome from day 1.

Last but not least, I have to thank my friends and family. Heike, Robin, Yvet (again), Chantal, Janneke, Myrna, I'm glad our surnames have brought us together. Jolien and Richelle, you really kept me motivated during the writing. Mom and Dad, you supported me, each in your own distinct way (sending me pictures of Jip vs. telling me it's normal that everything goes wrong). Joris, my lack of computer skills is never a problem thanks to you.

Difficilia quae pulchra

Supplements

Supplement 1: Genorm results of cDNA of the panel of 12 CMT cell lines

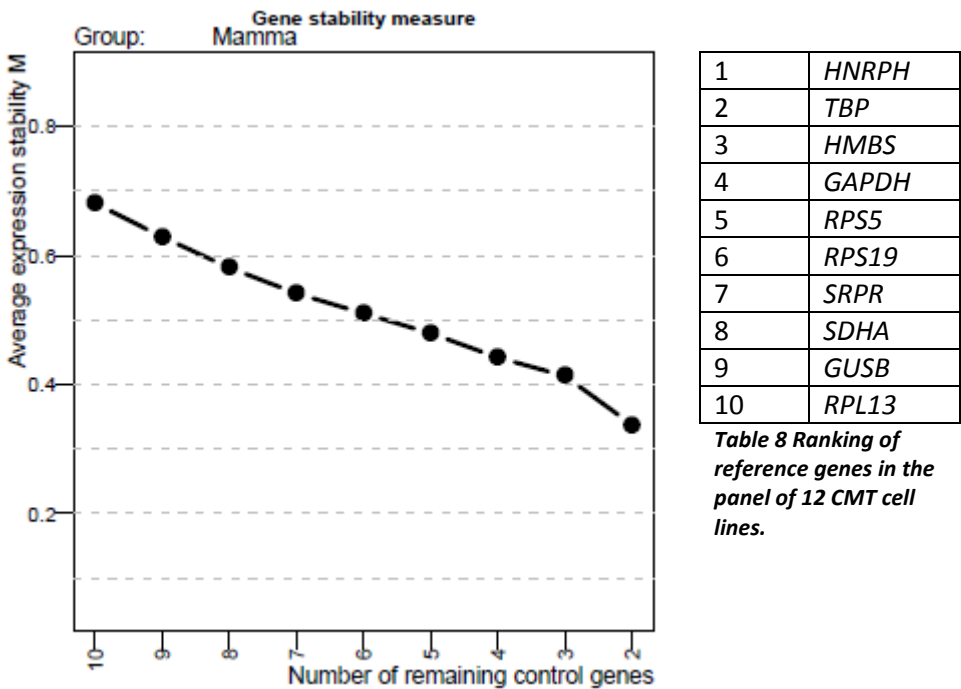


Figure 36 Stability of reference genes in the panel of 12 CMT cell lines.

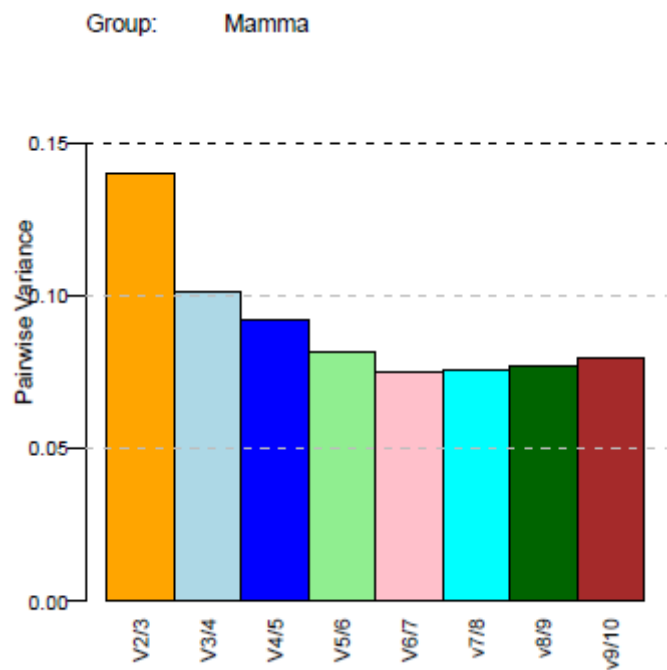


Figure 37 Variance using different numbers of reference genes in the panel of 12 CMT cell lines.

Supplement 2: PE CD49f^{high} and CD49f^{low} gates

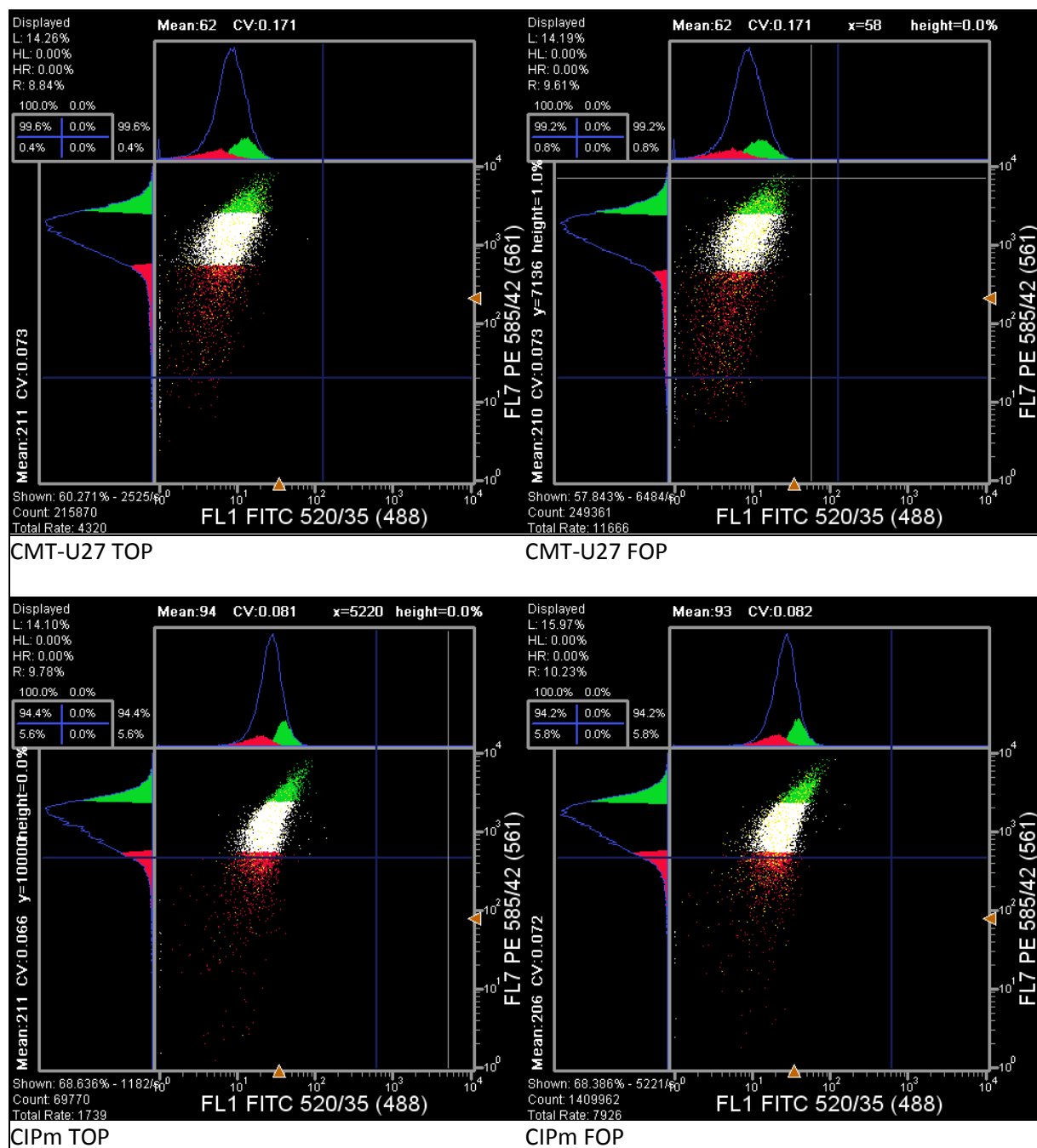


Figure 38 Gates drawn to sort PE anti-CD49f labeled cells from CMTU27 and CIPm cell lines into CD49f^{high} (green) and CD49f^{low} (red) populations. The white population is discarded. Experiment was performed once.

Supplement 3: Individual qPCR data of integrins in a panel of 12 CMT cell lines

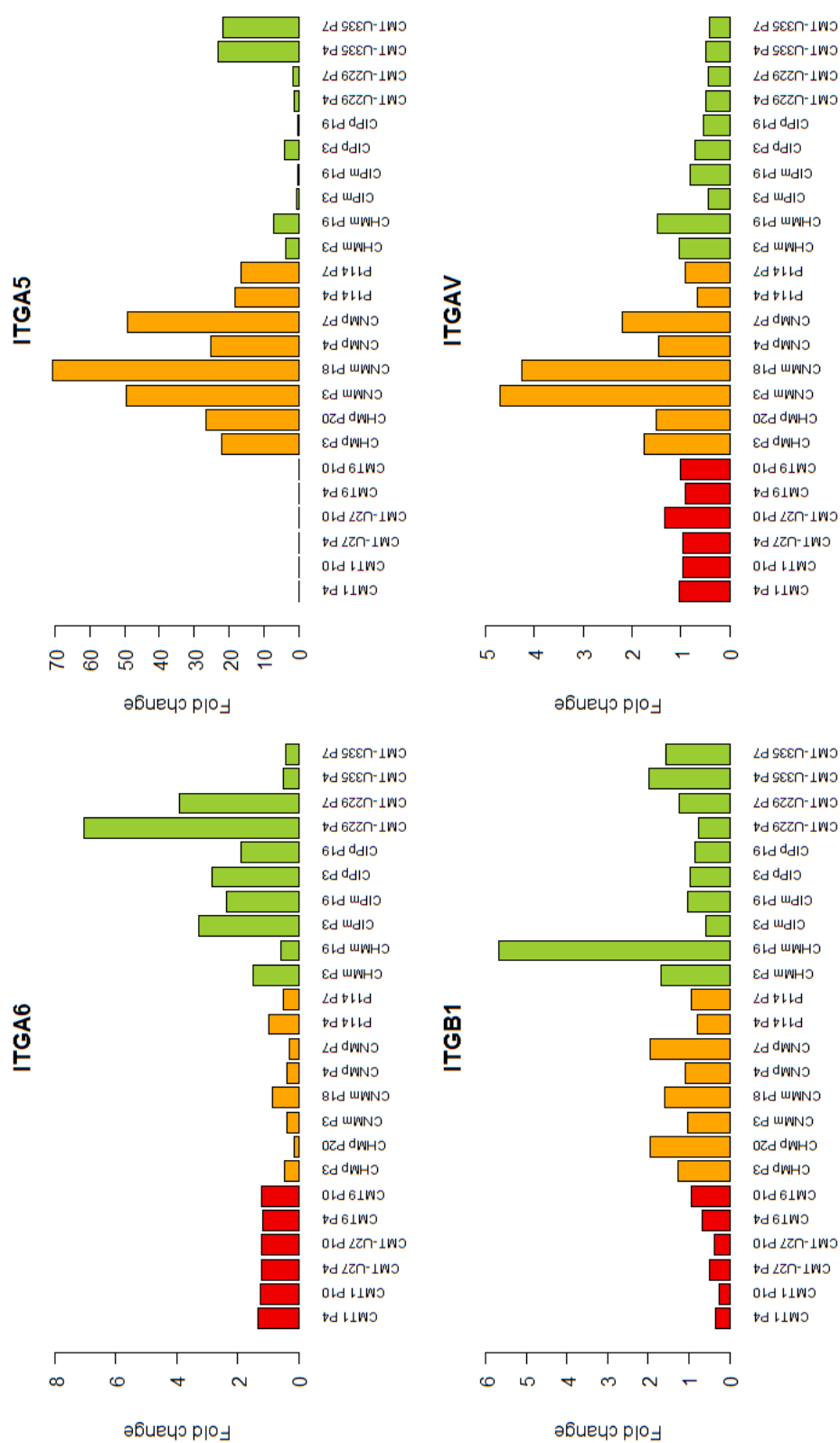
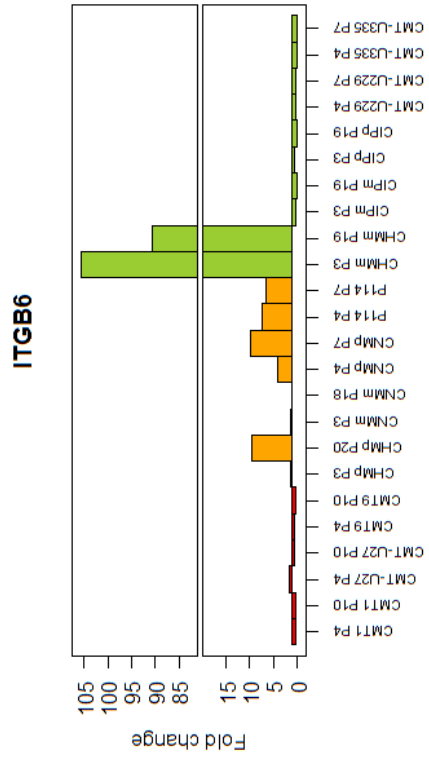
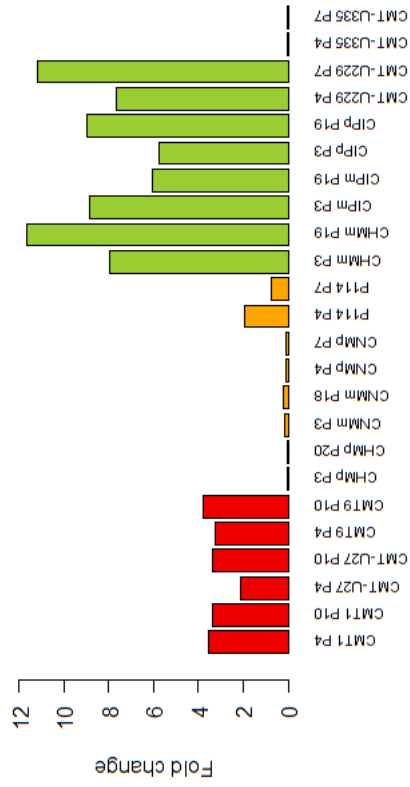
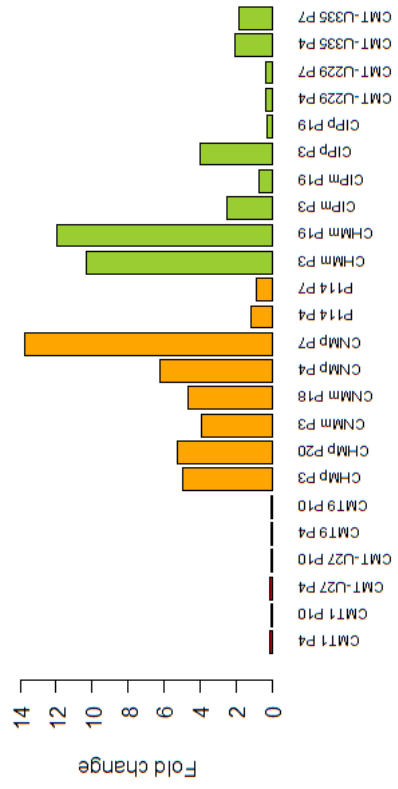


Figure 39 mRNA expression of integrins in a panel of 12 CMT cell lines. Data is expressed as fold change compared to the mean of all cell lines. 2 technical replicates were measured per cell line and passage number. Experiment was performed once. Continued on next page.



Supplement 4: Results FACS CD49f CIPm

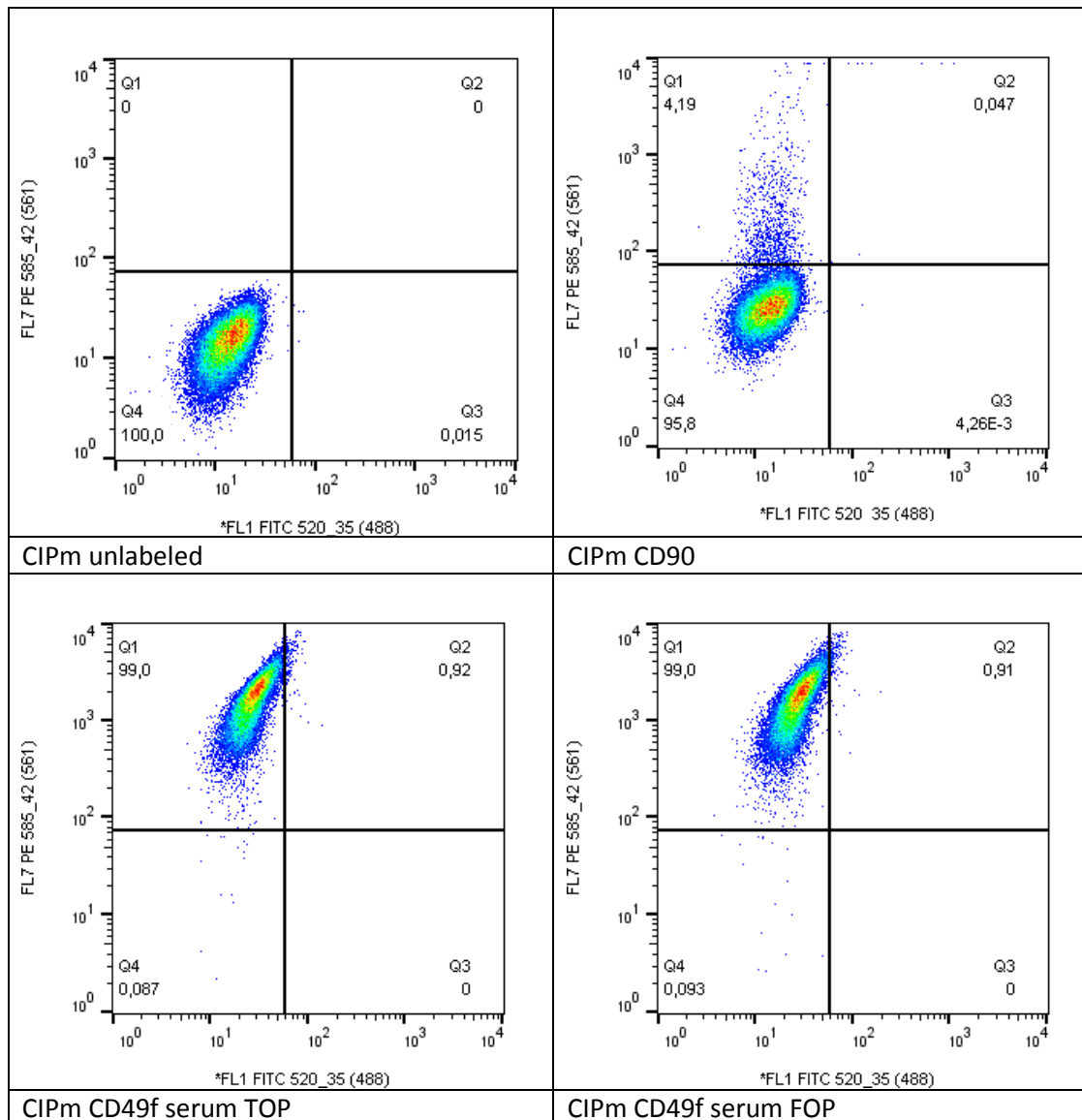


Figure 40 FACS results of unlabeled and anti-CD90 labeled untransfected CIPm and anti-CD49f labeled TOP/FOP transfected CIPm, from CD49^{high} CD49^{low} sorting experiment. Results are from 1 experiment.

Supplement 5: mRNA expression of ALDH1A1 and LGR5 in a panel of 12 CMT cell lines

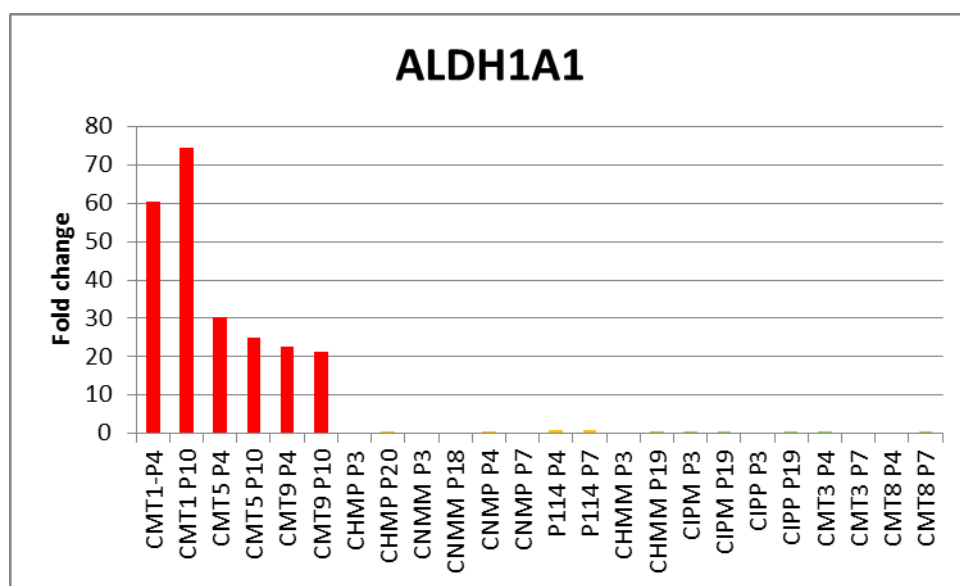


Figure 41 qPCR results of ALDH1A1 expression in a panel of 12 CMT cell lines. Data is expressed as fold change compared to mean of all measurements. 2 technical replicates were measured per cell line and passage number. Experiment was performed once.

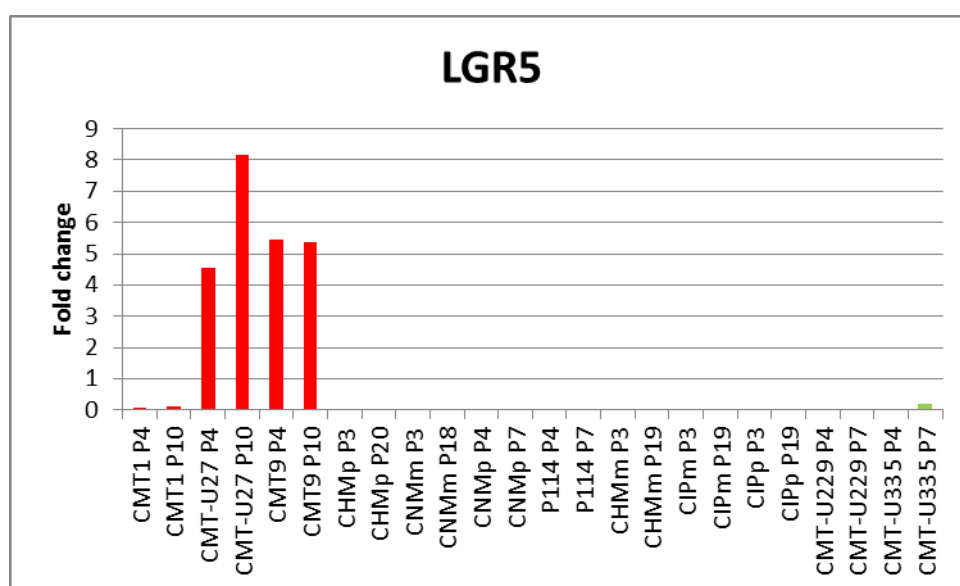


Figure 42 qPCR results of LGR5 expression in a panel of 12 CMT cell lines. Data is expressed as fold change compared to mean of all measurements. 2 technical replicates were measured per cell line and passage number. Experiment was performed once.

Supplement 6: Optimization of transfection conditions

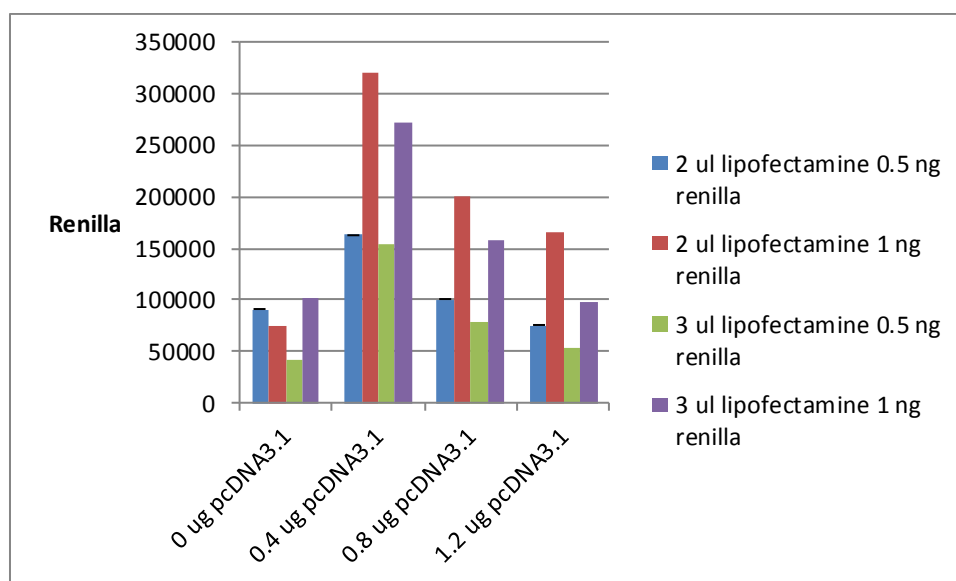
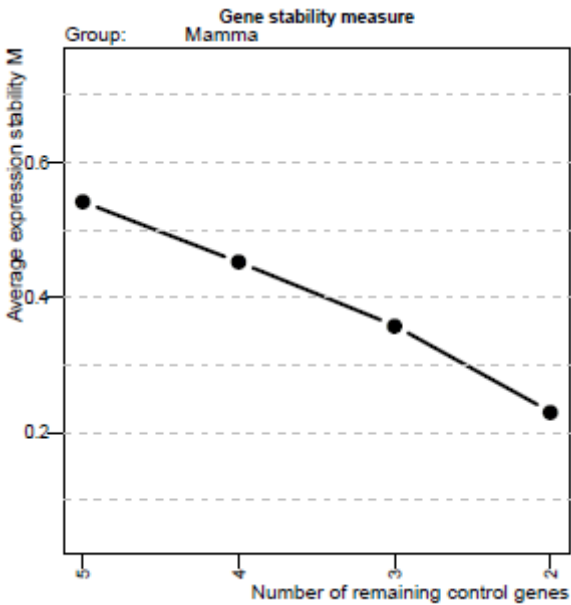


Figure 43 Results of optimization of transfection conditions in CMT-U27. CMT-U27 cells were transfected with varying amounts of pcDNA3.1 plasmid, 2 or 3 μ l Lipofectamine 2000 and 0.5 or 1 ng Renilla to determine the conditions giving the highest Renilla signal. 2 μ l Lipofectamine 200, 0.4 μ g DNA and 1 ng Renilla were optimal. Experiment was performed once.

Supplement 7: Genorm results of Wnt target qPCR



1	<i>RPS5</i>
2	<i>RPS19</i>
3	<i>TBP</i>
4	<i>GAPDH</i>
5	<i>HMBS</i>

Table 9 Ranking of reference genes in Wnt target qPCR samples.

Figure 44 Stability of reference genes in Wnt target qPCR samples.

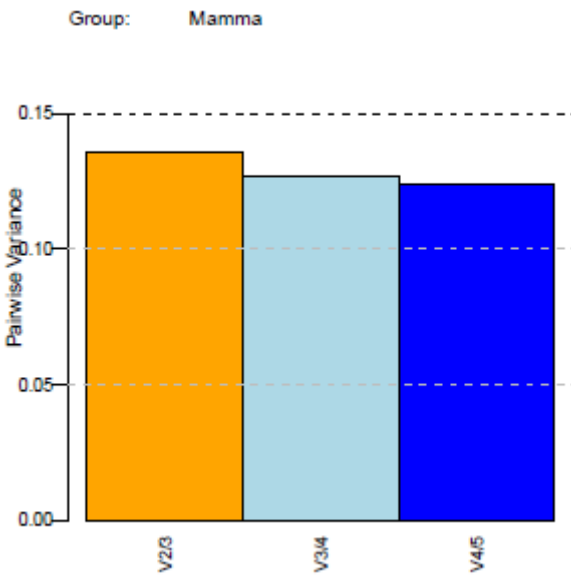


Figure 45 Variance using different numbers of reference genes in Wnt target qPCR samples.

Supplement 8: Results of *NEDD9* and *ILK*-complex qPCR

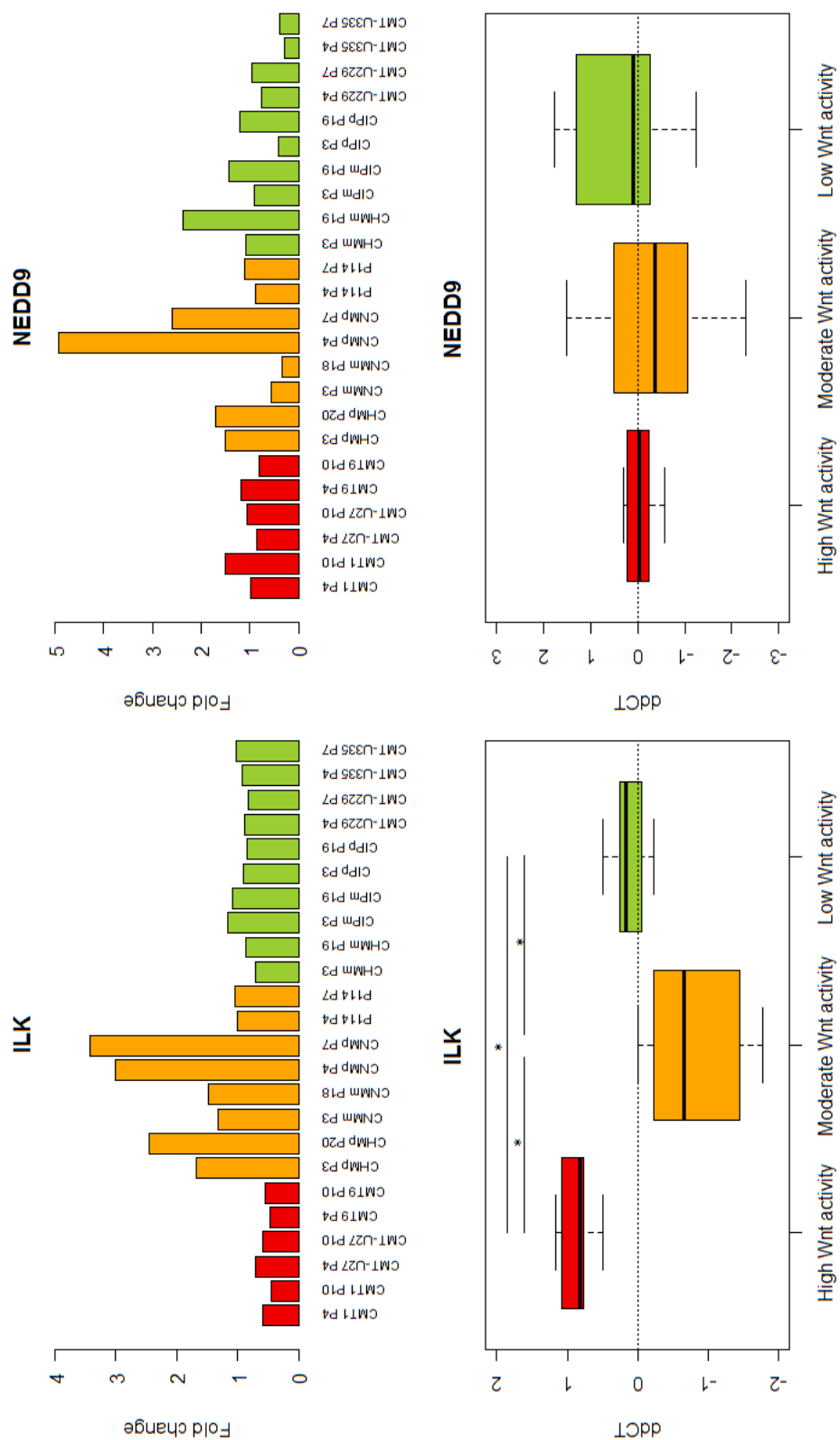
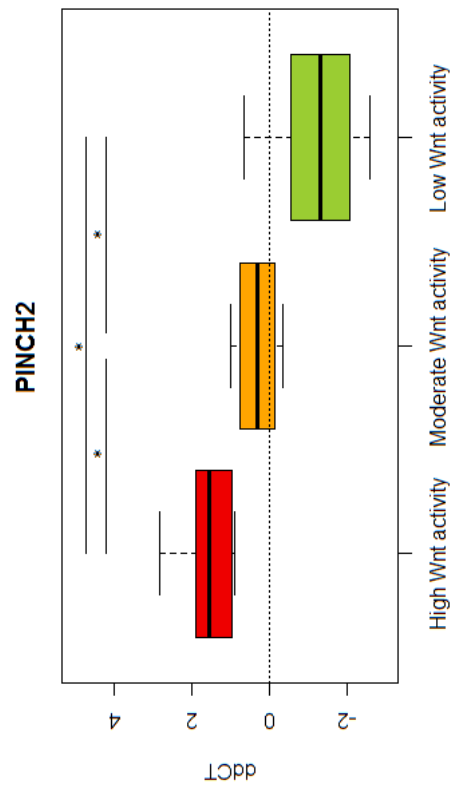
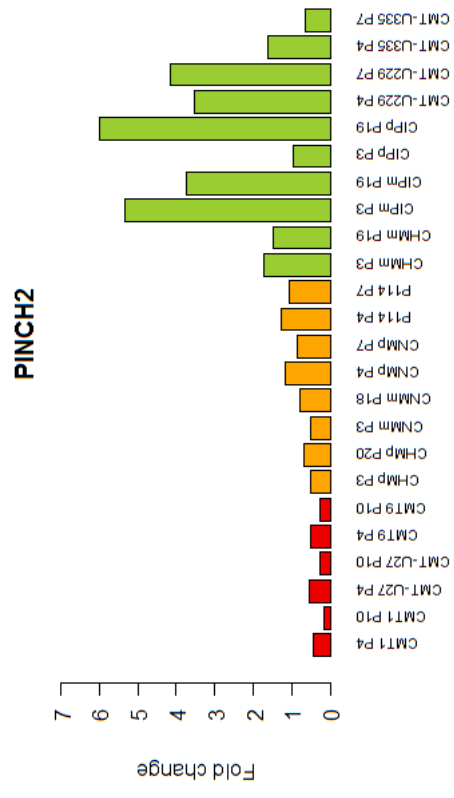
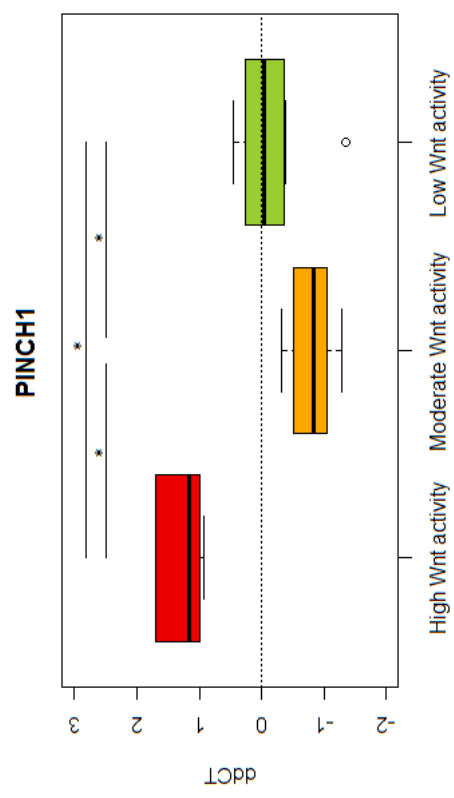
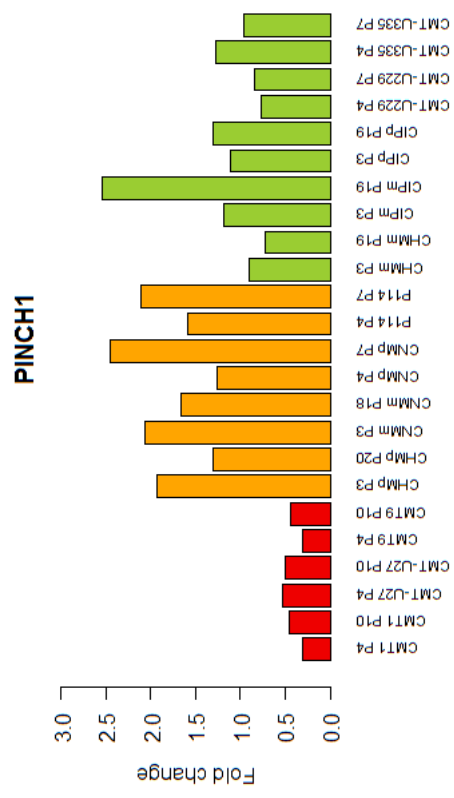
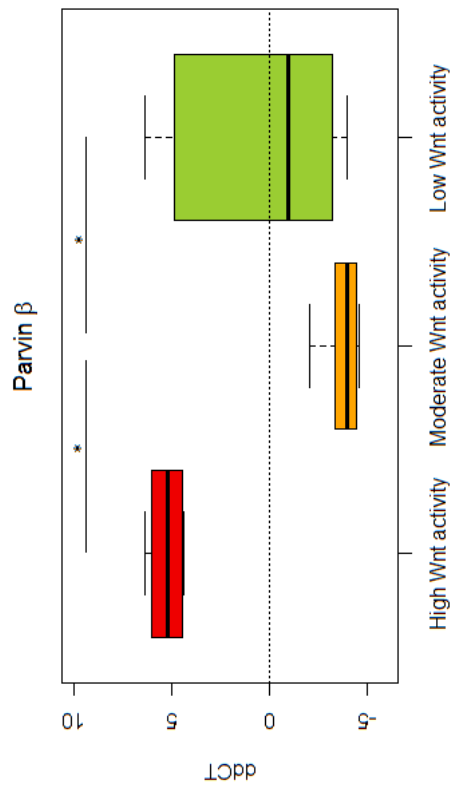
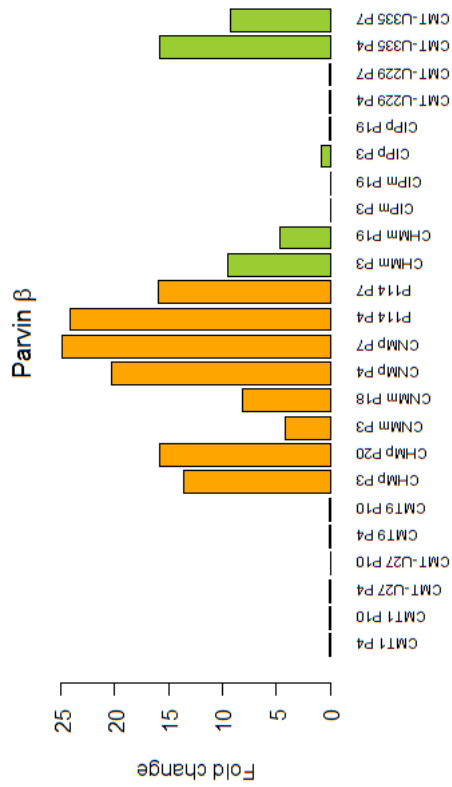
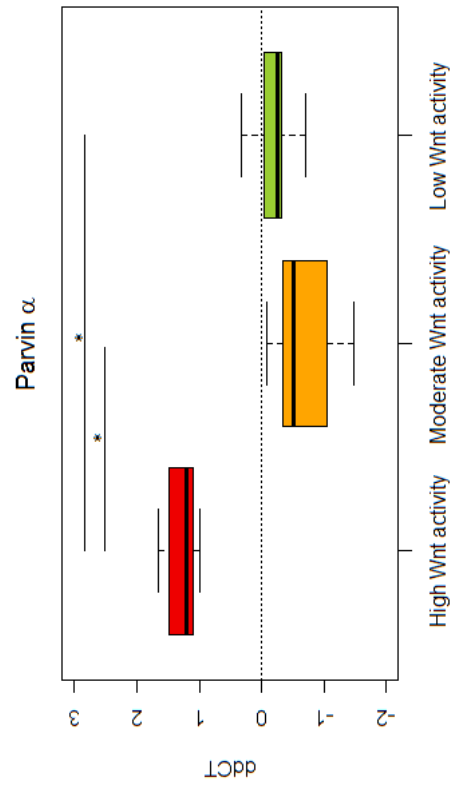
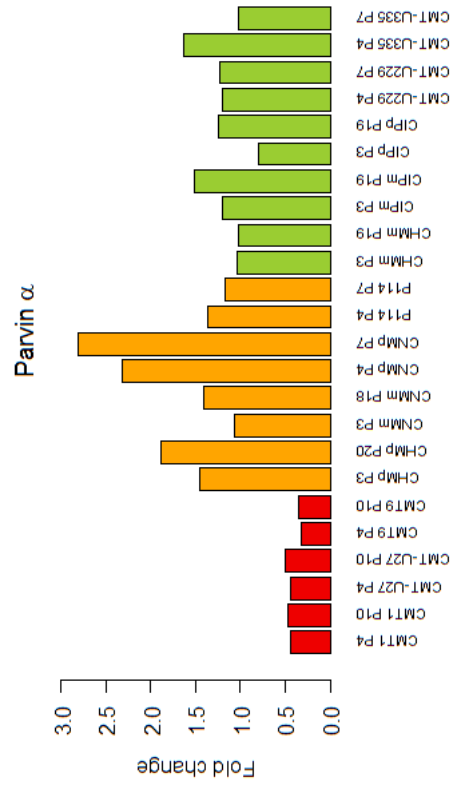


Figure 46 mRNA expression of integrin adaptors. Top figures: expression plotted as fold changes compared to mean expression. Bottom figures: expression plotted as $\Delta\Delta CT$, with mean expression = 0. 2 technical replicates were measured per cell line and passage number. Experiment was performed once. * indicates $p < 0.05$. Continued on next 2 pages.





Supplement 9: Results of preliminary P140CAP TCF/LEF reporter assays of CIPm

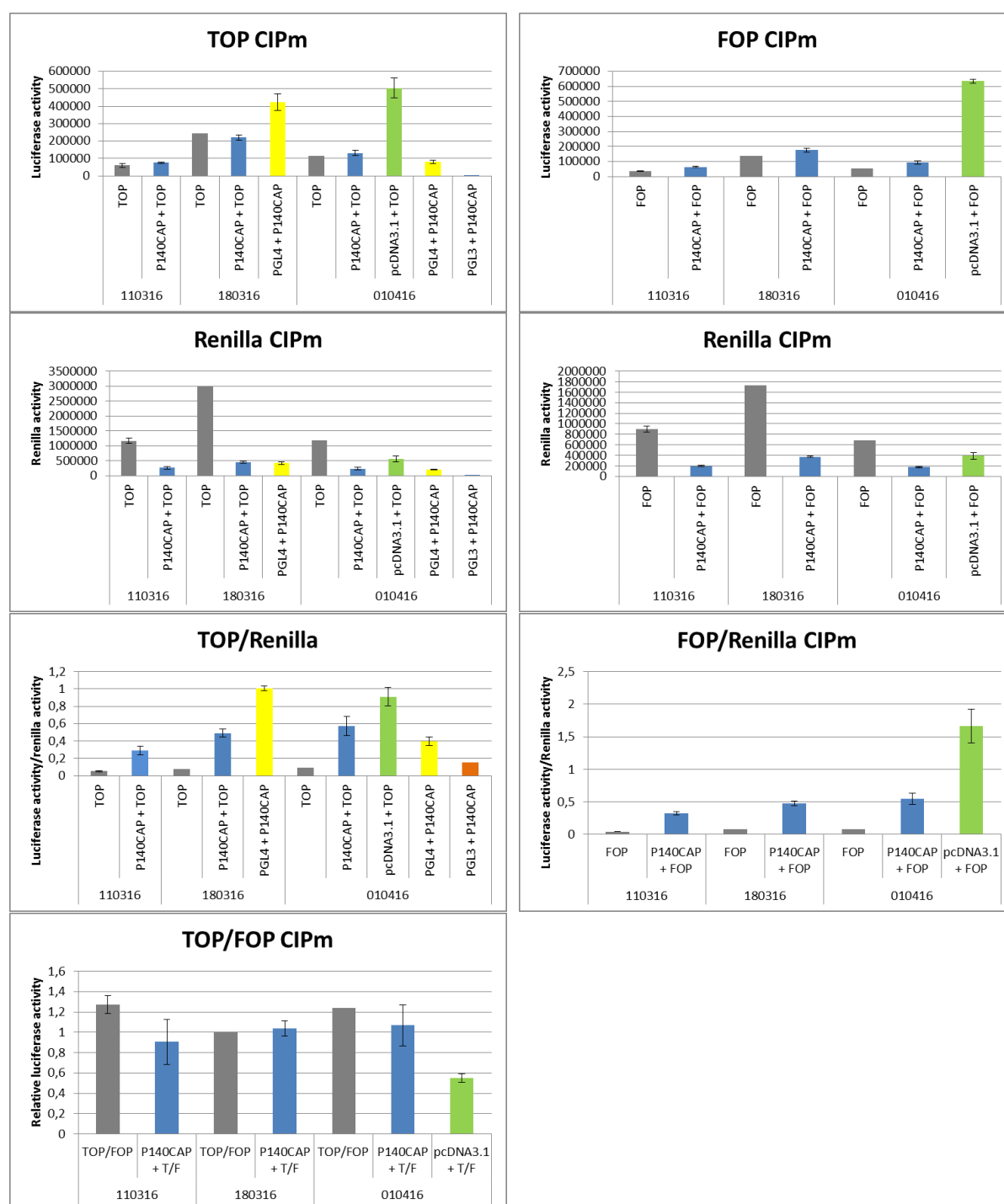


Figure 47 Luciferase activity, Renilla activity, normalized Renilla activity and relative luciferase activity of CIPm transfected with TOP/FOP, P140CAP + TOP/FOP, pcDNA3.1 + TOP/FOP, PGL4 + P140CAP, PGL3 + P140CAP. Left: TOP-transfected samples, right: FOP-transfected samples, bottom: resulting TOP/FOP ratio. Error bars represent SD. For details, refer to M&M of chapter III.

Supplement 10: Results of putative Wnt target gene qPCR

Gene	Cell line	P-Value control vs. Wnt3A	P-value control vs. Dasatinib	Suitable as a Wnt target gene?	P-value pcDNA3.1 vs. P140CAP	P-value pcDNA3.1 + Wnt3A vs. P140CAP + Wnt3A
AXIN2	CMT-U27	4.114e-05 (Corrected: 3.29e-04)	0.002756 (Corrected: 0.022)	Yes, clear effects in CMT-U27 (not significant in CIPm, but same pattern as CMT-U27)	1	0.7304
	CIPm	0.2581	0.1615		0.8633	0.6048
ALDH	CMT-U27	0.0004936 (Corrected: 3.94e-03)	0.1903	No, Wnt3A effect in CMT-U27 is very small		
	CIPm	0.6048	0.07701			
FOSL1	CMT-U27	0.4363	4.114e-05 (Corrected: 3.29e-04)	No, Dasatinib has opposite effects in CMT-U27 and CIPm		
	CIPm	0.9314	4.114e-05 (Corrected: 3.29e-04)			
HER3	CMT-U27	0.7304	0.01061 (Corrected: 0.085)	No, Dasatinib has opposite effects in CMT-U27 and CIPm		
	CIPm	1	8.227e-05 (Corrected: 6.58e-4)			
LBH	CMT-U27	4.114e-05 (Corrected: 3.29e-04)	4.114e-05 (Corrected: 3.29e-04)	No, Wnt3A and Dasatinib both decrease expression		
	CIPm	0.03147 (Corrected: 0.251)	0.3401			
LEF1	CMT-U27	0.7962	4.114e-05 (Corrected: 3.29e-04)	No, Dasatinib effect in CMT-U27 is very small, plus no Wnt3A effect		
	CIPm	0.06253	0.2224			
SURVIVIN	CMT-U27	0.1615	0.4363	No, Dasatinib effect is absent from CMT-U27, should be larger than in CIPm		
	CIPm	1	4.114e-05 (Corrected: 3.29e-04)			
EGFR	CMT-U27	0.002756 (Corrected: 0.022)	0.1903	No, Wnt3A effect in CMT-U27 is very small		
	CIPm	0.06253	0.2581			
MUC1	CMT-U27	4.114e-05 (Corrected: 3.29e-04)	4.114e-05 (Corrected: 3.29e-04)	Yes, larger effects in CMT-U27 than in CIPm	0.9314	0.8633
	CIPm	0.00399 (Corrected: 0.03192)	4.114e-05 (Corrected: 3.29e-04)		0.2581	0.7962
ID2	CMT-U27	0.6665	0.002756 (Corrected: 0.022)	No, no Wnt3A response in CMT-U27. Dasatinib has opposite effect in CMT-U27 and CIPm		
	CIPm	0.7304	4.114e-05 (Corrected: 3.29e-04)			

Table 10 Results of statistical analysis of putative Wnt target genes and genes of interest.

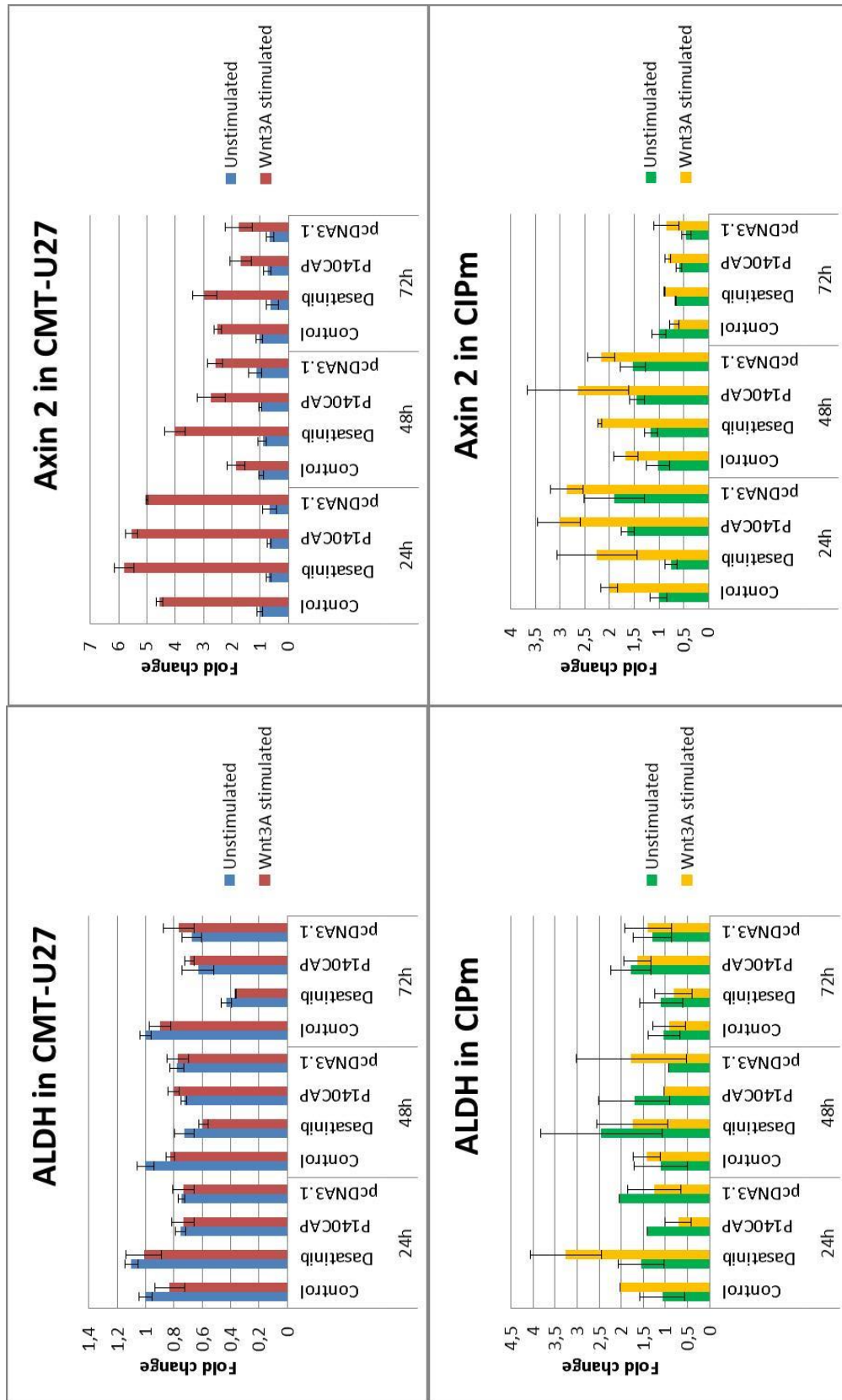
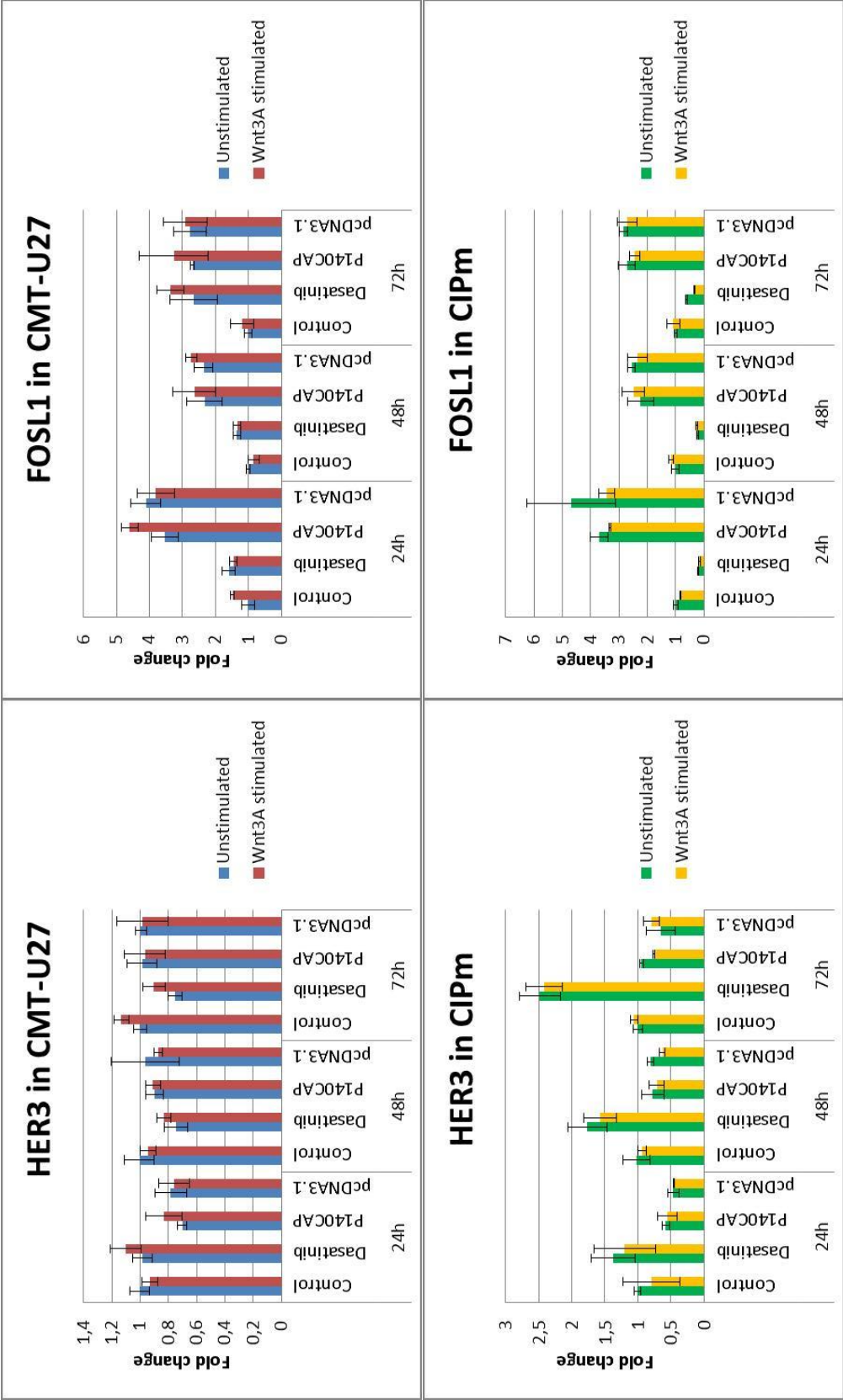
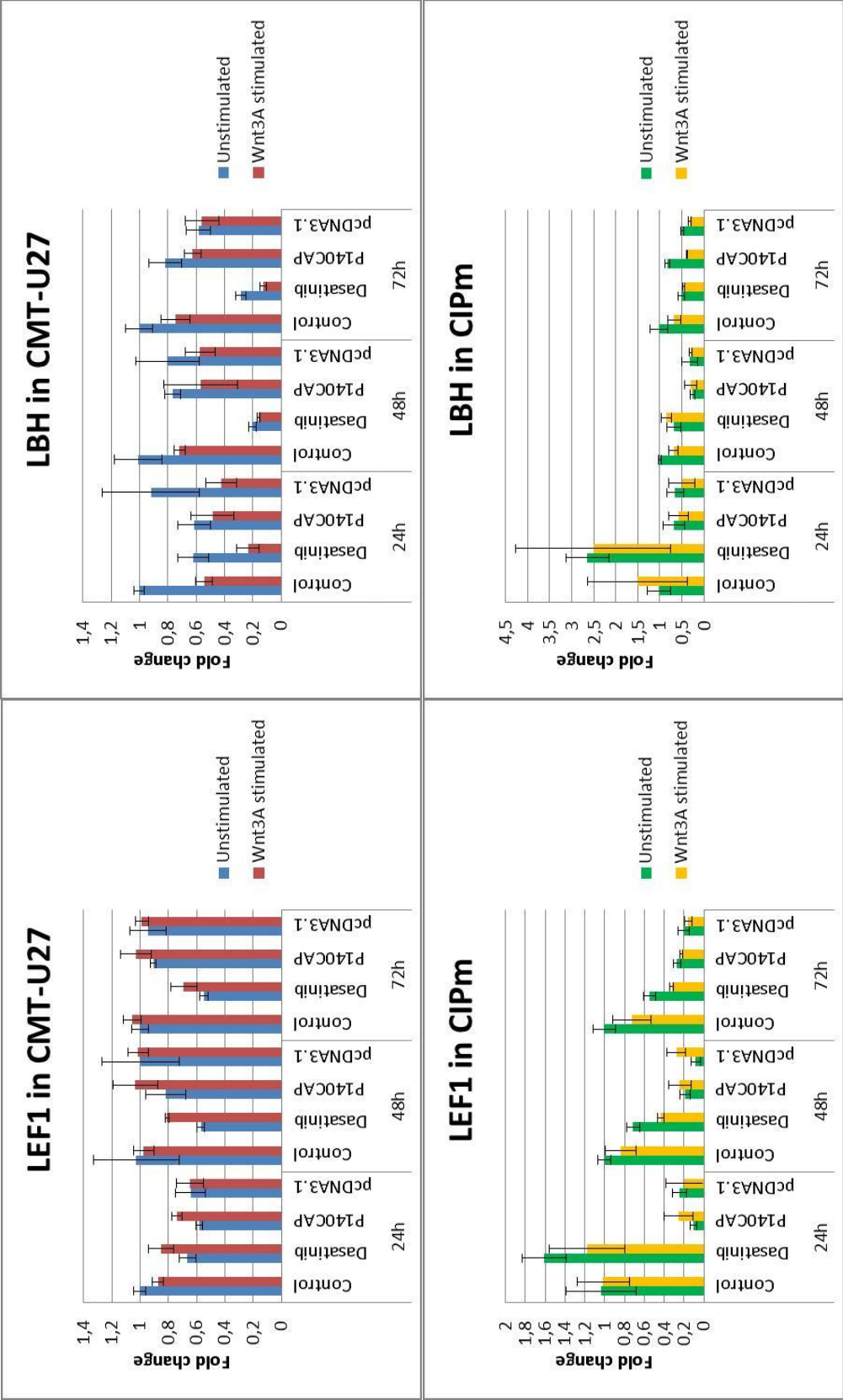
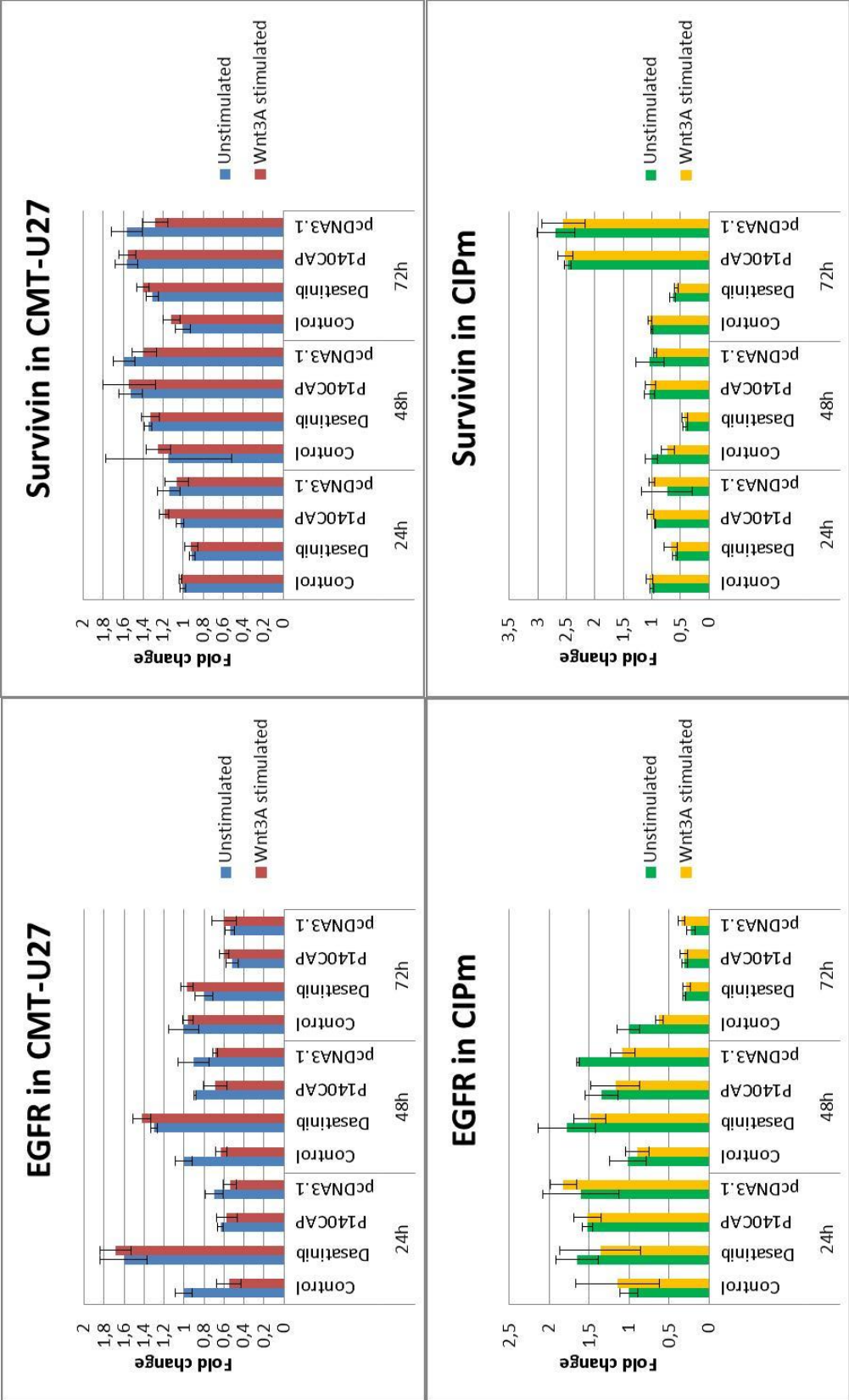
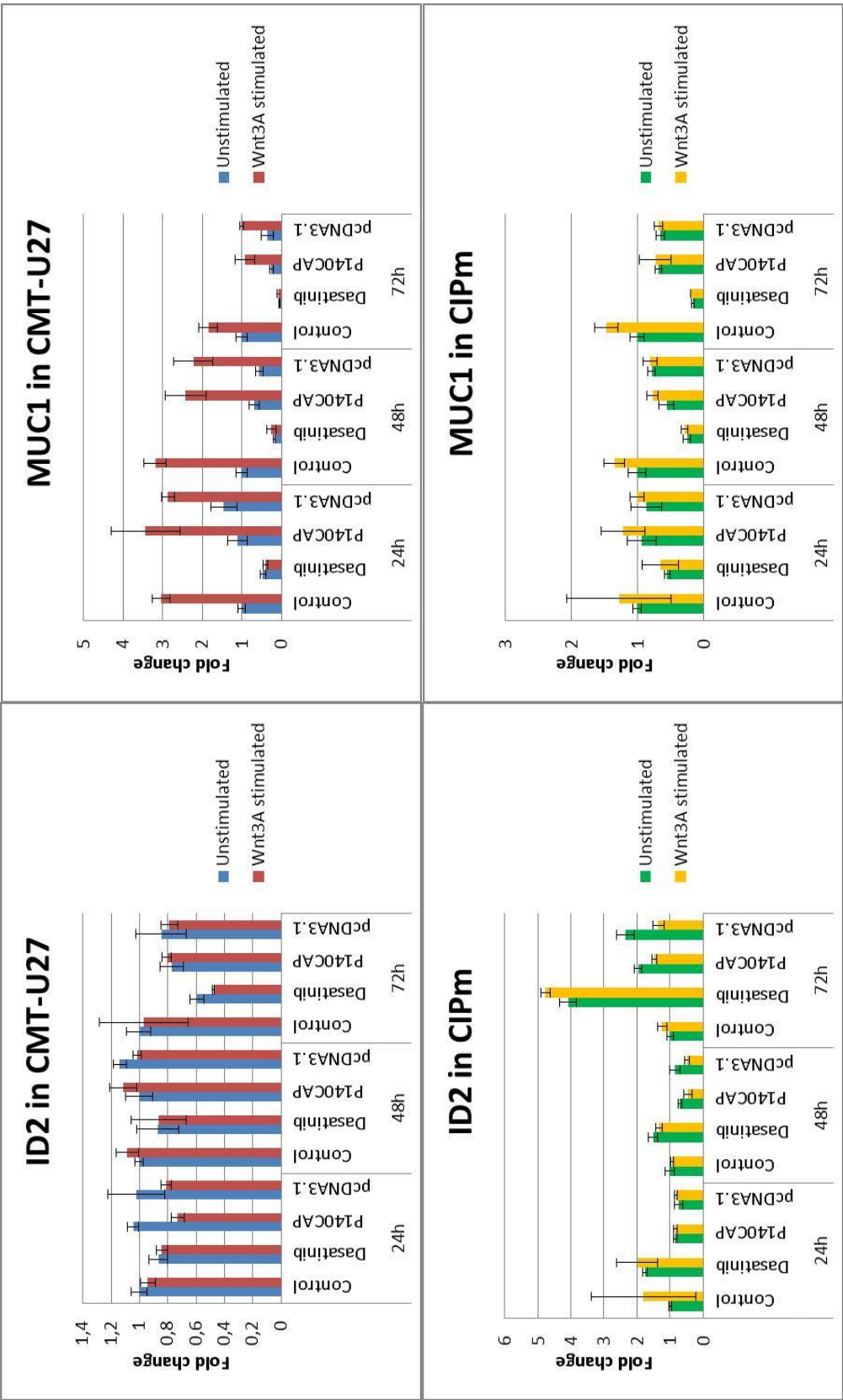


Figure 48 mRNA expression of putative Wnt target genes per individual timepoint, expressed as fold change compared to untransfected control of each timepoint. For each sample, $n = 3$. Experiment was performed once. Error bars represent SD. Continued on the next 4 pages.









Supplement 11: Courses followed during the HP year

Introductory statistics course

- 15 & 17 December 2015
- Course providers: Hans Vernooij en Jan van den Broek
- Faculty of Veterinary Medicine, Utrecht University

Modern methods in data analysis:

- 4-22 January 2016
- 3 weeks full time
- Course coordinator: Cas Kruitwagen
- Master epidemiology, Utrecht University
- 4.5 ECTS
- Grade: 8

Giving effective oral presentations

- 6, 13 & 20 April 2016, 13:00-16:00 h
- Course provider: Margo de Wolf
- Graduate School of Life Sciences, Utrecht University
- 1.0 ECTS

Scientific writing course

- 11 February, 7 & 14 March, 4 + 11 + 18 April, 2 + 9 May, 29 June 2016, 2 hours per meeting
- Course provider: Linda McPhee
- Graduate School of Life Sciences, Utrecht University